AN ABSTRACT OF THE DISSERTATION OF

D. Joseph Sexton for the degree of Doctor of Philosophy in Microbiology presented on May 8, 2017

Title: The Fitness Costs and Regulatory Strategies of Cooperative Siderophore Production in *Pseudomonas*

Abstract approved:

Martin Schuster

Cooperative behaviors in bacteria are increasingly appreciated for their relevance to microbial ecology and utility as model systems for social evolution. One example is the secretion of siderophores, a structurally diverse group of compounds that chelate extracellular iron. Siderophore production is considered cooperative because the benefits can be shared with neighboring cells, provided they have a suitable uptake system. As a cooperative behavior, evolutionary theory predicts siderophore production should be vulnerable to exploitation by free-loaders who reap the benefits without equal investment. Indeed, natural isolates often express receptors for siderophores they do not produce, indicating that social conflict is ecologically relevant. However, many questions remain unanswered regarding the influence of social conflict on the evolution of siderophore-producing populations. Specifically, the environmental conditions conducive to free-loading are not fully understood, obscuring efforts to distinguish whether siderophore-negative isolates evolved as social cheaters or are a result of non-social adaptations. It is also unknown how bacterial phenotypes are regulated to optimize fitness when competing with other siderophore producers. The results presented here provide insight into these two questions.

We first investigated the relationship between nutrient limitation and the fitness cost of pyoverdine (PVD) production, the primary siderophore of the medically relevant

model organism *Pseudomonas aeruginosa*. Using metabolic modeling, we showed PVD production, although energetically costly, does not influence growth rate unless a building block of PVD (carbon or nitrogen) is limiting. When growth is limited by any other nutrient such that carbon and nitrogen are in relative excess, PVD production does not compete with the generation of cellular biomass and therefore does not reduce the growth rate. We confirmed these results experimentally with a continuous-culture approach. We showed that isogenic PVD-negative mutants act as free-loaders in co-culture with a PVD-producing wild-type when limited by carbon, but not when limited by phosphorus.

Second, we focused on the competitive strategies of soil bacterium *Pseudomonas protegens* Pf-5, a biocontrol strain remarkable for its ability to use dozens of siderophores it does not make. We found that while Pf-5 is able to regulate its receptors dynamically to reflect siderophore availability, it continues to secrete its own primary siderophore $PVD_{Pf\text{-}5}$, declining the opportunity to free-load. We demonstrated that this strategy is beneficial in co-culture with a competing PVD producer, *P. aeruginosa* PAO1. Although Pf-5 can use PAO1's siderophore, Pf-5 must continue to produce its own to maintain a competitive advantage. We attribute this to an antagonistic effect of $PVD_{Pf\text{-}5}$ on the growth of PAO1, presumably through limiting access to iron. Our results demonstrate the benefits of excluding competitors exceed the incentives associated with a free-loader lifestyle for Pf-5.

Our findings are important not only for a fundamental understanding of microbial populations, but also for contexts highly relevant to humans, including human infections and agricultural applications. The principle of nutrient-dependent fitness costs has implications for the not only the stability of cooperation in the PVD model system, but also cooperation in general. Our work with Pf-5 emphasizes that complex strategies beyond free-loading are also relevant to siderophore social dynamics. Collectively, our findings contribute to a predictive understanding of how social dynamics influence the evolution and stability of siderophore production.

The Fitness Costs and Regulatory Strategies of Cooperative Siderophore Production in *Pseudomonas*

by

D. Joseph Sexton

A DISSERTATION

Submitted to

Oregon State University

In partial fulfillment of
the requirements for the
degree of

Doctor of Philosophy

Presented May 8, 2017

Commencement June 2017

Doctor of Philosophy dissertation of D. Joseph Sexton presented on May 8, 2017.

APPROVED:

_____

Major Professor, representing Microbiology

_____

Chair of the Department of Microbiology

_____

Dean of the Graduate School

I understand that my dissertation will become part of the permanent collection of Oregon State University libraries. My signature below authorizes release of my dissertation to any reader upon request.

_____

D. Joseph Sexton, Author

ACKNOWLEDGEMENTS

I would first like to extend my thanks to Martin Schuster for providing me with an opportunity to explore the social world of *Pseudomonas*. I greatly appreciate not only the opportunity to do my doctoral research in the Schuster Lab, but also the guidance I needed to succeed. I gratefully acknowledge my committee members, Drs. Jeff Chang, Walt Ream, Stephen Giovanonni and Valerian Dolja for their support through insightful conversations, as instructors of courses I took and in the case of Dr. Walt Ream, an invaluable opportunity to do rotational research on *Agrobacterium*. I also extend thanks to our collaborator Joyce Loper for providing numerous strains and expertise on Pf-5. I'd like to thank Brett Mellbye for teaching me how to use the chemostat. I also thank fellow graduate students including Kyle Asfahl, Tanner Robinson and Rashmi Gupta for sharing the graduate student experience. I appreciate the many undergraduates I have worked with, in particular Rochelle Glover and Amandip Singh, whose above average dedication contributed to novel discoveries. I would also like to say thanks to my friends for showing me the hidden swimming holes, swapping songs by the campfire, and the many other things that have created a positive and healthy life outside of the lab.

Most of all I thank my family. I thank my parents for the many years of hard work they invested to provide the foundation I needed to get here in the first place. They have always been there for me. I thank my wife Casey and my daughter Saylor, for leaving everything at home and sharing this journey to Oregon. I also want to acknowledge our newest daughter Max. You just got here but have been immediately appreciated for your uplifting smiles and waiting to teethe until after my dissertation defense.

CONTRIBUTION OF AUTHORS

Dr. Martin Schuster and D. Joseph Sexton were involved in designing and performing experiments, scientific discussions, data interpretation and writing of Chapter 2. Dr. Joyce Loper contributed to scientific discussions and helped revise the manuscript presented as Chapter 3. Rochelle Glover helped perform experiments and manuscript revisions of Chapter 3.

TABLE OF CONTENTS

TABLE OF CONTENTS (Continued)

Page

LIST OF FIGURES

LIST OF TABLES

LIST OF APPENDIX FIGURES

Chapter 1
Introduction

General introduction

In recent decades, an appreciation for the social complexity of bacteria has increased. The previous concept that bacteria live solitary and individually invested lives has now been overturned by many examples of cooperative activities (West, Diggle, *et al.*, 2007; Velicer and Vos, 2009; Xavier, 2011). One example is the secretion of siderophores, a class of compounds that chelate iron from the extracellular environment. This is considered cooperation because the benefits are shared with neighboring cells that express a suitable receptor. This possibility extends to cells that do not contribute to siderophore production, suggesting production might be vulnerable to exploitation by "free-loaders". The re-occurring isolation of strains that express receptors for siderophores they do not make provides evidence that social conflict is indeed relevant to natural populations (De Vos *et al.*, 2001; D'Onofrio *et al.*, 2010). However, the implications of social conflict remain unclear because the fitness costs of siderophore production are not fully understood. Complex multispecies dynamics characteristic of natural environments further obscure the fitness costs and benefits of siderophore production. Addressing these questions is relevant to not only to microbial ecology, but also human interest such as infections and the activity of agriculturally beneficial strains. This dissertation provides new insights with experiments focused on pyoverdine (PVD), the primary siderophore of the fluorescent pseudomonads. This introductory chapter provides background on the ecological and applied relevance of siderophores, with an emphasis on PVDs and their use as a model system for social dynamics.

Siderophores

The acquisition of iron is a challenge in many environments. Despite the abundance of elemental iron on the surface of the earth, it is rarely in a biologically accessible state. Iron tends to exist as insoluble oxides, bound to a wide variety of organic ligands or sequestered by proteins of host organisms (Ratledge and Dover, 2000; Gledhill

and Buck, 2012). Yet nearly all living organisms require iron because of its role in fundamental biological processes including respiration, DNA replication and transcription. Therefore microbial survival is often contingent on a sufficient iron acquisition strategy. One strategy common to many bacteria and fungi is the secretion of iron chelating molecules termed siderophores (Wandersman and Delepelaire, 2004). Siderophores are an incredibly large and diverse group of molecules that share only the ability to chelate iron from the environment, enabling subsequent uptake through a cognate receptor. Although diverse functional groups can be used, siderophores commonly use hydroxamate or catecholate groups to coordinate iron, arranged so that the charged oxygens are geometrically positioned around the iron center (Hider and Kong, 2010). The biosynthetic pathways of siderophores frequently involve non-ribosomal peptide synthetases (Crosa and Walsh, 2002). After binding extracellular iron, the ferric-siderophore complex is translocated back into the cell through a cognate receptor where the iron is often removed through a reductive process (Noinaj *et al.*, 2010). It is well established that siderophore production is stimulated when iron concentrations are low, an insight that has contributed to the successful identification of a number of siderophores as iron chelators (Hider and Kong, 2010). In many bacteria, this response is mediated by the global regulator Fur (Hassan and Troxell, 2013). Together with iron as a co-factor, Fur dimerizes and binds a conserved DNA motif known as the "Fur box" found in the promoter regions of iron related genes (Calderwood and Mekalanos, 1988). Fur binding prevents access to RNA polymerase resulting in transcriptional repression. When iron concentrations are low, iron is less available as a co-factor, and Fur no longer acts as a transcriptional repressor permitting expression. Fur boxes are found in the promoter regions of a large variety of genes related to iron acquisition, including those needed for siderophore biosynthesis (Hassan and Troxell, 2013). Fur can also regulate small RNAs and alternative sigma factors (ECF) which can influence expression of yet other genes, creating regulatory hierarchies that further refine the response to iron limitation (Cornelis *et al.*, 2009).

Siderophore production as cooperative behavior

Because siderophores are secreted into the extracellular environment, iron can be delivered to neighboring cells that express a compatible receptor. This suggests the potential for social conflict, as siderophore-producers may be vulnerable to exploitation by neighboring cells who gain access to the iron without equal investment. Evolutionary theory indicates that if unchecked, such "free-loaders" can pose a threat and potentially lead to the collapse of the entire population, a phenomenon referred to as a tragedy of the commons (Hardin, 1968).

The interpretation of siderophore production as a social trait has substantial merit; it is in fact common for natural isolates to carry receptors for siderophores they do not produce. This has been observed in diverse environments including human infections, marine environments and the rhizosphere (Loper and Buyer, 1991; De Vos *et al.*, 2001; D'Onofrio *et al.*, 2010). Several noteworthy distinctions can be made regarding the kinds of social interactions that have been observed. First, phylogenetic analysis provides strong evidence that some siderophore-negative strains isolated from human infections and marine environments appear to have evolved recently from siderophore-producing ancestors (Cordero *et al.*, 2012; Andersen *et al.*, 2015). This is indicative of what is typically considered "social cheating", where a non-producing strain initially evolves by exploiting the ancestral producer. In a second scenario, marine isolates have also been found that appear dependent on the siderophores produced by non-ancestral neighboring species (D'Onofrio *et al.*, 2010). This interaction is harder to classify; it is unclear if the relationship is exploitative in nature or is but one component of a stabile mutualism (Morris *et al.*, 2012). In a third category, many isolates carry receptors for siderophores originating from other species, yet retain the ability to produce their own siderophore and therefore avoid becoming dependent (Joshi *et al.*, 2006; Hartney *et al.*, 2013; Miethke *et al.*, 2013). Collectively, these examples demonstrate that siderophore production is an ecologically relevant social behavior, yet it remains unclear what the implications of these interactions are.

One interesting prediction is that social conflict may drive the evolution of novel siderophore structures. This is based on the premise that "free-loaders" impose a burden

on the producing strain; selection should favor modifications to the siderophore structure if the change excludes the free-loader (Smith *et al.*, 2005). This concept is supported by theoretical work, which suggests a cyclic pattern between the emergence of cheaters and the population's adaption to subsequently evade the burden (Lee *et al.*, 2012). It is therefore plausible that social conflict could explain the diversity of siderophore structures observed in nature. However, the foundational assumption of this prediction is that non-producers have a fitness advantage over the producing population and impose a selective pressure. Yet the variables that influence the fitness cost of siderophore production are not fully understood, and are further obscured by the complexity inherent to natural environments.

Pyoverdines

One sub-class of siderophores known as the pyoverdines (PVDs) has become a predominant model system to address these questions. PVD is the primary siderophore of the fluorescent pseudomonads and is comprised of a variable non-ribosomal peptide linked to a conserved chromophore (Visca *et al.*, 2007). This chromophore is in fact the source of the yellow-green pigmentation to which the fluorescent pseudomonads owe their name. This phenotype has been historically useful as a taxonomic marker for over half a century (King *et al.*, 1954), although the biological role as an iron chelator was not realized until decades later (Meyer and Abdallah, 1978). Over 60 PVDs have been characterized, with even closely related strains often producing unique PVD types (Meyer *et al.*, 2008). PVD production has been most extensively characterized in the opportunistic human pathogen and model organism *Pseudomonas aeruginosa*. Intriguingly, the PVD locus is the most divergent alignable locus in the *P. aeruginosa* genome, with some regions appearing to be under positive selection (Smith *et al.*, 2005). Social conflict provides one plausible explanation for this diversity. However, other potential selective pressures could also be involved, such as antimicrobial targeting of PVD receptors or changes to increase resistance to pH or enzymatic degradation (Hider and Kong, 2010).

Pyoverdine biosynthesis and regulation

Like many other siderophores, PVDs are synthesized by non-ribosomal peptide synthetases (NRPS), large multi-modular enzymes that synthesize peptides independent of an mRNA template and ribosomes (Challis and Naismith, 2004; Visca *et al.*, 2007). Each module incorporates a specific amino acid residue into the growing peptide. The sequence of the peptide is determined by the order of the NRPS modules in the genome, an insight which has facilitated the characterization of new PVDs and been exploited in other cases to engineer novel ones (Hartney *et al.*, 2011; Calcott *et al.*, 2014). This creates a mechanism for PVD structures to evolve through the loss, addition or duplication of entire modules. This was illustrated by the identification of a novel *P. aeruginosa* PVD type that differs from a known structure only by the absence of a single glycine residue. This modification was easily attributable to the absence of the corresponding NRPS module gene (Smith *et al.*, 2005).

In *P. aeruginosa* strain PAO1, PVD production and regulation is fairly well characterized at the molecular level. PVD biosynthesis starts with peptide assembly by NRPSs in the cytoplasm, leading up to a nearly complete non-fluorescent precursor known as ferribactin (Visca *et al.*, 2007). This precursor is transported through PvdE, an ABC transporter (McMorran *et al.*, 1996) into the periplasm where maturation of the chromophore and final modifications take place (Yeterian *et al.*, 2010). The mechanism of PVD export from the periplasm remains somewhat elusive. There is an efflux pump system known as PvdRT-OmpQ that has been suspected to export PVD. Supporting this prediction, PVD accumulates in the periplasm of *pvdRT-ompQ* mutants, presumably because export is inhibited (Hannauer *et al.*, 2010). However, PVD can still be detected in substantial quantities in the supernatant of *pvdRT-ompQ* mutants, indicating another export system is likely also involved (Imperi *et al.*, 2009).

Once outside the cell, PVD binds ferric iron and can then be recognized by a cognate receptor, FpvA. FpvA is large protein that forms a β-barrel spanning the outer membrane (Cobessi *et al.*, 2005) and is selective only for the ferric-PVD complex but not the apo-PVD (Greenwald *et al.*, 2008). Ferric-PVD transport is an energetic process that uses the proton motive force through a TonB-dependent mechanism (Noinaj *et al.*, 2010).

FpvA interacts with TonB through a conserved N-terminal domain known as the "TonB box"(Adams *et al.*, 2006). When bound to ferric-PVD, FpvA undergoes a conformational change that transduces a signal through the TonB box to activate transport. FpvA is part of a larger family of proteins often referred to as TonB-dependent transducers (Noinaj *et al.*, 2010; Hartney *et al.*, 2011). In the periplasm, the iron is removed from PVD in a reductive process (Greenwald *et al.*, 2007). PVD is exported back outside the cell where it can be reused. Like many siderophores, PVD is relatively stable as it must persist in natural environments (Hider and Kong, 2010). It is therefore possible for a single PVD to be used many times. Interestingly, a role of the PvdRT-OmpQ export system has been more conclusively demonstrated in PVD recycling; *pvdRT-ompQ* mutants are unable to export recycled PVD suggesting separate mechanisms may exist for exporting recycled vs. newly synthesized PVD (Imperi *et al.*, 2009).

The regulation of PVD production and uptake is mediated by the iron-binding transcriptional repressor Fur. Further levels of regulation are also integrated through ECFs PvdS and FpvI, which are required for transcription of the siderophore biosynthesis and receptor genes, respectively (Cornelis *et al.*, 2009). Interestingly, these cytoplasmic proteins simultaneously interact with the same transmembrane anti-ECF, FpvR (Edgar *et al.*, 2014). After binding ferric-PVD, the cognate receptor FpvA interacts with FpvR and induces a conformational change that releases PvdS and FpvI to further stimulate gene expression. This creates a positive feed-back loop leading to further upregulation of both PVD and FpvA (Lamont *et al.*, 2002).

Ecological and applied relevance of PVD production

PVD production is relevant to both ecological and applied contexts. In particular, there is a need to resolve the role of PVD in the chronic infections of cystic fibrosis patients. Cystic fibrosis patients carry a genetic mutation that impairs the ability to clear mucus from the lungs. The lungs are invariably colonized by *P. aeruginosa*, infections which are persistent and ultimately the cause of mortality (Lyczak *et al.*, 2002). PVD is known to be important for the progression of *P. aeruginosa* infections in mouse models (Meyer *et al.*, 1996; Minandri *et al.*, 2016) and has also been detected in the lungs of

cystic fibrosis patients, showing it is produced *in vivo* (Haas *et al.*, 1991). Curiously, PVD-negative isolates have been repeatedly isolated from the lungs of cystic fibrosis patients with increasing frequency as the infection progresses (De Vos *et al.*, 2001; Andersen *et al.*, 2015). It has been suggested these strains evolved as social cheaters. However, it is also possible they evolved due to non-social adaptations and acquire iron through alternative mechanisms. The former hypothesis is consistent with the observation that PVD-negative isolates are more likely to retain a functional PVD receptor when co-existing with a PVD-producer (Andersen *et al.*, 2015). While this is an interesting correlation, a caveat inherent to this comparison is that PVD-negatives were in some cases existing without PVD-producers. Indeed, iron concentrations are known to be orders of magnitude higher in the lungs of cystic fibrosis patients compared to healthy controls (Stites *et al.*, 1998; Reid *et al.*, 2007; Moreau-Marquis *et al.*, 2008). Furthermore, it has been shown that mutations enhancing the heme utilization pathway corresponds with the loss of siderophore production as *P. aeruginosa* adapts in the cystic fibrosis lung (Marvig *et al.*, 2014). An emerging picture that reconciles these observations suggests PVD production is important when establishing the infection, but is replaced by alternative uptake mechanisms as the infection progresses. Social cheating may play a role in driving this transition. A better understanding of the conditions where social cheaters enjoy a relative fitness advantage would greatly contribute to the ongoing conversation about the origin of PVD-negative isolates in the lungs of cystic fibrosis patients.

PVD production has also received attention for its potential in agricultural applications. A number of fluorescent pseudomonads, such as *P. protegens* Pf-5, have been successfully used to control plant pathogens (Loper *et al.*, 2007). PVD is believed to contribute to this activity in part by limiting local iron access to pathogens (Kloepper *et al.*, 1980; Haas and Défago, 2005). It has also been shown PVD can promote plant health by directly delivering iron to the plant (Vansuyt *et al.*, 2007; Nagata *et al.*, 2013). It is therefore valuable to understand the selective pressures influencing PVD production as plant-promoting activities may be compromised if social conflict selects for reduced production of a desired siderophore. This could conceivably occur if a free-loader

destabilizes siderophore production, as has been hypothesized in the progression of *P. aeruginosa* CF lung infections (Andersen *et al.*, 2015). Alternatively, a PVD-producer may down-regulate biosynthesis in favor of cross-feeding on siderophores secreted by a neighboring organism. However, relative to the cystic fibrosis lung, the microbial community in the rhizosphere is profoundly more complex, making it a much more challenging system to make predictions (Parray *et al.*, 2016).

Pyoverdine as model for siderophore cooperation

PVD initially gained attention as a model system for siderophore cooperation after it was shown that a PVD-negative strain derived from UV mutagenesis acted as a social cheater in *P. aeruginosa* (Griffin *et al.*, 2004). This report was particularly impactful as only a few other bacterial behaviors had been formally considered within the framework of social evolution at the time (West *et al.*, 2006). The inherent fluorescence of PVD provides an ideal marker because producers and non-producers can be distinguished based on the cooperative phenotype itself. Furthermore, access to a sequenced genome (Stover *et al.*, 2000), reliable methods for genetic manipulation (Horton, 1995; Choi and Schweizer, 2006), and a well-characterized physiological response to iron limitation made PVD production a very attractive system, especially for evolutionary biologists accustomed to the limitations of higher organisms as experimental model systems (West, Diggle, *et al.*, 2007). In the years since, *P. aeruginosa* PVD secretion has been used as a model system to empirically test basic tenets of social evolutionary theory, with a prominent focus on the principles that help avoid a tragedy of the commons (Hardin, 1968). These studies have shown that growth of PVD-negative strain can be restored when co-cultured with a PVD-producer under low iron conditions, and established a set of common methods for the study of social dynamics (Buckling *et al.*, 2007; Rolf Kümmerli, Gardner, *et al.*, 2009; Harrison and Buckling, 2009; Rolf Kümmerli, Griffin, *et al.*, 2009; Jiricny *et al.*, 2010; Kümmerli *et al.*, 2010).

Some principles are applicable to cooperation in general (Buckling *et al.*, 2007), such as the concept of frequency-dependent fitness benefits. A social cheater is predicted to have the highest relative fitness when it is rare in the population, and is surrounded by

cooperators to exploit. However, this fitness advantage depreciates as cheater frequency increases in the population, as the benefit provided by the cooperator becomes dilute (Ross-Gillespie *et al.*, 2007). Other work has shown spatial structure can help stabilize cooperation, which is especially relevant to microorganisms as clonal growth works to spatially exclude cheaters (Luján *et al.*, 2015). Density-dependent fitness effects have also been reported, where cooperation is more efficient and therefore less vulnerable to cheaters at higher densities (Ross-Gillespie *et al.*, 2009).

One characteristic likely to be particularly relevant for siderophores is "good durability", a concept extended from economic theory that describes how long the benefits from a cooperative behavior last (Brown and Taddei, 2007; Kümmerli and Brown, 2010). One study relates this concept to the recyclability of PVDs, which acts to increase durability. By reusing a single PVD to deliver multiple iron ions, the fitness costs can be greatly reduced. The cost may even be further minimized if secretion is repressed once a sufficient concentration has been reached (Kümmerli and Brown, 2010). Although not yet investigated explicitly for this purpose, other variables could influence the durability of siderophores, specifically those that influence its persistence in the environment such as pH or enzymatic degradation (Hider and Kong, 2010).

It has also been suggested that siderophores may be partially privatized, meaning that the producer strain has priority access (Scholz and Greenberg, 2015). Even minimal amounts of privatization can go far for repressing cheaters; it has been shown in yeast degradation of sucrose that priority access to just 1% of the breakdown products can be sufficient to avoid a tragedy of the commons (Gore *et al.*, 2009). As siderophores are secreted, it is perhaps counterintuitive to think they could be privatized. However, many siderophores in marine environments have hydrophobic domains that increase their association with cell membranes, presumably to reduce diffusion (Hider and Kong, 2010). One study investigated this idea more formally and found strains living in environments with greater diffusion tend to have less "diffusive" siderophores, consistent with the idea that selection may act to help retain the siderophore (Kümmerli *et al.*, 2014). This could work to provide an extent of privatization.

Many questions also remain about the strategies that influence siderophore-mediated interspecies competition. This topic was very recently addressed in theoretical work which modeled scenarios where multiple siderophore-producers co-exist, with varying abilities to use each other's siderophore (Niehus *et al.*, 2017). The authors found cross-feeding is likely to influence the evolution of siderophore production by selecting for more production of a siderophore that cannot be used by neighboring strains and vice-versa. Although this finding may seem intuitive, the study is valuable as it incorporated many variables true to the biochemistry of siderophores, such as binding affinities, and found a greater emphasis should be placed on the competitive nature of siderophores.

Research objectives

In this dissertation, we look at several aspects of siderophore cooperation that have not been previously considered. Specifically, recent work in other microbial social models suggests the growth-limiting nutrient plays a bigger role in the fitness costs of cooperation than currently appreciated (Xavier *et al.*, 2011; Mellbye and Schuster, 2014). However, relative resource availability has not been evaluated in the context of siderophore production. In the second chapter of this dissertation, we report that the growth limiting nutrient has a deterministic influence on the fitness cost of PVD production. We argue that the growth limiting nutrient is a valuable predictor of whether selection will favor the evolution of free-loaders.

In the third chapter, we evaluate the regulatory strategies of *P. protogens* Pf-5, a biocontrol strain that uses dozens of siderophores from other species but retains the ability to produce its own (Hartney *et al.*, 2013). Counter to what may be expected, we report Pf-5 continues to produce its native siderophore despite the availability of other siderophores. We find this behavior is essential in the interspecies competition for iron with *P. aerugionsa*, emphasizing the importance of strategies outside of the free-loader paradigm.

To summarize, the field of research interested in the social dynamics of siderophore production is in an exciting and dynamic state as diverse specialties are rapidly converging to address similar questions. This has ultimately accelerated the rate

of progress. Nonetheless, the ability to use a social dynamic framework to provide robust explanations for observations in natural environments remains out of reach. This dissertation presents novel insights to our understanding of how social dynamics shape the evolution of siderophore production.

Chapter 2

"Nutrient limitation determines the fitness of cheaters in bacterial siderophore cooperation"

D. Joseph Sexton and Martin Schuster

Nature Communications
In Review
April, 2017

Abstract

Cooperative behaviors provide a collective benefit, but are considered costly for the individual. Here we report that the costs of cooperation vary dramatically and have opposing effects on the selection for non-cooperating cheaters in different, ecologically relevant contexts. We investigate a prominent bacterial example of cooperative behavior, the secretion of the peptide siderophore pyoverdine by *Pseudomonas aeruginosa*, under different nutrient-limiting conditions. Using metabolic modeling, we show that pyoverdine, although energetically costly, incurs a fitness cost only when its building blocks carbon or nitrogen are growth-limiting and are diverted from cellular biomass production, but not when other nutrients are limiting such that building blocks are in relative excess. We confirm these results experimentally with an unconventional continuous-culture approach. We show that pyoverdine non-producers (cheaters) enjoy a large fitness advantage in co-culture with producers (cooperators) and spread to high frequency when limited by carbon, but not when limited by phosphorus. The principle of nutrient-dependent fitness costs has implications for the stability of cooperation in the pyoverdine model system, in pathogenic and non-pathogenic environments, in biotechnological applications, and beyond the microbial realm.

Introduction

Cooperative behaviors that provide a collective benefit abound across all domains of life, from animals to bacteria (Nowak and Sigmund, 1998; West, Diggle, *et al.*, 2007). Yet, their evolution and maintenance is difficult to explain given that non-contributing cheaters may reap the benefits of cooperation without incurring the costs (Hardin, 1968; West, Griffin, *et al.*, 2007; Rankin *et al.*, 2007). Primarily based on studies with animals, several behavioral and ecological factors have been proposed that can provide either direct or indirect benefits to cooperators (Lehmann and Keller, 2006; West, Griffin, *et al.*, 2007). Microbial cooperative behaviors, including cell-cell communication, nutrient acquisition, virulence and biofilm formation, have gained popularity as tractable model systems to experimentally test these factors within existing evolutionary theory (Nadell *et*

al., 2008; Schuster *et al.*, 2013). However, relatively little attention has been given to the costs and benefits of these behaviors in the context of microbial growth physiology. An important ecophysiological parameter that varies widely in nature is resource limitation (Harder and Dijkhuizen, 1983; Hall and Colegrave, 2007; Moore *et al.*, 2013). It has been argued that nutrient limitation generally affects cooperative behavior by increasing its costs, because resources must be diverted away from growth into cooperative functions (Buckling *et al.*, 2007). Recent work on cooperative secretion in the bacterial pathogen *Pseudomonas aeruginosa* indicates, however, that regulation in response to specific nutrient conditions can minimize these costs (Xavier *et al.*, 2011; Mellbye and Schuster, 2014). In a regulatory mechanism termed metabolic prudence, a carbon-rich surfactant is produced only when nitrogen is depleted from the growth medium and carbon is in relative excess, preventing non-producing strains from gaining an advantage (Xavier *et al.*, 2011).

Here we investigate the effects of nutrient limitation in one of the most prominent microbial models of cooperative behavior, iron acquisition via diffusible pyoverdine (PVD) molecules in *P. aeruginosa* (Buckling *et al.*, 2007). PVDs represent a class of non-ribosomal peptide siderophores that chelate iron with high affinity and are produced when iron levels are low (Visca *et al.*, 2007; Cornelis *et al.*, 2009; Schalk and Guillon, 2013) (Fig. 2.1A). Iron, an important micronutrient, is often scarce in the environment due to the formation of insoluble oxides under aerobic conditions, chelation by host proteins during infections, or scavenging by competing microbes (Ratledge and Dover, 2000; Caza and Kronstad, 2013). Siderophore production qualifies as a cooperative trait. As shown in numerous co-culturing studies, PVD molecules can be shared within a population of cells, benefitting cells other than the focal producer (Griffin *et al.*, 2004; Harrison *et al.*, 2006; Ross-Gillespie *et al.*, 2007; Ross-Gillespie *et al.*, 2009; R. Kümmerli *et al.*, 2009; Rolf Kümmerli, Gardner, *et al.*, 2009; Rolf Kümmerli, Griffin, *et al.*, 2009; Jiricny *et al.*, 2010; Kümmerli *et al.*, 2010). However, the growth advantage of non-producers compared with producers varies among strain pairs, is often marginal, and has only been investigated in complex medium. Consequently, the conditions that may select for the PVD-deficient variants commonly observed in infections and other

environments remain unclear (De Vos *et al.*, 2001; Cordero *et al.*, 2012; Andersen *et al.*, 2015).

We use a whole genome metabolic model paired with controlled *in vitro* evolution experiments to explore the relationship between the fitness cost of PVD production and the type of nutrient limitation. Modeling reveals two contrasting outcomes: PVD is costly when the limiting nutrient is a building block of PVD, such as carbon (C) or nitrogen (N), suggesting invasion of PVD-producers by non-producers. In contrast, PVD is not costly when other nutrients such as iron (Fe), phosphorous (P) or sulfur (S) are limiting as the building blocks are in relative excess, suggesting coexistence of PVD-producers and non-producers. We are able to confirm these results with continuous culture chemostats that allow precise adjustment of nutrient availability and require steady production of PVD, but not with batch cultures that have been customary in the field. In sum, we find that it is the intrinsic molecular composition of a secreted product that determines fitness costs and cooperator-cheater dynamics in the context of resource availability. We discuss the significance of this finding for the PVD model system and for social evolution in general.

Results

Metabolic modeling. We initially evaluated the resource-dependent metabolic costs of PVD production *in silico*, using a genome-scale metabolic model of *P. aeruginosa* strain PAO1 (Oberhardt *et al.*, 2008; Oberhardt *et al.*, 2011). This model contains all the basic metabolic pathways in PAO1 but lacks the PVD synthesis reactions. We therefore incorporated all the known biochemical reactions involved in PVD production based on the available literature, and added them to the model (Supplementary Table S2.1). These include accessory reactions, non-ribosomal peptide synthetases, siderophore maturation steps as well as export machinery (Visca *et al.*, 2007; Imperi *et al.*, 2009; Cornelis *et al.*, 2009). In all, 26 high-energy phosphates (~P) are required to produce and secrete 1 molecule of PVD. With PVD concentrations approaching 0.56 g per g of dry weight (DW) in *P. aeruginosa* batch cultures (Barbhaiya and Rao, 1985), we estimated that approximately 15% of the ATP needed to build a bacterial cell is used for PVD production (see Methods). In terms of both biomass and

energy demand, this appears to be a highly costly endeavor. Our model focused on this metabolic aspect and did not separately include synthesis reactions for the PVD biosynthetic enzymes themselves. This was justified as the energy and biomass requirement for the synthesis of the PVD enzymatic machinery is negligible compared with the synthesis of the PVD molecule from building blocks (Table 2.1 and Methods).

Table 2.1. Estimated energetic and biomass requirements for PVD biosynthesis

Category	~P requirement in mmol $(g\ DW)^{-1}$	Biomass requirement in g $(g\ DW)^{-1}$
PVD molecule	11	0.56
PVD biosynthesis machinery	0.26	0.0066

As a second step, we performed flux-balance analysis to model the relationship between bacterial growth and PVD secretion when different nutrients are growth-limiting. We modeled growth and secretion under aerobic conditions, with glucose as the sole C-source and other macronutrients provided as inorganic salts. Assuming a trade-off in resource allocation between cellular biomass production and secretion, we predicted a negative relationship between the two parameters: Increased PVD secretion should reduce biomass production and vice versa. We indeed found this to be the case under C or N-limiting conditions (Fig. 2.1B). This is because C and N are constituents of PVD (Fig. 2.1A), and growth and secretion are therefore competing for the same limiting pool of nutrients. We obtained equivalent results with the alternative C-sources glutamate and succinate (data not shown). In contrast, when we limited Fe, P, or S, secretion did not initially affect biomass production as the building blocks of PVD (C and N) were in relative excess. This held true until a secretion threshold was crossed and C again became the growth rate-limiting nutrient. Beyond this threshold, biomass production decreased because the carbon flux required for PVD production exceeded that necessary for cellular biomass production, at a cellular uptake rate set to the maximum possible value. The relative uptake rates of limiting and non-limiting nutrients are the key determinants in the trade-off between growth and secretion (Supplementary Fig. S2.1).

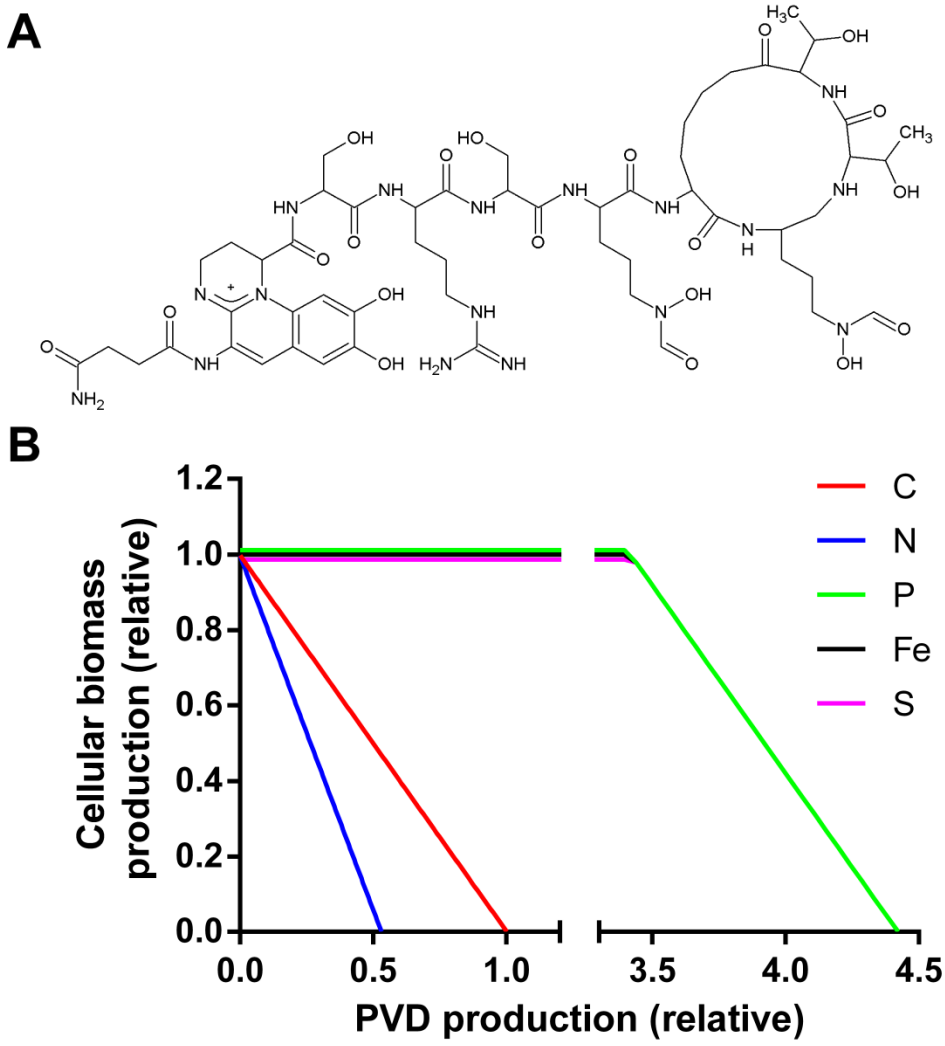

Figure 2.1 Relationship between PVD structure and metabolic cost of secretion. (A) Illustration of the PVD structure (*P. aeruginosa* PAO1 Type I), which is comprised primarily of C and N. (B) Metabolic model. Flux-balance analysis was performed to analyze the trade-off between the levels of cellular biomass production and PVD production. Different nutrient-limiting conditions were achieved by restricting the respective nutrient uptake rates. Graphs for Fe, P, and S-limitation are identical but are offset for visualization purposes.

Further interrogation of our metabolic model revealed that PVD secretion causes the highest flux increases in amino acid biosynthesis pathways that provide the building blocks for PVD peptide synthesis. Under C and N-limitation, this increase depletes the

precursor metabolites required for cellular biomass production. Taken together, we found that fitness cost is not merely a function of the total energetic and biomass requirements, but is also determined by the nature of the growth-rate limiting nutrient. This relationship between nutrient limitation and fitness costs has intriguing implications for the evolutionary stability of siderophore secretion by affecting the dynamics between siderophore-producers (cooperators) and non-producers (cheaters) in a mixed population.

Batch culture growth experiments. To empirically test the predictions of our metabolic model, we sought to compare the fitness of a PVD non-producing strain to a PVD-producing strain when different nutrients limit growth. According to our model, PVD production is most costly when a building block of the siderophore is growth limiting (Fig. 2.1). Hence, a non-producer should enjoy the greatest relative fitness benefit under these conditions. We constructed an isogenic *pvdS* gene (PA2426) deletion mutant in the background of the PAO1 parent that served as a non-producing strain. This gene encodes an alternative sigma factor that regulates transcription of a set of genes required for the synthesis of PVD (Ochsner *et al.*, 2002; Cornelis *et al.*, 2009). The deletion of *pvdS* is ecologically relevant because clinical PVD-deficient *P. aeruginosa* isolates are often mutated in this gene (Smith *et al.*, 2006; Marvig *et al.*, 2014; Andersen *et al.*, 2015).

For growth experiments, we chose to focus on media limited by either C or P; each representing conditions where we predict PVD production to come at a high and low fitness cost, respectively. We started with a defined, synthetic medium derived from Evan's minimal medium (Evans *et al.*, 1970), referred to herein as modified Evan's medium (MEM). MEM was limited by either glucose as the sole C-source (C-MEM) or phosphate as the sole P-source (P-MEM). Both media were supplemented with ethylenediamine-di (o-hydroxyphenylacetic acid) (EDDHA), a strong Fe^{3+} chelator that requires PVD for growth (Ochsner *et al.*, 2002). A second, low-affinity siderophore produced by *P. aeruginosa*, pyochelin, is insufficient for growth in the presence of this chelator. The Fe concentration was set at 1 μM, which is low enough to stimulate PVD production but high enough to not limit the growth yield set by C or P concentrations. We

chose C and P levels as well as cultivation times such that the WT reached virtually identical and saturating final cell densities in both media (Fig. 2.2 and Supplementary Fig. 2.2A). We verified that the intended nutrient was limiting by doubling its concentration and observing a proportional increase in culture density of the WT (Fig. 2.2). The *pvdS* mutant, in contrast, is unable to grow by itself under these conditions and does not produce any PVD (Fig. 2.2 and Supplementary Fig. S2.2). To overcome this growth defect in the pre-cultures used as inocula, we formulated an Fe-replete MEM that allows the mutant to grow as well as the WT (Supplementary Fig. S2.3).

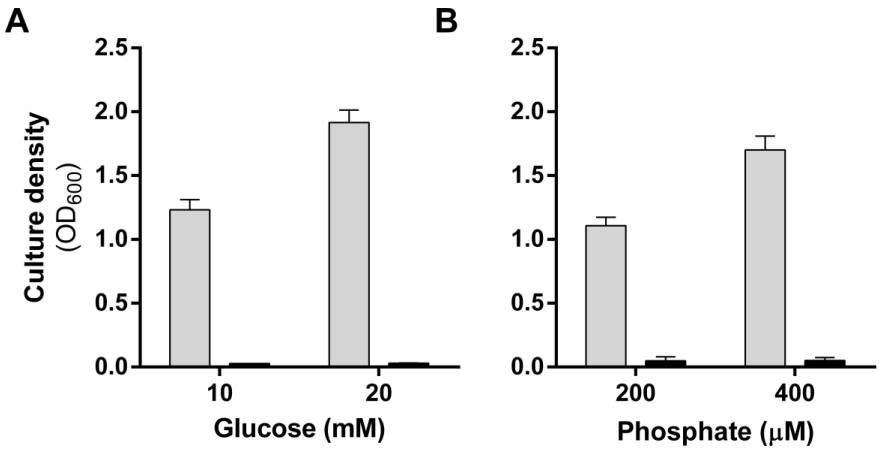

Figure. 2.2 Growth yield of *P. aeruginosa* in low-iron batch cultures. Individual cultures of the WT strain (gray bars) or the *pvdS* mutant (black bars) were grown in MEM for 24 h, and cell densities were measured as optical density at 600 nm (OD_{600}). In panel A, glucose concentrations vary while phosphate is held constant at 10 mM. In panel B, phosphate concentrations vary while glucose is held at 20 mM. The medium also contained 1 μM Fe and 40 μM of the chelator EDDHA that restricted growth of the *pvdS* mutant. Error bars show SEM, n = 3.

We then initiated batch culture competition experiments to compare the fitness of the *pvdS* mutant relative to the WT in C-MEM and P-MEM (Fig. 2.3A). In both cases the frequency of the mutant remained constant throughout the duration of co-culture. The frequency of the mutant also did not change in C-MEM after three additional subcultures (relative fitness $w = 1.07 \pm 0.06$ after 25 generations; no significant difference from 1 by one-sample t-test, $p = 0.33$). This shows that the *pvdS* mutant is indeed capable of utilizing the PVD produced by the WT, but it does not enjoy a relative growth advantage, regardless of the limiting nutrient. This result was similar to a variety of co-culturing

experiments we had conducted (Supplementary text, Supplementary Fig. S2.4 and Supplementary Table S2.2), which included conditions similar to those used in published studies (Griffin *et al.*, 2004; Ross-Gillespie *et al.*, 2007; R. Kümmerli *et al.*, 2009; Harrison and Buckling, 2009; Rolf Kümmerli, Griffin, *et al.*, 2009; Jiricny *et al.*, 2010; Kümmerli and Brown, 2010; Zhang and Rainey, 2013; Kümmerli and Ross-Gillespie, 2014). Collectively, we found that PVD non-producers grow at equal rates, but never faster, than the WT. This finding is inconsistent with the notion that non-producing cheater mutants can invade a producing population by avoiding the cost of cooperation, at least under the conditions explored thus far.

These results led us to carefully reconsider the use of a batch culture format, which has inherent limitations regardless of the media type used. Batch cultures are frequently used for the growth of microorganisms due to their low cost and ease of operation. However, the boom-bust pattern of growth alters the media composition over time, causing changes in the growth-rate limiting nutrient and causing accumulation of secreted metabolites, including PVD itself (Gresham and Dunham, 2014). This dynamic growth environment of batch cultures and consequently, the changing selective pressures experienced by bacterial populations, led us to pursue an alternative culturing approach with a higher degree of control.

Chemostat culture experiments. We eliminated the uncertainties associated with batch culture by turning to a chemostat format, an open system where fresh nutrients continuously displace spent medium. In this system, both cell density and growth rate are held constant, as determined by the concentration of the growth-rate limiting nutrient and the flow rate of the growth medium, respectively (Evans *et al.*, 1970). Furthermore, chemostat culturing ensures continuous PVD production from the WT, as the constant flow of medium limits PVD accumulation. Using this approach, we reasoned that the fitness cost associated with PVD production in relation to the limiting nutrient could be more clearly resolved. We again set out to compare the fitness of the *pvdS* mutant relative to the WT in C-MEM and P-MEM. Chemostats were operated at a dilution rate of 0.2 h^{-1} (corresponding to a generation time of 3.5 h), and sampled daily to determine strain frequencies and PVD concentrations.

We found that the *pvdS* mutant did indeed enjoy a significant relative fitness advantage in C-MEM, but not in P-MEM (Fig. 2.3B). This finding confirmed our prediction that the fitness cost of PVD production is contingent on the limiting nutrient. Importantly, we found that PVD secretion levels were comparable in both growth media, excluding the possibility that observed differences in relative fitness are merely a function of secretion activity (Fig. 2.3C). The measured PVD levels are somewhat lower than those cited in Table 1, but are still predicted to incur costs that are substantially above those for PVD synthesis machinery.

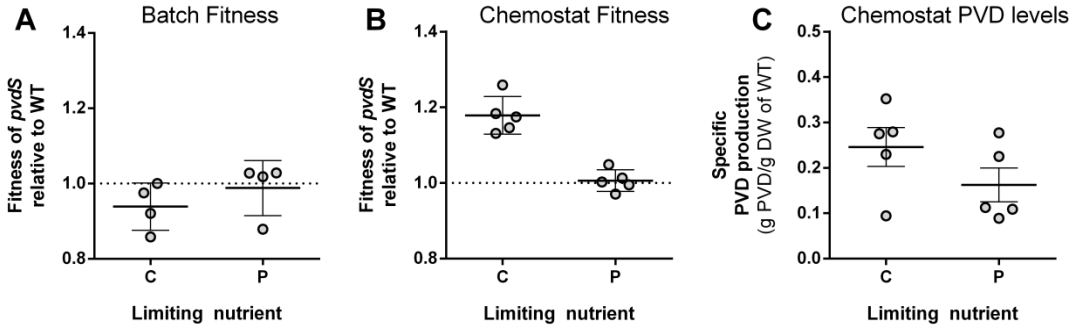

Figure 2.3 Fitness costs of PVD production according to growth-limiting nutrient and culturing format. (A, B) Relative fitness of the *P. aeruginosa pvdS* mutant in (A) batch culture and in (B) chemostat culture. Co-cultures of the WT and the *pvdS* mutant were initiated at a 1:1 ratio in either C-MEM or P-MEM. The duration of growth was 24 h in batch and 6 days in chemostat culture. Relative fitness *w* was calculated as the ratio of average growth rates, considering initial and final strain frequencies ($w > 1$ indicates an increase in mutant frequency, $w < 1$ indicates a decrease in mutant frequency, and $w = 0$ indicates no change in mutant frequency over time). Relative fitness is significantly different from 1 only in C-MEM chemostat culture, but not in C-MEM batch, P-MEM batch, and in P-MEM chemostat cultures (one-sample t-test; $p = 0.0013$, 0.15, 0.77, and 0.65, respectively). Relative fitness in C-MEM is significantly different than in P-MEM in chemostat culture but not in batch culture (two-sample t-test, $p = 0.00010$ and 0.34, respectively). (C) Specific PVD production levels in chemostat culture. Shown are the average PVD concentrations produced by the WT subpopulation over time. PVD levels in C-MEM were not significantly different than in P-MEM (two-sample t-test, $p = 0.18$). Each individual data point represents a separate biological replicate. Error bars indicate SEM.

The growth advantage of the *pvdS* mutant led to rapid invasion of the population, approaching an apparent equilibrium at a *pvdS* mutant frequency of ~95 % (Fig. 2.4B). The very high cheater tolerance in the C-limited chemostat without any reduction in total

cell density is interesting (Fig. 2.4A). One would expect a wash-out or population collapse to occur whenever the cheater burden exceeds the carrying capacity of the population (West *et al.*, 2006; Dandekar *et al.*, 2012). The mechanism that stabilizes cooperation is not currently clear, but it is notable that the decrease in cheater fitness correlates with a decrease in the total PVD concentration present in the chemostat (Fig. 2.4B). This substantial decrease in initially excessive PVD levels reduces Fe availability and hence could cause a change such that the limiting nutrient is no longer C but is Fe. Fe limitation, as predicted by modeling above, would again stabilize PVD cooperation.

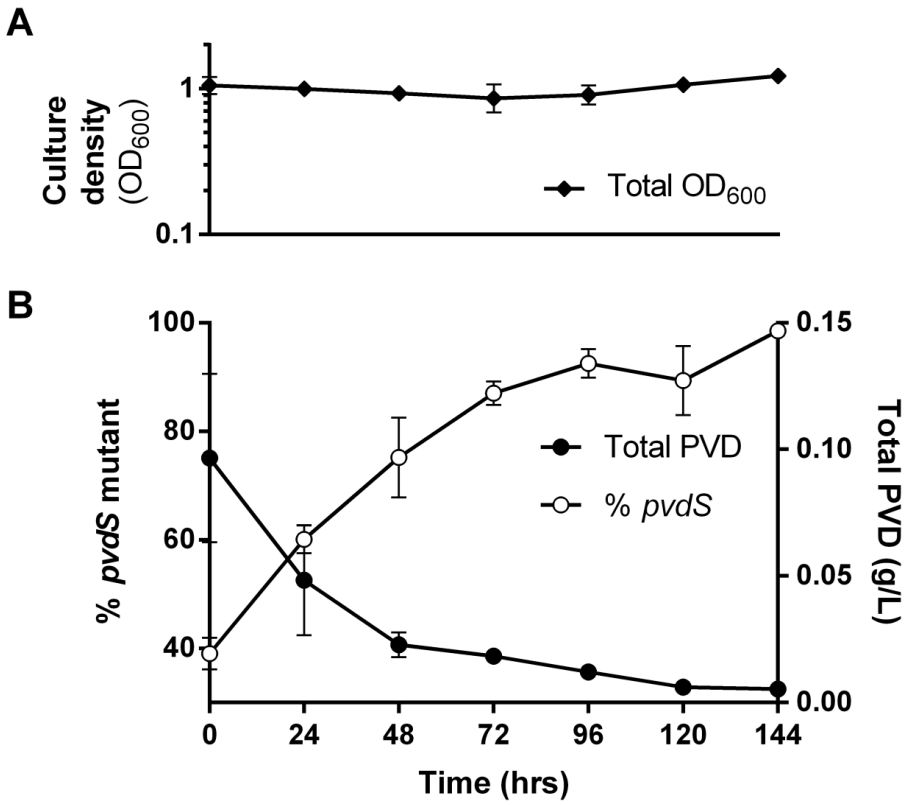

Figure 2.4 Change in population density, frequency and PVD concentration during C-limited chemostat culture. (A) Total population density. (B) Proportion of the *pvdS* mutant in WT co-culture, and total concentration of PVD in the chemostat over time. Co-cultures of WT and *pvdS* mutant were initiated in C-MEM at the indicated ratio. Error bars indicate SEM.

In order to relate experimental data to those from our metabolic model, we further determined growth and PVD secretion rates during the *pvdS* mutant enrichment phase in

C-limited conditions (up to 72 h of culturing), based on the measured dynamics of subpopulation densities and PVD concentrations. The growth rates of the WT and *pvdS* mutant are 0.181 ± 0.003 h^{-1} and 0.210 ± 0.002 h^{-1}, respectively, yielding a 13.8% reduction in growth attributable to PVD secretion. The PVD secretion rate of the WT is 0.044 ± 0.011 g (g DW h)$^{-1}$. Reinterrogating our metabolic model, we find that a PVD secretion rate of this magnitude reduces the growth rate from 0.210 h^{-1} to 0.184 h^{-1} under C-limitation, amounting to a 12.4% reduction. Thus, there is very good agreement between the two approaches.

Discussion

PVD production is one of the main microbial models for the evolution of cooperation. Because the costs of cooperation are an important determinant for its evolutionary stability, a detailed understanding of the environmental and physiological conditions that affect these costs is critical. Cost-benefit considerations seem particularly important in shaping the evolution of cooperative secretions that are lost to the environment (Smith and Chapman, 2010; Pai *et al.*, 2012; Gupta and Schuster, 2013).

In this study, we combined metabolic modeling with defined culturing experiments to demonstrate that the growth-limiting nutrient profoundly impacts the fitness costs and stability of PVD secretion in *P. aeruginosa*. When cell growth is limited by P, S or Fe, PVD production does not translate into a fitness costs because the resources needed to make the siderophore are in relative excess. In contrast, when C or N is growth-limiting, PVD production competes with cellular biomass synthesis for the same limited resource, resulting in a significant fitness cost. We experimentally verified our modeling predictions with a chemostat system. PVD production came at a fitness cost and allowed invasion of non-producing cheaters when C but not P was limiting, despite similar PVD secretion levels (Fig. 2.3B and C).

It is considered an established principle in microbial physiology that cells tightly couple biomass yield with ATP generation when limited by the C and energy source (Russell and Cook, 1995). In contrast, when limited by a nutrient other than C and energy source, cells tend to redirect the non-limiting cellular C flux to other functions, including

secretion (Harder and Dijkhuizen, 1983; Russell and Cook, 1995). Our results indicate that when secretion is nevertheless required under C limitation, a trade-off in nutrient allocation between growth and secretion is inevitable. P-limiting conditions in particular have been associated with low levels of phosphorylated compounds, including ATP (Dauner *et al.*, 2001; Boer *et al.*, 2010). In our case, however, ATP did not appear to be the growth-limiting intracellular metabolite because PVD production, along with its ATP demand, did not result in a growth disadvantage of producers compared with non-producers.

Furthermore, we found that PVD-producers are able to sustain a very high "cheater-load" of non-producers at an apparent equilibrium frequency in C-limited chemostat co-culture. This result is remarkable. In a well-mixed environment without assortment, a costly cooperative behavior should not be evolutionarily stable (Hardin, 1968; West, Griffin, *et al.*, 2007; Rankin *et al.*, 2007). Non-producing cheaters are expected to invade a population of cooperators and cause its collapse. We envision two explanations for our observation. First, as mentioned above, decreasing PVD levels over time could change growth conditions from C-limited to *de-facto* Fe-limited. Under these new conditions, PVD secretion would incur no costs as C and N are in relative excess. Second, *P. aeruginosa* PVD may not be a fully secreted product but may instead be partially retained by the producing cell(Yeterian *et al.*, 2010; Scholz and Greenberg, 2015). This property would be of increased significance at low producer frequencies when extracellular, secreted PVD levels available to non-producers are also low. In fact, retaining as little as 1% of a secreted product can favor cooperation in a way that leads to an equilibrium between producers and non-producers (Gore *et al.*, 2009).

Our findings have important implications for the use of PVD cooperation as a microbial model system for social evolution. The C-limited chemostat proved to be a unique condition where the non-producer had a fitness advantage and was able to invade a PVD-producing population, contrasting the P-limited chemostat and a wide collection of culturing permutations we explored in a batch culture format (Fig. 2.3A, Supplementary Fig. S2.4 and Supplementary Table S2.2). After comparing our findings with previous studies, we are led to conclude that the use of undefined media in a batch

culture format, an approach thematic to published literature, does not provide a consistent selective advantage for non-producers: Cheater invasion (i.e. a relative fitness > 1) is observed in some cases but is often marginal, and is less pronounced with isogenic than with non-isogenic strain pairs (see Supplementary text)(Griffin *et al.*, 2004; Ross-Gillespie *et al.*, 2007; R. Kümmerli *et al.*, 2009; Rolf Kümmerli, Gardner, *et al.*, 2009; Harrison and Buckling, 2009; Rolf Kümmerli, Griffin, *et al.*, 2009; Jiricny *et al.*, 2010; Kümmerli and Brown, 2010).

A first step we have taken here towards clearly defining growth conditions was the use of a synthetic medium. Heated debates have emerged in recent years regarding the selective conditions created by CAA-based medium, as well as another commonly used undefined medium known as King's B (Zhang and Rainey, 2013; Kümmerli and Ross-Gillespie, 2014). This dispute challenges the interpretation of an entire collection of social studies on siderophores. Exacerbating this issue further, distinct PVD phenotypes have been observed in CAA preparations originating from different manufactures, suggesting efforts to characterize the attributes of this media may be chasing a moving target (Kümmerli and Ross-Gillespie, 2014).

A second step we have taken was the use of a continuous-culture chemostat system. As we demonstrated, the relationship between the limiting nutrient and the fitness cost of PVD production was obscured in our batch culture experiments (Fig. 2.3A). There are two plausible explanations for this. The first relates to the dynamic changes in media composition due to the influence of bacterial growth physiology (Gresham and Dunham, 2014). This fact is relevant in our context, as we could only confirm the intended limiting nutrient was the first to be depleted (Fig. 2.2). It is likely that Fe is the limiting nutrient early in growth, as *de-novo* PVD production is required to scavenge iron from the strong chelator EDDHA. The second explanation considers the ability of *Pseudomonas* to recycle PVD and adapt its phenotype accordingly. Indeed, after Fe is unloaded into the periplasm, PVD is returned to the extracellular environment and can be reused many times (Imperi *et al.*, 2009). As PVD accumulates, the producing strain reduces costs by suppressing PVD biosynthesis and benefits from the PVD produced by previous generations. This intrinsic property has been suggested to affect the evolutionary stability

of PVD cooperation (Kümmerli and Brown, 2010). Although both explanations have merit, the very nature of the batch culture format makes it difficult to distinguish the two. Our continuous-culture approach avoids these uncertainties as it provides the ability to hold a known selective pressure constant, a feature that is desirable for experimental evolution studies in general (Gresham and Dunham, 2014).

Distinguishing the conditions that select for secretion deficiency or instead stabilize secretion remains a challenging yet important goal. Microbial secretions have an important role in natural microbial communities, in pathogenesis and agriculture, in biotechnological applications, and in antimicrobial intervention (Baron, 2010; Cornforth and Foster, 2013; Green and Mecsas, 2016; Saha *et al.*, 2016). Medical relevance is apparent in the chronic lung infections of cystic fibrosis patients, where secretion-deficient strains of *P. aeruginosa* are consistently isolated (De Vos *et al.*, 2001; Smith *et al.*, 2006; Andersen *et al.*, 2015). Recent evidence suggests that PVD-negative strains evolved as social cheaters, because they tend to retain their PVD receptor when cross-feeding on a co-infecting PVD-producing is possible (Andersen *et al.*, 2015). However, our data indicate that the ability to cross-feed is not alone sufficient to conclude that non-producers have a fitness advantage, even when siderophores are required for growth (Fig. 2.3, Supplementary Fig. S2.4 and Supplementary Table S2.2). This highlights the challenges to understanding social dynamics in natural environments and emphasizes the need to better characterize the selective pressures in a given context.

The principles we have demonstrated *in vitro* provide a framework to consider the evolutionary origin of secretion-deficient isolates observed in natural environments. By pairing knowledge about the composition of a given secreted product with local resource availability, general predictions can be made. This approach can be illustrated by considering marine ecosystems, where many strains have been isolated that require siderophores for growth but do not produce them (D'Onofrio *et al.*, 2010; Cordero *et al.*, 2012). Our findings suggest peptide siderophores should be particularly costly when N is limiting, which is often characteristic of low latitude surface waters with minimal nutrient inputs (Moore *et al.*, 2013). In contrast, Fe can be limiting in sub-surface waters when upwelling or other sources increase nutrient concentrations beyond what can be fixed

from the atmosphere (Moore *et al.*, 2013). Here production may come at little to no cost, due to the relative excess of carbon and nitrogen. Other features which impact the stability of production, such as spatial structure and siderophore durability, should not be neglected in aquatic environments, even though they are expected to play stronger roles in highly structured environments, such as in soil for example (Nadell *et al.*, 2016). The principle of nutrient-dependent fitness costs can be used in an analogous fashion to devise culture conditions that stabilize the production of secreted enzymes or metabolites in biotechnological applications.

Taken together, our results exemplify how the relationship between resource availability and the molecular properties of the secreted product itself impact the stability of cooperation. The limiting resource is likely to impact the stability of many social behaviors that involve shared products, generally referred to as public goods. In *P. aeruginosa*, it has already been shown that quorum-sensing dependent secretions are "prudently" regulated in a way that ensures sufficient supply of building blocks(Xavier *et al.*, 2011; Mellbye and Schuster, 2014). This suggests that the regulatory network has adapted to minimize the fitness cost of public goods production by responding to the available resources. Although we did not focus our study on the regulation of PVD expression, it is known that production is stimulated when environmental Fe concentrations are low (Cornelis *et al.*, 2009). This alone may be sufficient in many cases to prevent cheaters, namely if Fe levels are so low that they are growth-limiting. Consequently, the PVD building blocks C and N are in relative excess such that PVD production comes at no cost. In general, our work highlights the importance of ecophysiological context for the evolution and maintenance of cooperative behavior. Fitness costs may vary more widely and social interactions may be more dynamic than currently appreciated.

Methods

Metabolic model. For flux-balance analysis, we used the whole-genome metabolic model of *P. aeruginosa*, iMO1086 (Oberhardt *et al.*, 2008; Oberhardt *et al.*, 2011). PVD synthesis reactions were added to the metabolic model as described in

Supplemental Table S2.1. All computations were performed with the COBRA toolbox in Matlab (version R2013b, Mathworks, Natick MA) (Becker *et al.*, 2007). To assess the trade-off between growth (i.e. cellular biomass production) and PVD secretion as shown in Fig. 2.1B, we performed a robustness analysis that calculates the growth rate as a function of the PVD secretion rate. C, N, P, S, or Fe limitation was achieved by constraining the respective nutrient uptake rate such that the resulting growth rate in the absence of any PVD secretion is identical to the experimental value of 0.2 h^{-1}. The uptake rates of the non-limiting nutrients remained effectively unconstrained, with the exception of the C (glucose) uptake rate which was set to the maximally possible rate of 12 mmol $(g\ DW\ h)^{-1}$, as experimentally determined (Jain and Srivastava, 2009). For graphing, the growth rate in the absence of secretion (0.2 h^{-1}) and the PVD secretion rate that yields zero growth under C-limitation (0.25 mmol $[g\ DW\ h]^{-1}$, equal to 0.38 g $[g\ DW]^{-1}$) were normalized to one. Different, physiologically relevant C-sources (Mellbye and Schuster, 2014) were tested by constraining the uptake rates for glutamate or succinate instead of glucose.

To examine the effect of PVD secretion on the relative reduction in growth rate under a range of different C and P levels, we decreased the respective uptake rates in two-fold increments, starting with the rates that permit maximal growth in the absence of PVD secretion (C uptake rate of 12 mmol $[g\ DW\ h]^{-1}$ and P uptake rate of 0.8 mmol $[g\ DW\ h]^{-1}$).

To investigate the metabolic basis for the trade-off between growth and secretion, we determined the ratios of reaction fluxes in the presence vs. the absence of PVD secretion (growth rate of 0.2 h^{-1} and PVD secretion rate of 0.05 mmol $(g\ DW\ h)^{-1}$, equal to 0.068 g $(g\ DW^{-1})$, and sorted them by magnitude.

Estimation of energetic and biomass requirements for PVD production. We estimated the requirements for PVD biosynthesis, as presented in the main text, in terms of high-energy phosphates (mol ~P per g DW) (Neidhardt *et al.*, 1990) and in terms of biomass (g PVD per g DW). We separately considered PVD molecule biosynthesis, and manufacturing of the PVD synthesis machinery. We estimated energetic requirements from building blocks, and we assumed that the requirements of cellular synthesis in *P.*

aeruginosa are similar to those in *E. coli*, for which most values have been determined (Farmer and Jones, 1976). In minimal medium with good aeration, 1 g of culture produces 0.56 g of PVD, equal to 0.41 mmol (*M*r = 1350 for PVD Type I) (Barbhaiya and Rao, 1985). To estimate the energetic requirement for PVD molecule synthesis from building blocks, we considered that, according to our calculation, 1 molecule PVD demands 26 ~P. The energetic requirement is then 0.41 mmol PVD $(g\ DW)^{-1}$ x 26 mol ~P $(mol\ PVD)^{-1}$ = 11 mmol ~P $(g\ DW)^{-1}$.

To approximate the requirement of building the PVD synthesis machinery, we considered that the energy demand for the production of total protein in 1 g of cells is 22 mmol ~P $(g\ DW)^{-1}$ (Neidhardt *et al.*, 1990). Without any information about expression levels of PVD machinery, we assumed that the contribution of PVD protein biosynthesis to total protein biosynthesis is equal to the length of the coding sequence for annotated PVD biosynthesis genes (69,729 bp) in relation to the length of the entire coding sequence in the *P. aeruginosa* genome (90% of the total 6.26 Mbp sequence) (Dumas *et al.*, 2013; Toll-Riera *et al.*, 2016). We could then estimate that the requirement for the PVD synthesis machinery is 22 mmol ~P $(g\ DW)^{-1}$ x 1.2% = 0.26 mmol ~P $(g\ DW)^{-1}$. We further related these results to total cellular biosynthesis, which requires 72 mmol ~P to generate 1 g DW of *E. coli* cells under aerobic conditions, in minimal medium with glucose as the sole C-source (Farmer and Jones, 1976). We finally estimated the biomass requirement for the PVD biosynthesis machinery. Given that about 55% of cell dry weight is protein (Neidhardt *et al.*, 1990), the respective biomass requirement is 1 g DW x 55% $(g\ DW)^{-1}$ x 1.2% = 6.6 mg $(g\ DW)^{-1}$.

Bacterial strains and growth media. We used the PVD-producing *P. aeruginosa* WT strain PAO1 (ATCC 15692) and a derived, non-producing *pvdS* in-frame deletion mutant, which was constructed in the same genetic background by splicing-by-overlap-extension PCR and allelic exchange as described (Horton, 1995). The *pvdS* gene deletion was generated using 5'-N_6<u>GAGCTC</u>GACATCGTTTTCGGCGGGCGGG-3' and 5'-N_6<u>TCTAGA</u>GATGCTGGCGCGCTCGGGCATCCAG-3' as flanking primers and 5'-TTCCGACATGGAAATCACCTTGCTGCGGAG-3' and 5'-AGCAAGGTGATTTCCATGTCGGAAGCCCGCCGCTGACGGCGGCGAGCATTCC

TCA-3' as overlapping internal primers. Restriction enzyme sites (*Sac*I and *Xba*I, respectively) for cloning into an allelic exchange vector are underlined.

Cultures were routinely maintained in Lennox LB liquid medium or on Lennox LB agar plates at 37 °C. The synthetic minimal medium used for batch culture and chemostat experiments is a modification of Evan's minimal medium (MEM) (Evans *et al.*, 1970). The base salt composition is 10 mM KCl, 1.25 mM $MgCl_2 \cdot 6H_2O$, 50 mM NH_4Cl, 2 mM Na_2SO_4, $CaCl_2 \cdot 2H_2O$, 50 mM 3-(N-morpholino) propanesulfonic acid (pH = 7), 10 µM ZnO, 20 µM $MnCl_2 \cdot 4\ H_2O$, 2 µM $CuCl_2 \cdot 2H_2O$, 4 µM $CoCl_2 \cdot 6H_2O$, 2 µM H_3BO_3, 33 nM $Na_2MoO_4 \cdot 2H_20$, 1 µM $FeCl_3 \cdot 6H_2O$. Fe was chelated by adding 40 µM EDDHA. C-MEM had 10 mM D-glucose and 10 mM NaH_2PO_4. P-MEM had 20 mM D-glucose and 200 µM NaH_2PO_4. Before initiating experiments in C-MEM or P-MEM, single colonies were used to inoculate an unchelated, Fe-replete medium of otherwise identical salt composition with 20 mM D-glucose, 10 mM NaH_2PO_4 and 50 µM $FeCl_3 \cdot 6H_2O$. This provided a culturing medium in which both the WT and the *pvdS* mutant could grow independently. Cells were washed twice in MEM lacking EDDHA, D-glucose, NaH_2PO_4 and $FeCl_3 \cdot 6H_2O$ before sub-culturing into C-MEM or P-MEM. Culture densities were routinely monitored by culture optical density at 600 nm (OD_{600}).

Batch culture experiments. Batch cultures were grown at 37 °C with shaking. To demonstrate the growth-limiting nutrient, mono-culture growth experiments with WT and *pvdS* mutant were performed in MEM with varying glucose or phosphate concentrations. Cultures were inoculated at an OD_{600} of 0.01. Growth was measured as OD_{600} after 24 h of cultivation. For time courses, growth and PVD production were measured in 6 h intervals. For co-culture competitions, the WT and *pvdS* mutant were mixed to 1:1 ratios and diluted to an OD_{600} of 0.01 in either C-MEM or P-MEM. Cultures were sampled at 0 and 24 h to measure strain frequencies and calculate fitness values for each of the four biological replicates. In the case of successive subculturing, C-MEM co-cultures were diluted into fresh medium and incubated again for 24 h, for a total of four growth cycles.

Chemostat operation. Chemostats were built in-house as described previously, with minor modifications[14]. They were operated at 37 °C, well aerated, stirred, and

maintained at volumes of 100 ml. Cultures of the WT and *pvdS* mutant were mixed to 1:1 ratios, inoculated to an OD_{600} of 0.05 and grown in batch mode until reaching an OD_{600} of 1 in late exponential phase. At this point, chemostat mode was initiated. Fresh culture medium was pumped into the culture vessel at a dilution rate (D) of 0.2 h^{-1} using a peristaltic pump. Chemostats were sampled every 24 h to determine culture densities, PVD concentrations and frequencies of strain populations. A total of five biological replicates were performed.

Strain frequencies and relative fitness. The relative frequencies of WT and *pvdS* mutant sub-populations were distinguished by patching 100 randomly selected colonies onto King's B agar, which stimulates production of PVD (King *et al.*, 1954). Strains were identified as PVD-producers or non-producers based on a distinct green or white phenotype, respectively (King *et al.*, 1954). Relative fitness (*w*) of non-producers was subsequently calculated as the ratio of average growth rates or Malthusian parameters (μ_{pvdS}/μ_{WT}) as described (Lenski, 1991). Calculation of the average growth rate μ for each sub-population considers the initial and final sub-population densities N_0 and N_1, respectively, and the culturing time t. For batch cultures, $\mu = \ln(N_1/N_0)/t$ (with t = 24 h), and for chemostat cultures, $\mu = \ln(N_1/N_0)/t + D$, which considers the dilution rate (with t = 144 h).

Specific PVD production. PVD concentrations were estimated from culture supernatants. Relative fluorescence units (excitation and emission wavelengths of 400 and 460 nm, respectively) were measured with a TECAN Infinite 200 plate reader (Tecan Group Ltd, Männedorf, Switzerland). PVD concentrations were interpolated from a standard curve generated with purified PVD_{PAO1} (EMC Micro-collections, Tübingen, Germany). To obtain a specific PVD concentration, values were divided by the subpopulation density of the PVD-producing WT measured at the same time point. The specific PVD concentration is expressed as g per g DW of WT. Dry weight of cells was quantified by operating dedicated chemostats under conditions identical to those used for population and PVD measurements. This approach avoided perturbations from the withdrawal of large sample volumes needed for dry weight measurements. Based on these measurements, an OD-to-dry weight conversion factor was calculated (OD_{600} of 1

equals 0.48 g DW/l). For each biological replicate, specific PVD production values were determined at 24 h intervals. Data presented show the average specific PVD production level for each replicate.

Quantitative comparison of metabolic model and chemostat experiment. As a first step, we determined specific growth and PVD secretion rates in the C-limited chemostat, only considering the *pvdS* mutant enrichment phase (0 to 72 h) before an equilibrium was reached. A growth rate μ for the WT and *pvdS* mutant subpopulations was determined by fitting replicate time courses of subpopulation densities to a standard growth rate equation of the form $N_t = N_0 e^{(\mu-D)t}$ using linear regression. N_t and N_0 denote subpopulation densities at time t and at time zero, respectively. A PVD secretion rate q was determined by fitting replicate time courses of PVD concentrations to a model that considers the change in PVD concentrations and the WT growth rate during the *pvdS* mutant enrichment phase. Changes in the PVD concentrations over time are given by the differential equation $dPVD/dt = q\ N_t - D\ PVD_t$. Integration and incorporation of the growth rate equation yields $PVD_t = (PVD_0 - N_0\ q/\mu_{WT})\ e^{-D\ t} + N_0\ q/\mu_{WT}\ e^{-(\mu-D)\ t}$, with PVD_t as PVD concentrations at time t and PVD_0 as initial PVD concentration. Graphpad Prism software was used for linear and non-linear regression analysis. Rates μ and q are reported with SEM in the main text.

In a second step, we matched empirical data to modeling data. In the model, we set the C uptake rate such that the growth rate, in the absence of any secretion, is identical to the experimentally determined growth rate of the *pvdS* mutant. Next, we modeled PVD secretion under C-limiting conditions at the experimentally determined PVD secretion rate of the WT, and we determined the corresponding reduction in growth rate.

Supporting information

SI Results and discussion

PVD production is immune to cheater invasion in a wide variety of batch culture conditions. In the main text, we report that the *pvdS* mutant has a relative fitness equal to, but not greater than, 1 when co-cultured with the WT in C-MEM and P-MEM batch cultures (Fig. 2.3A). This outcome was strikingly similar to a collection of related co-culture experiments we had conducted using growth conditions modeled after previous studies. Generally, the experimental approach entails batch cultures with casamino acids (CAA) medium (Griffin *et al.*, 2004; Ross-Gillespie *et al.*, 2007; Ross-Gillespie *et al.*, 2009; R. Kümmerli *et al.*, 2009; Rolf Kümmerli, Gardner, *et al.*, 2009; Rolf Kümmerli, Griffin, *et al.*, 2009; Jiricny *et al.*, 2010; Kümmerli and Brown, 2010). CAA are derived from hydrolyzed casein protein, providing a mixture of carbon and nitrogen in the form of amino acids and small peptides. We present our culturing data in Supplementary Fig. S2.4 and associated Supplementary Table S2.2, where the relative fitness of non-producing strains was measured in a total of 17 different permutations.

Within this data set, we manipulated variables that could plausibly impact the relative fitness of a non-producer. Some variables tested are specifically predicted to impact the stability of cooperation, such as starting population density and initial mutant frequency (West *et al.*, 2006; Ross-Gillespie *et al.*, 2007; Ross-Gillespie *et al.*, 2009; Darch *et al.*, 2012). Others were manipulated to exactly reflect conditions in other studies, such as the temperature, iron chelator of choice, and whether cultures were incubated statically or with shaking (Rolf Kümmerli, Gardner, *et al.*, 2009; Rolf Kümmerli, Griffin, *et al.*, 2009; Kümmerli and Brown, 2010). We also carefully considered the specific genetic mutations conferring the non-producer phenotype, and explored several different defined non-producer/producer strain pairs. A few permutations also contained glucose, succinate and glutamate as alternative C sources. However, we collectively found that these variations had little influence, as the relative fitness of non-producers was always equal to or below 1 (Supplementary Fig. S2.4 and Supplementary Table 2.2).

We found this outcome to be intriguing. Although non-producers could restore their individual growth by utilizing the PVD secreted by the WT, they did not have a selective advantage. These results began to question the social cheating hypothesis as an explanation for the evolution of PVD-negative isolates observed in nature. Furthermore, our findings appear to contrast previous descriptions of social cheating which use conditions similar or even identical to those we explored (Supplementary Fig. S2.4 and Supplementary Table S2.2) (Griffin *et al.*, 2004; Ross-Gillespie *et al.*, 2007; R. Kümmerli *et al.*, 2009; Rolf Kümmerli, Gardner, *et al.*, 2009; Rolf Kümmerli, Griffin, *et al.*, 2009; Jiricny *et al.*, 2010; Kümmerli and Brown, 2010; Darch *et al.*, 2012). Although it is not entirely clear how to reconcile our results with the previous literature, we believe that two experimental design choices in particular can at least partially explain this discrepancy.

The first such design choice is the use of non-isogenic PVD-producer/non-producer strain pairs that differ by mutations other than that conferring the PVD phenotype. In fact, many studies, including some of the first and most influential reports of social cheating, used such strains (Griffin *et al.*, 2004; Ross-Gillespie *et al.*, 2007; Brockhurst *et al.*, 2008; Jiricny *et al.*, 2010; Kümmerli *et al.*, 2010; Kümmerli and Brown, 2010; Darch *et al.*, 2012). A prominent strain pair used was *P. aeruginosa* PAO1, a PVD-producer, and PAO6609, a PVD-deficient mutant derived by UV-mutagenesis (Griffin *et al.*, 2004). PAO6609 carries at least four mutations, *met-9011, amiE200, strA,* and *pvd9*, compared to the PAO1 parent strain. These mutations, uncharacterized by sequence analysis, confer methionine auxotrophy, amidase-deficiency and streptomycin-resistance, in addition to PVD deficiency (Rella *et al.*, 1985; Meyer *et al.*, 1996).

We note that the use of non-isogenic or undefined strains does not by definition negate these studies. However, it complicates the process of attributing an observed fitness outcome to the PVD phenotype, as one cannot exclude the possibility that other, possibly unknown mutations contribute to the results. Fortunately, a number of studies have been published that also employ isogenic producer/non-producer pairs (Ross-Gillespie *et al.*, 2007; Ross-Gillespie *et al.*, 2009; Jiricny *et al.*, 2010; Kümmerli and Brown, 2010; Harrison, 2013). These studies indicate that non-isogenic PVD non-

producers tend to have higher relative fitness values compared to their isogenic counterparts, which often only have a marginal fitness advantage, if any. It therefore seems that additional mutations present in non-isogenic PVD non-producers contributed to results in early studies. Whether these putative mutations are a prerequisite of the cheating phenotype, or would confer a fitness benefit independent of siderophore cooperation is unclear. Our findings presented in the main text largely suggest that the batch-culturing format is not conducive to social cheating. However, it may indeed be that these strains are capable of cheating in batch culture conditions, but that the field has not recognized additional important underlying mutations supporting this behavior.

A second possible explanation for the discrepancy could be variation in the growth media itself. Batches of commercially available hydrolyzed caseinate can differ in their composition, and different sources of CAA have even been shown to stimulate different PVD production phenotypes (Kümmerli and Ross-Gillespie, 2014). It is therefore plausible that our media preparations differed from those of previous authors, which further emphasizes the value of defined growth media.

Together with the data presented in the main text, we are led to conclude that batch culture formats, including when CAA is used as a growth substrate, do not create selective pressures conducive to social cheating. We have outlined some plausible explanations that may account for the discrepancies between our findings and those of others, although the definitive cause remains unclear.

SI Methods

Bacterial growth conditions for undefined batch culture experiments. For all co-culture experiments presented in Supplementary Fig. S2.4 and Supplementary Table S2.2, bacterial strains were routinely grown to stationary phase in LB, washed in a low iron salts base and mixed to desired ratios before inoculating co-cultures. For all permutations, we used 0.118 % (w/v) $K_2HPO_4 \cdot 3H_2O$, 0.025% (w/v) $MgSO_4 \cdot 7H_2O$ as a low Fe salt base, following previous precedent (Griffin *et al.*, 2004; Ross-Gillespie *et al.*, 2007; R. Kümmerli *et al.*, 2009; Rolf Kümmerli, Gardner, *et al.*, 2009; Rolf Kümmerli, Griffin, *et al.*, 2009; Jiricny *et al.*, 2010; Kümmerli and Brown, 2010). As pH can impact

PVD properties and Fe solubility, we also buffered all media to a pH of 7 with 25 mM MOPS (Sandoz *et al.*, 2007; Hider and Kong, 2010; Luján *et al.*, 2015). Where indicated, media were supplemented with 0.5% (w/v) CAA, which provides enough C and N to achieve final densities of ~ $1.25x10^9$ CFU/ml. In conditions L, M, and N, glucose, succinate or glutamate was added instead of CAA, to a final concentration of 25 mM. Because N is not available in glucose, and to a lesser degree in succinate and glutamate (compared to CAA), 25 mM NH_4Cl was added to these conditions. In all conditions, 1 µM $FeCl_3 \cdot 6H_2O$ was added. The Fe chelator EDDHA (Complete Green Company, El Segundo, CA) was added to a final concentration of 0.5 mg/ml. In some cases, 100 µg/ml apo-transferrin (Sigma) replaced EDDHA as the Fe chelator as indicated.

Bacterial strains and method of differentiation used in undefined batch culture experiments. All strains described in Supplementary Table S2.2 are derived from the PAO1 wild-type (ATCC 15692). PAO1 Δ*pvdD* Δ*pchEF* and PAO1 Δ*pvdS*::Gm^R were generously provided by Dr. Michael Vasil (Ochsner *et al.*, 1996; Ghysels *et al.*, 2004). PAO1 Δ*pvdS* was constructed by splicing-by-overlap-extension PCR as described in the main text. Trimethoprim and tetracycline resistance markers were chromosomally integrated to create PAO1 Tp^R and PAO1 Δ*pvdS* Tet^R, respectively, using the miniTn7 system (Choi and Schweizer, 2006). PVD producers and non-producers were differentiated using a selection scheme compatible with their respective genotype. Strains lacking antibiotic markers were differentiated by phenotypic screening on Kings B medium based on the characteristic green colony morphology of PVD producers (King *et al.*, 1954). Trimethoprim, gentamicin or tetracycline was used at 100 µg/ml to select for PAO1 Tp^R, PAO1 Δ*pvdS*::Gm^R or PAO1 Δ*pvdS*::Tet^R, respectively. Relative fitness (*w*) was subsequently calculated as the ratio of average growth rates (μ_{pvdS}/μ_{WT}), as described (Lenski, 1991).

SI Figures

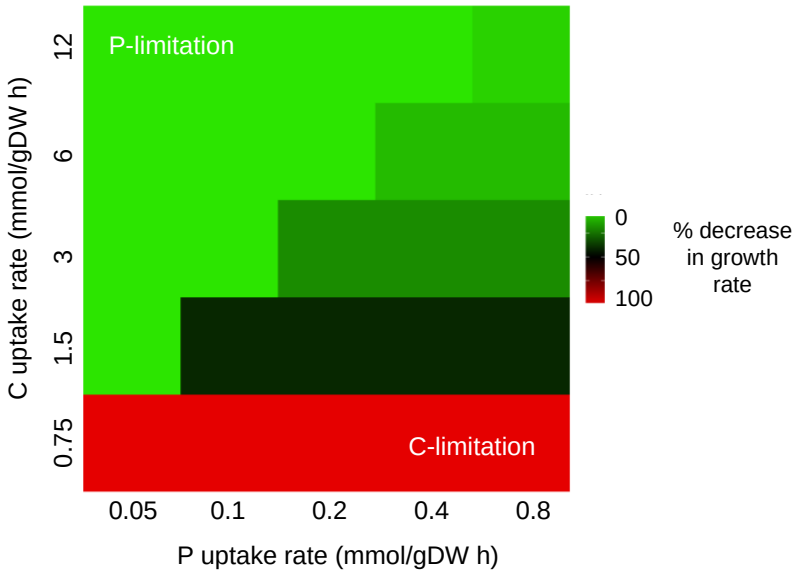

Figure S2.1. Relative C and P availabilities determine the impact of secretion on cellular biomass production. The heat map shows the percent-decrease in growth rate from PVD secretion as a function of C and P-uptake rates. For each nutrient combination, growth rates were compared in the presence and in the absence of secretion. The PVD secretion rate was set to a constant value (0.050 mmol (g DW h)$^{-1}$, equal to 0.068 g (g DW h)$^{-1}$), such that it reduces the growth rate by almost 100% at the lowest nutrient uptake rates. Relatively low C and high P uptake rates yield C-limiting conditions, whereas relatively low P and high C uptake rates yield P-limiting conditions.

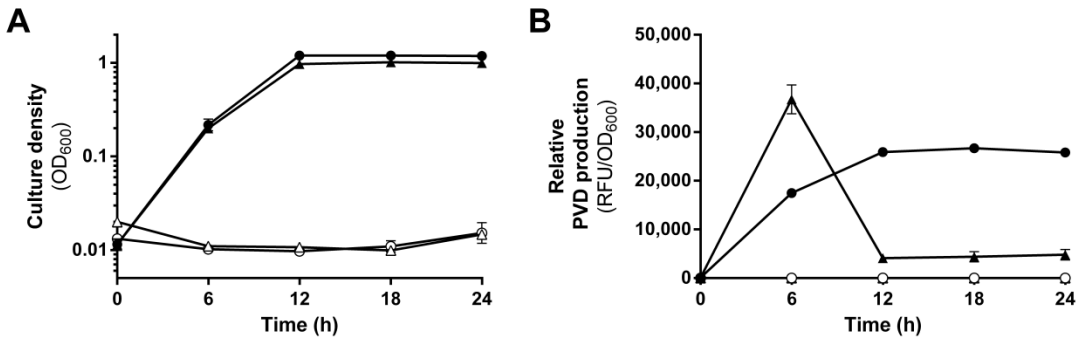

Figure S2.2. Time-courses of *P. aeruginosa* growth and PVD production. (A) Culture density, measured as optical density at 600 nm (OD_{600}). (B) Relative PVD production, expressed as relative fluorescence units (RFU) per OD_{600}. Individual cultures of the WT (filled symbols) and *pvdS* mutant (open symbols) were grown for 24 h in either C-MEM

(circles) or P-MEM (triangles). Error bars show SEM and are too small to be seen in some cases, n=3.

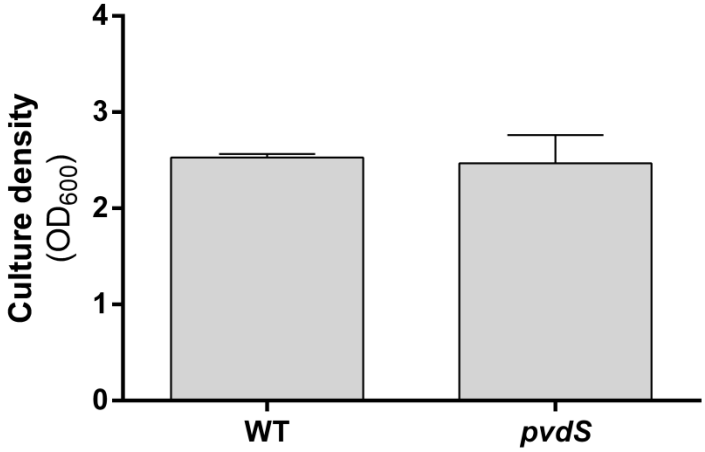

Figure S2.3. Growth yield of *P. aeruginosa* in Fe-replete batch culture. Individual cultures of the WT and *pvdS* mutant were grown for 24 h in MEM containing 20 mM C (glucose), 10 mM P, and 50 μM Fe. Culture density was measured as optical density at 600 nm (OD_{600}). Error bars show SEM, n=3. Means are not significantly different as determined by two sample t-test ($p > 0.05$).

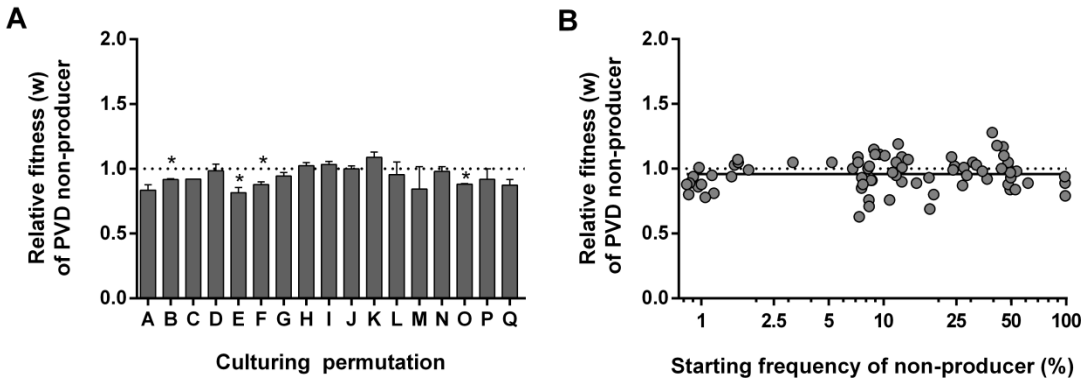

Figure S2.4. Relative fitness of PVD non-producers in a variety of batch culture permutations. (A) Relative fitness values grouped by the 17 different co-culturing permutations (see Supplementary Table 2). * indicates significant difference from 1, as determined by one sample t-test ($p < 0.05$). In no cases was fitness greater than 1. Error bars indicate SEM. (B) Individual relative fitness values as a function of starting frequency of non-producer. Each individual replicate from all 17 permutations was plotted and analyzed for frequency-dependent fitness patterns. Line represents linear

regression of data with a slope that is not significantly different from 1 (one-sample t-test, $p > 0.05$), indicating no increase or decrease in fitness.

Table S2.1. PVD biosynthesis reactions added to the *P. aeruginosa* whole-genome metabolic model

Protein name	Activity	Reaction equation*
Precursor reactions		
PvdA	L-ornithine N5-oxygenase	L-Orn + O_2 + 2NADPH + H^+ → L-OHOrn + NADP + H_2O
PvdF	Transformylase	L-OHOrn + For + ATP → L-fOHOrn + ADP + P_i
PvdH	Aminotransferase	Already in the model
Peptide synthesis		
PvdL†	NRPS‡	L-Glu + L-Tyr + L-Dab + 3 ATP → L-Glu-D-Tyr-L-Dab + 3 AMP + 3 PP_i + 3H^+
PvdI	NRPS	L-Glu-D-Tyr-L-Dab + L-Ser + L-Arg + L-Ser + L-fOHOrn + 4 ATP → L-Glu-D-Tyr-L-Dab-D-Ser-L-Arg-D-Ser-LFOHORN + 4 AMP + 4 PP_i + 4 H^+
PvdJ	NRPS	L-Glu-D-Tyr-L-Dab-D-Ser-L-Arg-D-Ser-L-fOHOrn + L-Lys + L-fOHOrn + 2 ATP → L-Glu-D-Tyr-L-Dab-D-Ser-L-Arg-D-Ser-L-fOHOrn-L-Lys-L-fOHOrn + 2 AMP + 2 PP_i + 2 H^+
PvdD	NRPS	L-Glu-D-Tyr-L-Dab-D-Ser-L-Arg-D-Ser-L-fOHOrn-L-Lys-L-fOHOrn + L-Thr + L-Thr + 2 ATP → L-Glu-D-Tyr-L-Dab-D-Ser-L-Arg-D-Ser-L-fOHOrn-L-Lys-L-fOHOrn-L-Thr-L-Thr + 2 AMP + 2 PP_i + 2 H^+
Secretion§		
PvdE/PvdRT-OpmQ	Membrane transport	PVD + 3 ATP → PVD(e) + 3 ADP + 3 P_i + 3 H^+

* Standard abbreviations for molecules and biochemical compounds are used. Orn, ornithine; fOHOrn, N_5-formyl-N_5-hydroxyornithine; Dab, 2,4-aminobutyrate; PVD(e), extracellular (secreted) PVD.

† Initial amino acid acylation via CoA-ligase is considered energetically in the PvdL reaction above. In terms of biomass, the acyl group is again removed prior to secretion and is therefore not lost from the cell.

‡ NRPS, non-ribosomal peptide synthetase

§ Periplasmic maturation is not considered here. The roles of periplasmic enzymes Pvd N, M, O, P are not clear, and the enzymes involved in chromophore formation have yet to be identified. Consequently, the energy demand, if any, is not known. Therefore, the product of the last NRPS (PvdD), is considered to be the mature, intracellular PVD. Transport of PVD across cytoplasmic membrane by PvdE, and across outer membrane by PvdRT-OpmQ are combined here, because the model does not separately consider a periplasmic compartment. The precise stoichiometry of ATP per PVD molecule is not known, but we estimate 2 ATP for PvdE and 1 ATP for PvdRT-OpmQ.

Table S2.2 Characterization of PVD producer and non-producer co-culture permutations

Group	Relative fitness (w)*[†]	p-value[‡]	Initial % of PVD non-producer[†]	n[§]	Starting density, (CFU mL^{-1})	Growth medium plus Fe chelator[¶]	Temp (°C)	Shaken (+) or static (-)	Strain pair	
									pvd^+	pvd^-
A	0.84 ± 0.04	0.058	10.3 ± 1.5	3	$3.55x10^7$	CAA + EDDHA	30	+	PAO1	PAO1 Δ*pvdD* Δ*pchEF*
B	0.92 ± 0.01	0.0063	8.47 ± 0.06	3	$1.66x10^5$	CAA + EDDHA	30	+		
C	0.92	N/A	8.05	1	$1.74x10^4$	CAA + EDDHA	30	+		
D	0.99 ± 0.05	0.81	46.7 ± 9.0	3	$1.04x10^4$	CAA + EDDHA	30	+		
E	0.82 ± 0.04	0.041	14.1 ± 3.1	3	$8.97x10^4$	CAA + Transferrin	37	-		
F	0.88 ± 0.02	0.0077	43.5 ± 5.5	4	$6.36x10^4$	CAA + Transferrin	37	-		
G	0.95 ± 0.03	0.074	1.40 ± 0.17	13	$1.08x10^5$	CAA + EDDHA	30	+	PAO1	PAO1 Δ*pvdS*:: Gm^R
H	1.03 ± 0.02	0.50	5.97 ± 0.78	2	$5.10x10^4$	CAA + EDDHA	30	+		
I	1.04 ± 0.02	0.19	11.4 ± 0.8	11	$1.64x10^5$	CAA + EDDHA	30	+		
J	1.00 ± 0.02	0.95	28.1 ± 1.9	7	$7.00x10^4$	CAA + EDDHA	30	+		
K	1.09 ± 0.04	0.064	44.6 ± 2.1	8	$2.24x10^5$	CAA + EDDHA	30	+		
L	0.95 ± 0.10	0.68	10.4 ± 2.5	4	$1.92x10^5$	25 mM Glucose + EDDHA	30	+		
M	0.84 ± 0.17	0.46	9.20 ± 1.42	3	$2.10x10^5$	25 mM Succinate + EDDHA	30	+		
N	0.98 ± 0.04	0.63	8.60 ± 0.89	4	$1.97x10^5$	25 mM Glutamate + EDDHA	30	+		
O	0.88 ± 0.01	0.00080	0.900 ± 0.054	3	$6.55x10^6$	CAA + EDDHA	30	+	PAO1 Tp^R	PAO1 Δ*pvdS* Tet^R
P	0.92 ± 0.08	0.50	48.4 ± 4.2	2	$5.76x10^6$	CAA + EDDHA	30	+		
Q	0.84 ± 0.05	0.10	98.4 ± 0.2	3	$4.88x10^6$	CAA + EDDHA	30	+		

N/A, not applicable
* Relative fitness (w) of PVD non-producer strain
[†] Values are given as the average ± SEM
[‡] p-value of one-sample t-test to assess whether fitness values are significantly different than 1
[§] Number of biological replicates for corresponding permutation
[¶] All media shared low iron salt base (see *Supplementary methods*), with specific C-source as indicated; CAA, 0.5% w/v casamino acids

Chapter 3

"*Pseudomonas protegens* Pf-5 favors self-produced siderophore over free-loading in interspecies competition for iron"

D. Joseph Sexton, Rochelle C. Glover, Joyce E. Loper and Martin Schuster

Environmental Microbiology
In Review
April 7th, 2017

Originality-Significance Statement. Microbial siderophores influence local ecology by restricting iron access away from neighboring organisms. This has led to interspecific competition for siderophores, evidenced by the ubiquity of bacteria that carry receptors for heterologous siderophores they do not make themselves. Consequently, there is an increasing interest to better understand cross-feeding interactions and their implications for microbial ecology and evolution. In this study, we demonstrate that the soilborne biocontrol strain *Pseudomonas protegens* Pf-5 maintains a competitive edge by capitalizing on the antagonistic role of its own siderophore, rather than adopting a free-loading lifestyle. This work documents an alternative strategy to success in the interspecies competition for iron, contrasting the more frequently studied "free-loader" approach.

Summary

Many microorganisms use strain-specific chelators, known as siderophores, to compete for extracellular iron. The ferric-siderophore complex limits local access to iron because import requires a suitable cognate receptor. Interestingly, many species carry receptors that enable "cross-feeding" on heterologous siderophores made by neighboring organisms, although little is known about how this ubiquitous behavior is regulated. Here, we investigated the soil bacterium *Pseudomonas protegens* Pf-5, a strain remarkable for its ability to use dozens of heterologous siderophores. We characterized the expression of six pyoverdine-type (PVD) siderophore receptors in response to their cognate PVD. In general, we found expression is tightly regulated to reflect availability of their cognate PVD. In contrast, Pf-5 continues to secrete its own primary siderophore, $PVD_{Pf\text{-}5}$, despite the capability and opportunity to cross-feed. We demonstrate that this strategy is beneficial in co-culture with a competing PVD_{PAO1}-producer, *P. aeruginosa* PAO1. Although Pf-5 can cross-feed on PVD_{PAO1}, production of $PVD_{Pf\text{-}5}$ is required to maintain a competitive advantage. We attribute this to an antagonistic effect of $PVD_{Pf\text{-}5}$ on the growth of PAO1, presumably through limiting access to iron. Our results demonstrate the benefits of excluding competitors out-weigh the incentives associated with a free-loader lifestyle for Pf-5.

Introduction

Iron is essential for a wide variety of biological functions ranging from DNA synthesis to electron transport (Hider and Kong, 2010). However, iron is most often present in an insoluble form or is bound to a variety of organic ligands, making iron acquisition a significant challenge for microorganisms in most environments (Ratledge and Dover, 2000; Gledhill and Buck, 2012). To overcome this barrier, many bacteria and fungi secrete siderophores, a structurally diverse class of secondary metabolites which chelate ferric iron with high affinity (Meyer and Abdallah, 1978; Visca *et al.*, 2007). The ferric-siderophore complex is subsequently transported back into the cell through cognate surface receptors (Hider and Kong, 2010). Siderophores exhibit great structural diversity, and even closely related bacterial strains often produce distinct siderophores (Meyer *et al.*, 2002). The structural specificity of siderophores confers an element of excludability, as iron bound to a siderophore becomes unavailable to strains lacking a suitable receptor. By limiting access to iron, siderophores can strongly influence the composition of local microbial communities. This effect is believed to contribute to the success in using siderophore-producing bacteria in controlling pathogens (Haas and Défago, 2005). However, the extent of excludability is finite; because the siderophores are secreted, there is an opportunity for competitors, provided they have a suitable receptor, to intercept the siderophore. Indeed, many bacteria and fungi carry receptors for siderophores they do not produce, indicating that stealing iron from a neighboring cell's siderophore is a common and worthwhile strategy. Evidence of siderophore cross-feeding within and between species has been reported in contexts such as the soil, ocean and even human infections, highlighting a need to better understand cross-feeding and its ecological implications (De Vos *et al.*, 2001; D'Onofrio *et al.*, 2010; Hartney *et al.*, 2011; Cordero *et al.*, 2012; Miethke *et al.*, 2013; Andersen *et al.*, 2015).

The Gram-negative soil bacterium *Pseudomonas protegens* Pf-5 is a metabolically versatile strain recognized for its secondary metabolite production and applications in plant pathogen control (Loper *et al.*, 2007). Pf-5 produces a pyoverdine type siderophore ($PVD_{Pf\text{-}5}$) and a secondary siderophore known as entantio-pyochelin

(Youard *et al.*, 2007; Hartney *et al.*, 2013). PVDs are a sub-class of siderophores with a particularly high affinity (10^{-32} M^{-1}) for iron (Meyer and Abdallah, 1978; Albrecht-Gary *et al.*, 1994). PVDs are composed of a variable non-ribosomal peptide chain linked to a naturally fluorescent dihydroxyquinoline chromophore, to which the "fluorescent pseudomonads" owe their name (King *et al.*, 1954; Visca *et al.*, 2007).

Although $PVD_{Pf\text{-}5}$ production by Pf-5 has been known for some time, the structure was only recently characterized, along with the identification of its cognate TonB-dependent surface receptor, FpvZ (Hartney *et al.*, 2013). In addition to using its own siderophores, Pf-5 is remarkably proficient in the acquisition of siderophores produced by other organisms, a behavior attributable to the large number of additional TonB-dependent surface receptors encoded in its genome (Hartney *et al.*, 2011). Six of these receptors have been identified as PVD-type receptors and have been shown to collectively permit uptake of more than a dozen PVDs (Hartney *et al.*, 2013). While efforts have been made to characterize the global response of Pf-5 to iron stress (Lim *et al.*, 2012), less is known about how the availability of siderophores from neighboring species is incorporated into this response.

The regulation of PVD production and uptake is best understood in the opportunistic pathogen *Pseudomonas aeruginosa* strain PAO1. Both functions fit within the global iron starvation response, mediated by the iron-binding transcriptional repressor Fur. Furthermore, binding of ferric-PVD_{PAO1} to the cognate receptor FpvA transduces a signal across the periplasm through a transmembrane protein FpvR (Edgar *et al.*, 2014). FpvR functions as an anti-extracytoplasmic sigma factor (ECF). When FpvR perceives signal from PVD binding, it stimulates the release of the alternative extracytoplasmic sigma factors (ECFs) PvdS and FpvI, which up-regulate PVD biosynthesis and cognate receptor FpvA genes, respectively (Rédly and Poole, 2003; Cornelis *et al.*, 2009). In *P. putida* WCS358, a similar mechanism has been shown to regulate PupB, a receptor which permits uptake of heterologous PVDs. PupB expression is regulated by a specific ECF/anti-ECF pair PupI/R, which activate PupB expression when the cognate heterologous PVDs are present (Koster *et al.*, 1994). Indeed, the genes of many TonB-dependent receptors in pseudomonads are directly adjacent to the genes for ECF/anti-

ECF pairs, reflective of a common model for the regulation of siderophore receptors (Winsor *et al.*, 2016). Likewise, the heterologous ferric-PVD receptors in Pf-5 also have adjacent ECF/anti-ECF pairs, although whether these ECF/anti-ECF pairs regulate the expression of the adjacent receptor has not been empirically investigated (Hartney *et al.*, 2011).

There is also an increasing interest in siderophore production as a cooperative behavior, and how the social environment influences siderophore production. In P. aeruginosa, it has been shown that PVD-positive cooperators increase production in the presence of PVD-negative cheaters (Kümmerli et al., 2009; Harrison, 2013). Other studies have shown that native siderophore production increases in the presence of different siderophores produced by competing species (Harrison et al., 2007; Traxler et al., 2013). Recent theoretical work looking more specifically at cross-feeding suggests that the more "shared" a siderophore is, the lower the optimum secretion rate should be (Niehus et al., 2017). However, less is known about how the opportunity to cross-feed may influence the regulation of PVD production. Considering the available literature on within-species siderophore cheaters, it is plausible that a cross-feeding strain may reduce production of its native siderophore to conserve resources, therefore acting as an opportunistic free-loader (Griffin et al., 2004). . However, to better address this question more empirical evidence is needed.

In this study, we considered how two key aspects, receptor expression and PVD biosynthesis, of the cross-feeding behavior, are regulated in Pf-5. We report that while the PVD receptors are predominately regulated to reflect the presence of their cognate PVD, biosynthesis of the endogenous siderophore $PVD_{Pf\text{-}5}$ is not impacted. We demonstrate this behavior confers an important fitness advantage when co-cultured with competing strain PAO1. Collectively our work provides new insights into the strategies at play as species compete for iron.

Results

Regulation of PVD receptors in response to cognate, heterologous PVDs

The Pf-5 genome encodes six ferric-PVD receptors which collectively permit uptake of PVDs from over a dozen of the tested *Pseudomonas* strains (Hartney *et al.*, 2013). Acknowledging that one receptor can permit uptake of multiple PVDs, we chose to focus our study on a single representative PVD for each receptor (Table 3.1). *Pseudomonas* species secreting these PVDs were cultured in a buffered low-iron casamino-acid (CAA) medium that stimulates high levels of PVD production. All strains grew well under these conditions (final culture densities, OD_{600} of 1.5 – 2.0) and produced PVD concentrations ranging from 200-1200 μM. PVD concentrations were determined based on fluorescence intensity (Supporting Information Fig. S3.1) (Meyer and Abdallah, 1978; Hoegy *et al.*, 2014).

Table 3.1 Ferric-PVD receptors and matching PVD

Ferric PVD receptor	Matching PVD structure[b]	PVD producing strain
FpvU (PFL_2391)[a]	Ser-Arg-Ser-FOHOrn-(Lys-FOHOrn-Thr-Thr)	*P. aeruginosa* PAO1
FpvV (PFL_2527)	Unknown	*P. putida* Bn7
FpvW (PFL_2293)	εLys-OHAsp-Ala-aThr-Ala-cOHOrn	*P. fluorescens* B10
FpvX (PFL_3315)	*Ala-Lys-Thr-Ser-OHOrn-OHOrn*	*P. putida* CS111
FpvY (PFL_3485)	*Ser-Lys-FOHOrn-Ser-Ser-Gly-(Lys-FOHOrn-Ser–Ser)*	*P. rhodesia* CFML 92-104
FpvZ (PFL_4092)	Asp-FOHOrn-Lys-(Thr-Ala-Ala-FOHOrn-Lys)	*P. protegens Pf-5*

[a] Gene locus tag
[b] Italics indicate structure computationally predicted

To confirm the previously reported cross-feeding phenotypes, we measured the effect of each supernatant on growth of two siderophore-negative strains, Pf-5 Δ*pvdI* Δ*pchA* and Pf-5 Δ*pvdS*, which have in-frame deletions in the siderophore biosynthesis and regulatory ECF genes, respectively (Table 3.2). As neither strain can produce $PVD_{Pf\text{-}5}$, they are unable to grow independently when CAA is supplemented with the synthetic iron chelator ethylenediamine-dihydroxy-o-phenylacetic acid (CAA-EDDHA) (Supporting Information Fig. S3.2). Consistent with previous reports, we found each supernatant rescued growth of Pf-5 Δ*pvdI* Δ*pchA* and Pf-5 Δ*pvdS*, confirming the expected cross-feeding phenotype. Using the two strains provided a form of independent verification.

Table 3.2 Bacterial strains and plasmids used in this study

Strains or plasmids	Notes	Reference
Strains		
P. putida CS111	Producer of PVD_{CS111}	Meyer, 2007
P. rhodesiae CFML 92-104	Producer of $PVD_{CFML\ 92\text{-}104}$	Meyer, 2007
Pseudomonas sp. B10	Producer of PVD_{B10}	Teintze *et al*., 1981
P. putida Bn7	Producer of PVD_{Bn7}	Koster *et al.,* 1993
P. protegens Pf-5	Producer of $PVD_{Pf\text{-}5}$	Hartney *et al*., 2013
Pf-5 Gm^R	Pf-5 marked with Gm^R using miniTn7 system	This study
Pf-5 *ΔpchA*	Entantio-pyochelin biosynthesis mutant	Hartney *et al.,* 2011
Pf-5 *ΔpvdI ΔpchA*	Entantio-pyochelin, $PVD_{Pf\text{-}5}$ biosynthesis double mutant	Hartney *et al.,* 2011
Pf-5 *ΔpvdS*	Deletion in alternative ECF that controls PVD regulon	This study
Pf-5 *ΔpvdS* Tet^R	Pf-5 Δ*pvdS* marked with Tet^R using miniTn7 system	This study
P.aeruginosa PAO1	Producer of PVD_{PAO1}	Demange *et al.,* 1990
PAO1 *ΔpchEF*	Pyochelin biosynthesis mutant	Ghysels *et al.,* 2004
PAO1 *ΔpvdD ΔpchEF*	Pyochelin, PVD_{PAO1} biosynthesis double mutant	Ghysels *et al.,* 2004
PAO1 *ΔpvdS*	Deletion in alternative ECF which controls PVD regulon	Sexton and Schuster, 2017
Escherichia coli SM10	*thi thr leu tonA lacY supE recA*::RP4-2-Tc::Mu Km λ*pir*	Simon 1983
E. coli DH5α	F-Φ80*lacZYA-argF* U169 *recA1 hsdR17* (rk−, mk+) phoA *supE44* λ- *thi-1 gyrA96 relA1*	Invitrogen
Plasmids		
pUC18RKT-mini-Tn7-Tet^R	Broad host-range mini-Tn7 vector with Tet^R gene cassette	Choi and Schweizer, 2006
pUC18RKT-mini-Tn7-Gm^R	Broad host range mini-Tn7 vector with Gm^R gene cassette	Choi and Schweizer, 2006
pEX18Tet^R	Conjugative suicide plasmid; Tet^R	Hoang *et al.,* 1998
pEX18Tet^R.ΔPA2426	pEX18Tet^R carrying ΔPA_2426 (*pvdS*) allele	This study
pEX19Gm^R	Conjugative suicide plasmid; Gm^R	Hoang *et al.,* 1998
pEX19Gm^R.ΔPFL4190	pEX19Gm^R carrying ΔPFL_4190 (*pvdS*) allele	This study

We proceeded to evaluate how Pf-5 Δ*pvdI* Δ*pchA* responds when exposed to six culture supernatants, each containing a different PVD. We used quantitative real-time PCR (qRT-PCR) to measure mRNA transcript levels of each receptor-encoding gene in bacteria grown in media supplemented with supernatants containing PVD. To isolate the effects of the specific PVD of interest from siderophores produced endogenously by Pf-5, it was necessary to use a $PVD_{Pf\text{-}5}$ negative strain. For this purpose we chose Pf-5 Δ*pvdI* Δ*pchA*. Supernatants were normalized to provide 10 µM PVD. This concentration was high enough to permit robust cross-feeding while remaining low enough to avoid the non-specific binding and entry through other receptors, which we have observed at higher concentrations (Supporting Information Fig. S3.2 and S3.3). Receptor transcript levels of Pf-5 Δ*pvdI* Δ*pchA* were quantified after 18 hours of growth of the bacteria in CAA medium alone, or CAA supplemented with each PVD-containing supernatants.

We found five of six supernatants (those containing $PVD_{Pf\text{-}5}$, PVD_{PAO1}, $PVD_{CFML\ 92\text{-}104}$, PVD_{B10} and PVD_{CS111}) significantly induced expression of the anticipated cognate receptor relative to the no supernatant control (Fig. 3.1). In all of these cases except for one, induction was exclusive to the cognate receptor and did not stimulate expression of

other receptors. Moreover, FpvU and FpvZ were induced concurrently when the medium was supplemented with both supernatants containing PVD_{PAO1} and $PVD_{Pf\text{-}5}$. These observations suggest that the underlying regulatory mechanisms operate independently.

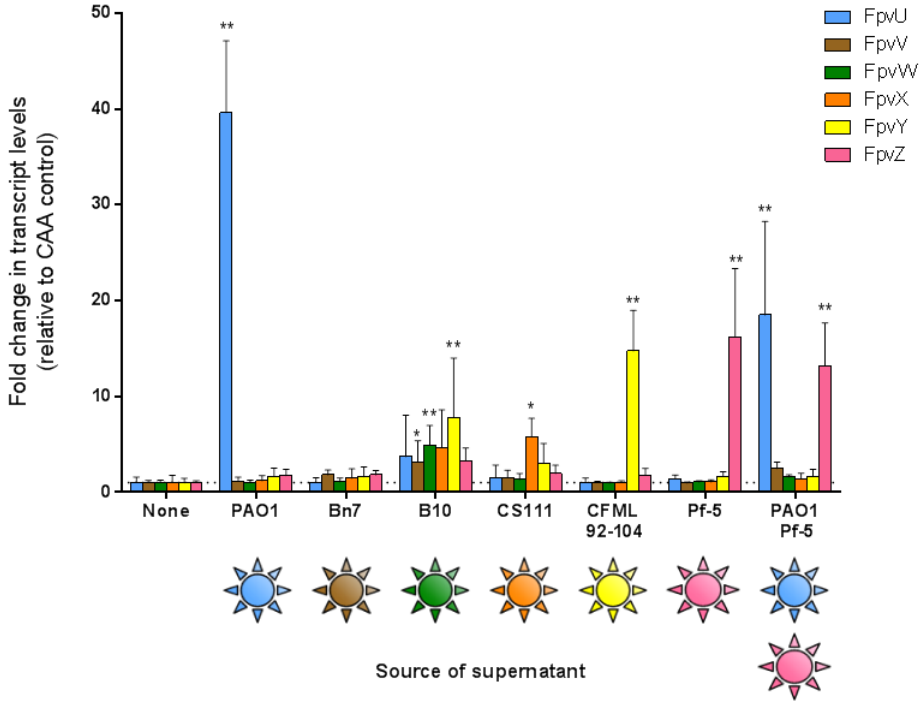

Figure 3.1 Expression of ferric-PVD receptors in response to heterologous PVDs. The y-axis shows transcript levels of each receptor when *P. protegens* Pf-5 Δ*pvdI* Δ*pchA* is supplemented with supernatant from the strain designated on the x-axis. Supernatant concentrations were adjusted to provide 10 µM of PVD. Data are expressed as fold-change relative to the media only (CAA) no supernatant control. The symbols along the bottom of the x-axis depict the PVDs produced by the respective strains. They are color-coded to reflect their cognate receptor. Statistical significance was determined by comparing mean values of each treatment to the respective control (n=3) using a one-way ANOVA with Dunnett's multiple comparison test. Single asterisks indicates p-value = 0.05-0.01, double asterisks indicate p-value <0.01.

However, two noteworthy deviations from the general trend were observed. First, the inductive effect of supernatant containing PVD_{B10} was not exclusive to its cognate receptor FpvW, but also significantly induced expression of FpvV and FpvY. Furthermore, supernatant with PVD_{Bn7} was unique in that it did not increase transcription of any receptors, including its cognate receptor FpvV. Considering that the growth of Pf-

5 Δ*pvdI* Δ*pchA* in EDDHA-supplemented CAA medium was restored by the same concentration of PVD_{Bn7} (Supporting Information, Fig. S3.2), the basal level of FpvV must be sufficient to permit robust growth without further induction. In sum, these data demonstrated that Pf-5 expresses genes encoding its TonB-dependent receptors to reflect availability of their cognate PVD, although FpvV represents a noteworthy exception.

$PVD_{Pf\text{-}5}$ production continues despite the presence of other pyoverdines

We then considered how biosynthesis of the endogenous siderophore $PVD_{Pf\text{-}5}$ responds to the availability of heterologous PVDs. Specifically, does Pf-5 continue to produce $PVD_{Pf\text{-}5}$ or does it reduce production in favor of cross-feeding? To address this question, we cultured the Pf-5 WT in CAA supplemented with each bacterial supernatant normalized to 10 μM PVD. The PVD present in these supernatants creates a baseline fluorescence which can be detected (~1,000 RFU) but remains well below the upper limit of linear detection (~15,000 RFU, Supporting information Fig. S3.1). We reasoned that if Pf-5 represses biosynthesis of $PVD_{Pf\text{-}5}$ in favor of cross-feeding behavior, fluorescence intensity should stay constant throughout the growth experiment. In contrast, active production of $PVD_{Pf\text{-}5}$ would lead to an increase of fluorescence intensity above the baseline. Corroborating the latter, we see that in all cases, fluorescent values emerge from the background levels at around 6 hours of growth, indicating $PVD_{Pf\text{-}5}$ is being actively produced (Fig. 3.2). Fluorescence intensity continued to increase over an order of magnitude until saturating the linear range of detection at around 9 hours of growth.

To ensure that the PVD concentration in each supernatant was indeed sufficient for robust growth, we performed the experiment with Pf-5 Δ*pvdI* Δ*pchA* and again for independent verification, Pf-5 Δ*pvdS*. We found that PVD supplementation consistently restores growth of both mutants to wild-type levels, indicating that 10 μM PVD in the supernatants was sufficient for effective cross-feeding (Fig. 3.2). Taken together, our data provide compelling evidence that Pf-5 does not repress biosynthesis of its own siderophore despite the presence of heterologous PVDs.

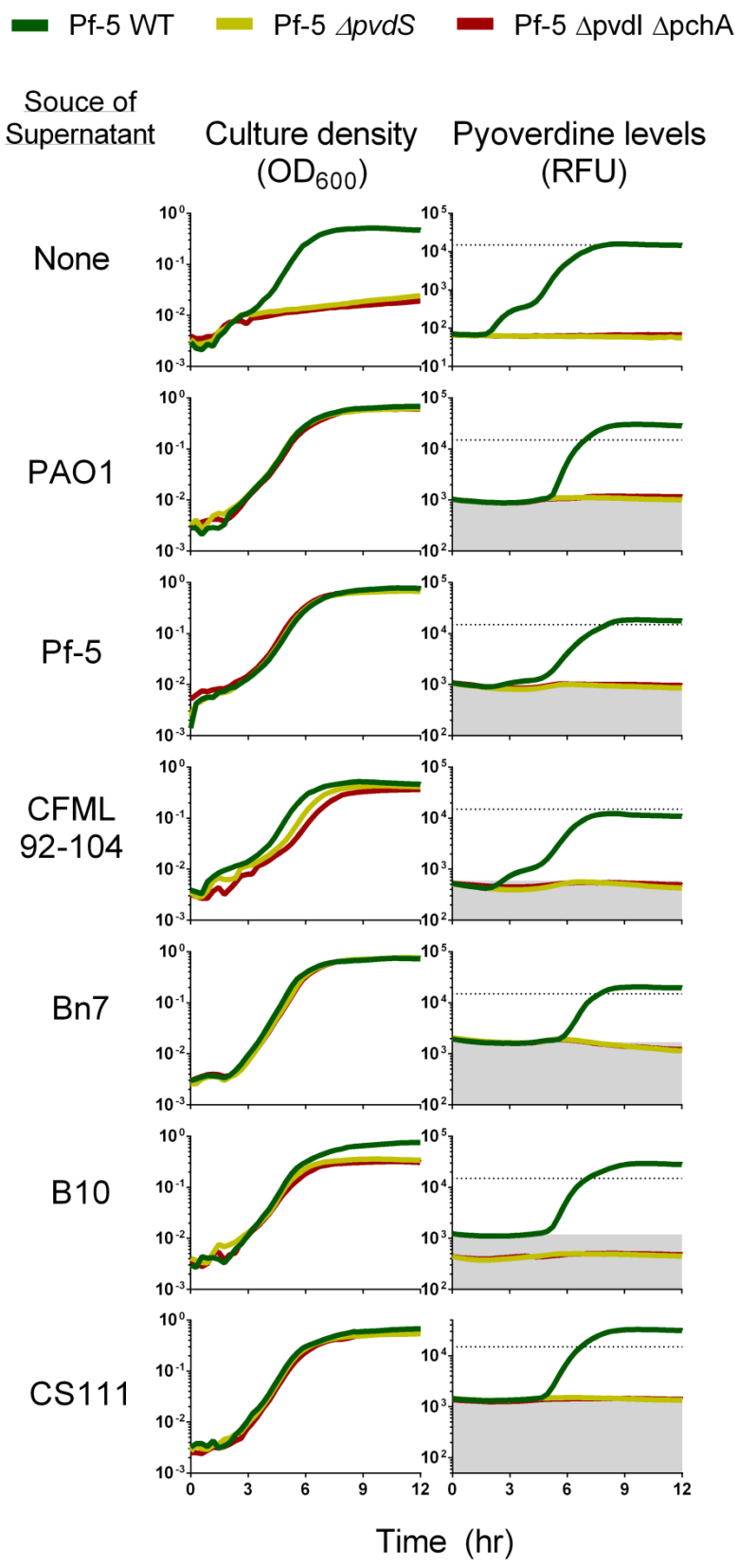
Pf-5 WT
Pf-5 ΔpvdS
Pf-5 ΔpvdI ΔpchA
Souce of Supernatant
Culture density (OD600)
Pyoverdine levels (RFU)
None
PAO1
Pf-5
CFML 92-104
Bn7
B10
CS111
Time (hr)

Figure 3.2 Production of $PVD_{Pf\text{-}5}$ by *P. protegens* Pf-5 in response to heterologous PVDs. Growth of Pf-5 WT (green), Pf-5 Δ*pvdS* (yellow) and Pf-5 Δ*pvdI* Δ*pchA* (red) in CAA-EDDHA when provided with supernatant from the strain designated to the right of the panel. Supernatants were adjusted to provide 10 µM of the indicated PVD. The left panels show culture density (OD_{600}), and the right panels show corresponding PVD levels, expressed as relative fluorescence units (RFU). Gray shade indicates background levels of RFU contributed by PVD present in the supernatants. Continued $PVD_{Pf\text{-}5}$ production by Pf-5 WT is observed as an increase in fluorescence intensity above the background, which is not seen with either mutant.

Fitness contribution of $PVD_{Pf\text{-}5}$ in interspecies competition

Considering our finding that receptor expression is adapted to cross-feeding opportunities, it was unclear why biosynthesis of $PVD_{Pf\text{-}5}$ is not. To better understand this observation, we considered the fitness benefits of $PVD_{Pf\text{-}5}$ when in co-culture with a competing PVD-producing strain. For this purpose, we designed a co-culturing system between Pf-5 and PAO1. We chose PAO1 for several reasons. First, while Pf-5 is able to take up PVD_{PAO1} using FpvZ, PAO1 does not carry a suitable receptor to take up $PVD_{Pf\text{-}5}$, creating unidirectional cross-feeding (Fig. 3.3) (Stover *et al.*, 2000; Hartney *et al.*, 2013). This allowed us to study the fitness benefits of cross-feeding of Pf-5 by PVD_{PAO1}, while avoiding the complications of two-way cross-feeding. PAO1 is a genetically tractable strain and model organism, whose response to iron stringency has been extensively characterized (Cornelis *et al.*, 2009). Furthermore, we recently constructed and characterized a PAO1 Δ*pvdS* in-frame deletion mutant (Sexton and Schuster, 2017), that could be compared to the Pf-5 Δ*pvdS* strain we had used thus far.

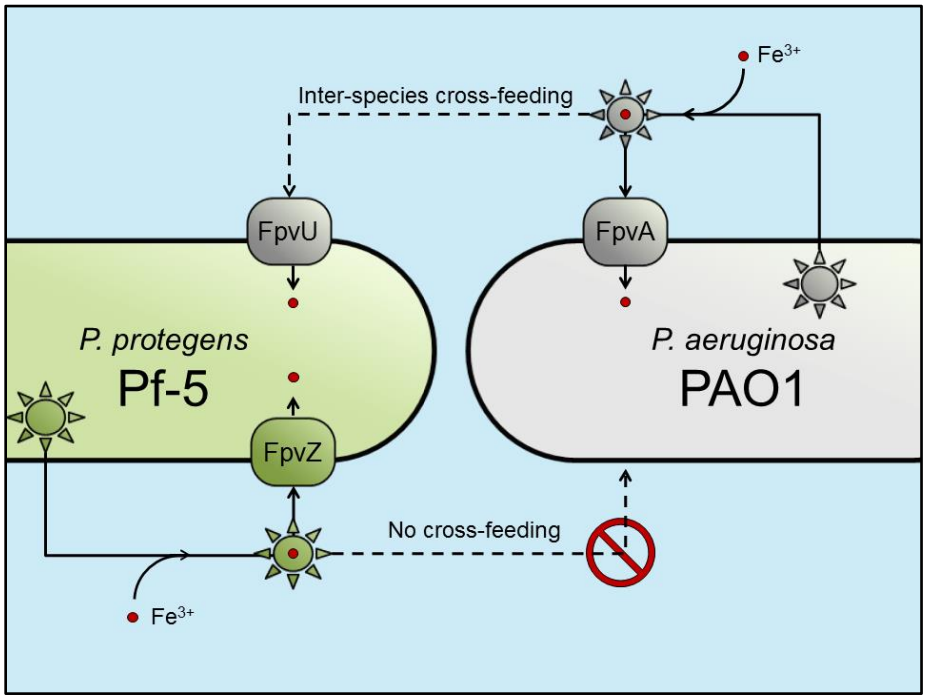

Figure 3.3 Illustration of interspecies co-culture model. *P. aeruginosa* PAO1 (gray) and *P. protegens* Pf-5 (green) secrete structurally distinct strain-specific PVDs. PVD_{PAO1} and $PVD_{Pf\text{-}5}$ are imported though cognate cell surface receptors FpvA and FpvZ, respectively. In addition to using its own $PVD_{Pf\text{-}5}$, Pf-5 is also able to steal iron from PVD_{PAO1} using additional receptor FpvU. However, PAO1 lacks a comparable receptor and is therefore unable to use $PVD_{Pf\text{-}5}$, creating unilateral cross-feeding.

Before initiating co-cultures, we confirmed that cross-feeding was unilateral using the Pf-5 *ΔpvdS* and PAO1 Δ*pvdS* mutants in CAA-EDDHA, where neither strain can grow independently (Fig. 3.4). As anticipated, the growth of PAO1 Δ*pvdS* was only restored by supernatant from its parental PAO1, but not Pf-5 (Fig. 3.4A). Consistent with previous observations, growth of Pf-5 Δ*pvdS* was restored when provided supernatant from either Pf-5 or PAO1 WT strains (Fig. 3.4B). We note that the growth curves of Pf-5 Δ*pvdS* with either supernatant are superimposable, indicating similar preference for both siderophores under our conditions.

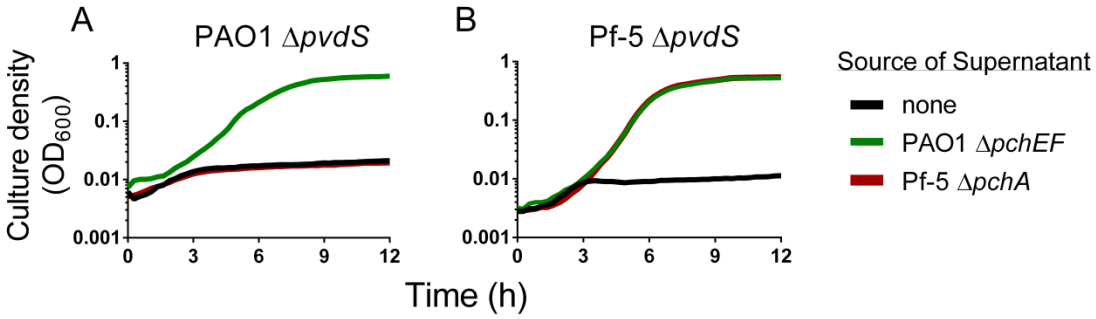

Figure 3.4 Confirmation of interspecies cross-feeding phenotypes in pure cultures. PAO1 Δ*pvdS* (A) and Pf-5 Δ*pvdS* (B) were grown in CAA-EDDHA without supplementation (gray), or supplemented with supernatants from strain PAO1 Δ*pchEF* (green) or Pf-5 Δ*pchA* (red). Supernatants were adjusted to provide 10 µM of PVD. In panel B, symbols for Pf-5 ΔpvdS growth on CAA + supernatant from Pf-5 Δ*pchA* are largely hidden behind symbols for growth on CAA + supernatant from PAO1 Δ*pchEF*.

After empirically confirming the premise of our co-culture model system, we measured the fitness of Pf-5 relative to PAO1 WT in CAA-EDDHA (Fig. 3.5). Strains were inoculated at a 1:1 ratio, and subpopulation frequencies were distinguished at 0 and 24 hours by selective plating, using LB plates at 37°C to select for *P. aeruginosa*, and LB + 200µg/mL Carbenicillin to select for *P. protegens.* Fitness was defined as the ratio of Malthusian growth parameters as described (Lenski, 1991). Pf-5 consistently outcompeted PAO1 (Fig. 3.5, white circles), with an average fitness significantly greater than 1 as determined by a one-sample t-test ($\alpha = 0.05$). In stark contrast, Pf-5 Δ*pvdS* suffered a distinct disadvantage in co-culture, dropping to less than 0.5% of the total population (Fig. 3.5, white triangles). This result was unexpected, considering the proficiency Pf-5 Δ*pvdS* demonstrated when cross-feeding on PVD_{PAO1} in mono-culture (Fig. 3.2, Supporting Information Fig. S3.2, Fig. 3.4). To ensure this strain did not suffer an unintended defect as a cross-feeder, we performed a control competition with its parental strain Pf-5, a scenario where Pf-5 Δ*pvdS* could be described as an intraspecies social cheater (West *et al.*, 2006). To distinguish these strains, gentamicin (Gm^R) and tetracycline (Tet^R) resistance genes were inserted into the genomes of Pf-5 WT and Pf-5 Δ*pvdS*, respectively. After competing antibiotic resistant strains, we found Pf-5 Δ*pvdS* Tet^R had an average relative fitness of 1.05 (SD = 0.044) which was not significantly different than 1 (one-sample t-test, p-value = 0.18). This shows that in co-culture Pf-5

Δ*pvdS* Tet^R and Pf-5 Gm^R grow at equal rates. The poor performance of Pf-5 Δ*pvdS* against PAO1 therefore cannot be attributed to an inherent defect of Pf-5 Δ*pvdS*, but instead suggests that the production of $PVD_{Pf\text{-}5}$ offers an important fitness benefit in co-culture.

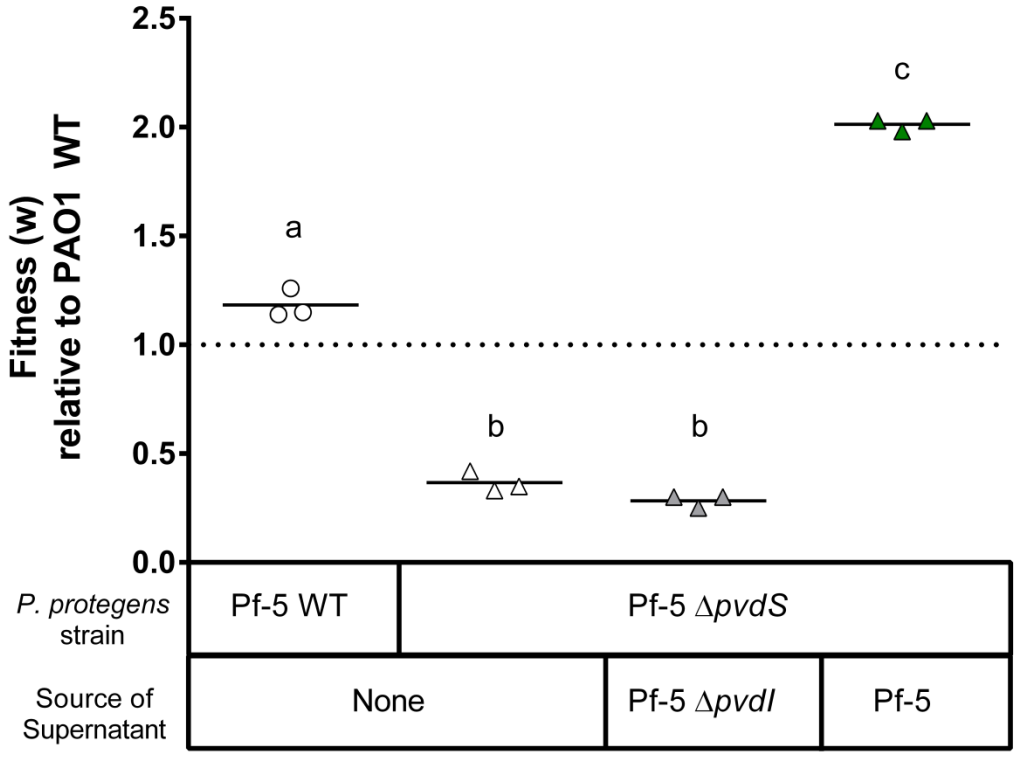

Figure 3.5. Contribution of $PVD_{Pf\text{-}5}$ to the fitness of *P. protegens* Pf-5 when competing with *P. aeruginosa* PAO1. Strain pairs were inoculated at a 1:1 ratio and co-cultured in CAA-EDDHA for 21 hours. Fitness (w) of Pf-5 WT (circles) or Pf-5 *ΔpvdS* (triangles) relative to PAO1 was calculated as ratio of Malthusian growth parameters (Materials and methods). A fitness above 1 indicates an increase in *P. protegens* frequency, while fitness below 1 indicates a decrease in frequency. Where indicated, supernatants were added to the co-culture growth medium adjusted to 100 µM $PVD_{Pf\text{-}5}$ (green triangles) or as a comparable dilution for supernatant from Pf-5 Δ*pvdI* (gray triangles), which lacks $PVD_{Pf\text{-}5}$. Mean values with different lowercase letter are significantly different from each other as determined with a one-way ANOVA followed by Tukey's multiple comparison test ($\alpha = 0.05$).

To further test this interpretation, we performed a complementation experiment where PAO1 and Pf-5 Δ*pvdS* were again competed, but this time supplemented with supernatant from the Pf-5 WT, normalized to provide ~ 100 µM $PVD_{Pf\text{-}5}$. This higher

concentration was chosen to more closely reflect the amount produced by the WT under these conditions. Corroborating our hypothesis, we found this restored the relative fitness of Pf-5 Δ*pvdS* back above 1, and even to a higher fitness than the WT alone (Fig. 3.5, green triangles). This increase in fitness is likely related to early exposure to high concentrations of $PVD_{Pf\text{-}5}$, contrasting the gradual accumulation when produced endogenously by Pf-5 WT. Rescued fitness of Pf-5 Δ*pvdS* can be specifically attributed to the $PVD_{Pf\text{-}5}$ in the supernatant, because supernatant from a Pf-5 Δ*pvdI* biosynthesis mutant did not improve the relative fitness of Pf-5 Δ*pvdS* (Fig. 3.5, gray triangles).

The collective results from these experiments demonstrate that $PVD_{Pf\text{-}5}$ plays an essential role during interspecies competition for iron despite the opportunity for the bacteria to cross-feed. Because PAO1 is unable to access iron bound by $PVD_{Pf\text{-}5}$, we considered a plausible mechanism where growth of PAO1 is delayed by the presence of $PVD_{Pf\text{-}5}$. To test this hypothesis, we measured PAO1 WT mono-culture growth in CAA alone, or supplemented with supernatant from Pf-5 WT normalized again to provide 100 μM $PVD_{Pf\text{-}5}$ (Fig. 3.6). As an additional control, we also included supernatant from a culture of Pf-5 Δ*pvdI*, at an equal dilution. We found supernatant from the Pf-5 WT, but not Pf-5 Δ*pvdI*, significantly reduced the growth rate of PAO1 (two-sample t-test, $\alpha = 0.05$). This finding demonstrates an antagonism that can be specifically attributed to $PVD_{Pf\text{-}5}$. This role is essential during interspecies competition with PAO1, providing a parsimonious explanation as to why biosynthesis of $PVD_{Pf\text{-}5}$ continues even when iron can be acquired through heterologous siderophores.

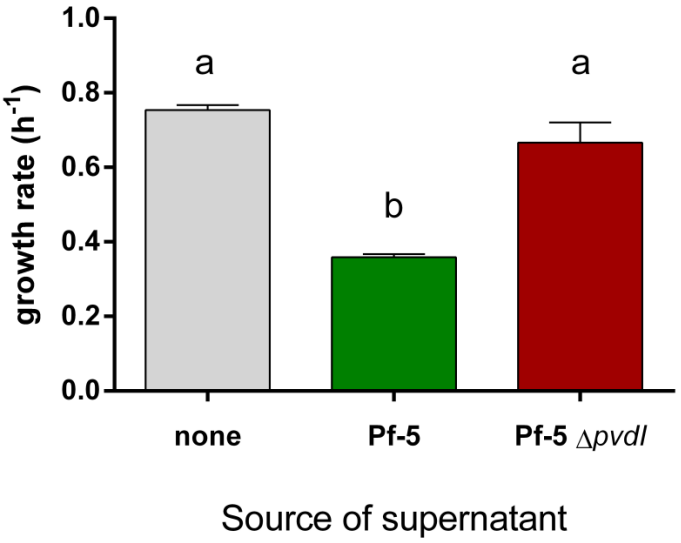

Figure 3.6. $PVD_{Pf\text{-}5}$ reduces the growth rate of *P. aeruginosa* PAO1. The y-axis shows growth rate (h^{-1}) of the PAO1 WT in mono-culture in CAA-EDDHA medium alone (gray), supplemented with supernatant from either Pf-5 WT (green) or Pf-5 Δ*pvdI* (red). Supernatants were adjusted to provide 100 µM PVD or the comparable dilution in the case of Pf-5 Δ*pvdI*. Error bars show standard deviation of the mean (n=3). Mean values with different lowercase letter are significantly different from each other (two-sample t-test, $\alpha = 0.05$).

Conclusions

P. protegens Pf-5 is highly adapted to the interspecies competition for iron. In addition to producing two siderophores of its own, it has been empirically shown to intercept dozens of siderophores produced by other species and is predicted to uptake many more still based on the large number of TonB-dependent receptors which have not yet been fully characterized (Hartney *et al.*, 2011; Hartney *et al.*, 2013). Using molecular techniques in combination with innovatively applied co-culturing methods, we provide novel insights into how Pf-5 regulates its behavior to optimize cross-feeding.

First, we found that the regulation of its ferric-PVD receptors is finely tuned (Fig. 3.1). In five of the six ferric-PVD receptors, we see that expression is only induced when the cognate PVD type is present. The ability of these receptors to be regulated independently was demonstrated when both heterologous and homologous PVD (PVD_{PAO1} and $PVD_{Pf\text{-}5}$, respectively) were present at the same time (Fig. 3.1). Although we did not explore the underlying mechanisms, there is good reason to suspect that ECFs

are involved, as has been shown in other systems (Koster *et al.*, 1994). In *P. aeruginosa* PAO1, expression of ferric-PVD receptor FpvA is controlled by the ECF FpvI (Rédly and Poole, 2005). While transcription of FpvI is under control of the global iron regulator Fur, it remains inactive on the cytoplasmic side of the inner membrane, bound to transmembrane anti-ECF FpvR. FpvR interacts directly with FpvA, and after binding ferric-PVD_{PAO1}, undergoes a conformational change that releases and thereby activates FpvI to induce FpvA expression (Rédly and Poole, 2005; Edgar *et al.*, 2014). It is plausible that Pf-5 uses a similar mechanism to regulate receptors in response to their cognate siderophore. Indeed, each of Pf-5's heterologous PVD receptor genes is directly adjacent to a predicted ECF/anti-ECF gene pair (Winsor *et al.*, 2016). This proximity is noteworthy, considering these receptors are dispersed throughout the genome and not clustered with the rest of the PVD locus, suggestive of acquisition through horizontal gene transfer (Hartney *et al.*, 2013; Winsor *et al.*, 2016). If horizontally transferred as a package with the ECF/anti-ECF pair, newly acquired ferric-PVD receptors may come with a regulatory mechanism already in place.

There are a number of reasons why selection might favor tight regulation of these receptors. One consideration is the conservation of resources. Ferric-PVD receptors are about three times larger than the average bacterial protein (Poole *et al.*, 1993; Brocchieri and Karlin, 2005). It is therefore conceivable that receptors are tightly regulated to avoid unnecessary synthesis costs. However, discerning whether receptor synthesis translates into an appreciable evolutionary fitness cost is less clear. Recent work has emphasized the underappreciated relationship between resource availability and the fitness cost of microbial behaviors (Xavier *et al.*, 2011; Mellbye and Schuster, 2014; Sexton and Schuster, 2017).

Alternatively, tight regulation of these receptors may be important as a defense mechanism. Viruses and antimicrobials often target outer-membrane receptors. Of particular relevance are a class of antimicrobials known as pyocins, which are secreted by pseudomonads to kill closely related strains (Parret and De Mot, 2002). Although not fully understood, the few which have been studied were found to target PVD receptors (Baysse *et al.*, 2002; Denayer *et al.*, 2007). By targeting ferric-PVD receptors, pyocins

may play a role antagonizing closely related strains specifically while competing for iron. It is therefore possible that pyocins specifically select for tight regulation of PVD receptors.

One of the six receptors, FpvV, was unique in that it was not stimulated by the presence of its cognate siderophore, PVD_{Bn7}. We know that PVD_{Bn7} was indeed taken up by the cell, based on the restored growth observed by both Pf-5 Δ*pvdI* Δ*pchA* and Pf-5 Δ*pvdS* (Fig. 3.2, supporting information Fig. S3.2). This indicates that basal levels of FpvV were sufficient to import PVD_{Bn7}. Furthermore, like the other ferric-PVD receptors, FpvV also has an adjacent ECF/anti-ECF pair which should permit regulation. Our result could potentially be explained by the degradation of the regulatory system if selection has not been maintaining preservation of the signaling domains of the receptor, ECF or anti-ECF. In contrast, supernatants containing PVD_{B10} induced expression of three *fpv* genes, those encoding FpvV, FpvX, and the cognate receptor for PVD_{B10}, FpvW. This likely reflects a degree of structural promiscuity that can occur between PVDs and receptors (Hartney *et al.*, 2013). Although uptake of PVD_{B10} has been shown to require FpvW, it may interact enough other ECFs to activate *fpvV* and *fpvX*.

The observation that Pf-5 continues to produce $PVD_{Pf\text{-}5}$ despite the opportunity and capability to cross-feed on siderophores from other organisms was very intriguing (Fig. 3.2). Considering that many bacteria have adapted to an obligate free-loading lifestyle, exclusive use of siderophores from neighboring cells (D'Onofrio *et al.*, 2010; Cordero *et al.*, 2012; Andersen *et al.*, 2015), one might expect $PVD_{Pf\text{-}5}$ production to decrease as a strategy to conserve resources in favor of cross-feeding (West *et al.*, 2006). However, our data were very clear that Pf-5 does not adopt such a "free-loader" strategy, as regulation of endogenous $PVD_{Pf\text{-}5}$ biosynthesis was not impacted by the availability of heterologous PVDs (Fig. 3.2). Although the benefits of this behavior could not be seen in our mono-culture experiments, a clear benefit emerged in the context of interspecies competition. We found that the success of Pf-5 against inter-species competitor PAO1 was contingent on production of $PVD_{Pf\text{-}5}$ (Fig. 3.5), which we subsequently demonstrated reduces growth rate of PAO1 (Fig. 3.6), presumably by sequestering iron from PAO1.

Our findings collectively demonstrate the fitness benefits of continued $PVD_{Pf\text{-}5}$ production outweigh the benefits of free-loading, at least in the conditions used in our study. In fact, we did not observe any appreciable fitness cost associated with $PVD_{Pf\text{-}5}$ production, contrasting previous studies on the social evolution of siderophore cooperation in *P. aeruginosa* (Griffin *et al.*, 2004). Such a fitness cost should be discernable as slower growth of a strain that produces a secreted product, compared to one that does not (West *et al.*, 2006). This was not observed in our mono-culture growth experiments, where cross-feeding Pf-5 Δ*pvdI* Δ*pchA* and Pf-5 Δ*pvdS* grow at similar rates to the Pf-5 WT (Fig. 3.2). Furthermore, we would predict a cost of production to manifest in direct competitions between a PVD producer and a PVD-negative cheater (Griffin *et al.*, 2004; West *et al.*, 2006). However, we found Pf-5 Δ*pvdS* and its parental Pf-5 WT grow at equal rates in co-culture. This result is consistent with an emerging body of literature indicating fitness costs are contingent on resource availability (Mellbye and Schuster, 2011; Xavier *et al.*, 2011; Sexton and Schuster, 2017). Because our growth medium is composed of amino acids, there is a relative surplus of carbon and nitrogen thereby reducing the effect of PVD biosynthesis on growth rate. Although it is plausible that the free-loading strategy may offer more measurable benefits under other contexts, it is clear that the antagonistic role of $PVD_{Pf\text{-}5}$ against PAO1 warrants its continued production under the conditions explored here.

Considering Pf-5 continues to manufacture its own siderophore, questions are raised regarding the benefits of carrying receptors for heterologous siderophores at all. One explanation consistent with our data emphasizes a role in niche invasion. By secreting siderophores, micro-organisms construct niches for themselves by excluding iron access to competitors (Loper and Buyer, 1991; McNally and Brown, 2015). Pf-5 could therefore use its collection of heterologous siderophore receptors to break into niches previously established by competing siderophore-producers. This explanation does not require the benefit to manifest as an immediate relative growth advantage but simply provides an opportunity to become established. The competitive advantage is realized subsequently as active biosynthesis of its own siderophore $PVD_{Pf\text{-}5}$ impedes the original resident and provides an opportunity to take over the niche. It is also noteworthy that Pf-5

continues to produce PVD even when provided with sufficient levels of its own $PVD_{Pf\text{-}5}$ for robust growth (Fig. 3.2). Taken together, our data show $PVD_{Pf\text{-}5}$ expression is tuned to exceed what is necessary for iron acquisition, and are consistent with an additional role in competition.

The crucial role siderophores play in shaping microbial community composition is increasingly appreciated (Haas and Défago, 2005; Loper *et al.*, 2007; D'Onofrio *et al.*, 2010; Andersen *et al.*, 2015; Niehus *et al.*, 2017). In addition to solubilizing ferric iron from minerals for the initial establishment of microbial communities, they can further influence local community composition through their exclusivity. We have provided novel insights into how soil bacterium *P. protegens* Pf-5 optimizes its behavior to not only intercept siderophores from neighboring species, but to also actively exclude them through production of its own siderophore. These findings have implications for understanding the interactions that mediate iron availability in many diverse and important environments.

Materials and methods

Bacterial strains, growth conditions and media

Bacterial strains used in this study are described in Table 3.2. *Pseudomonas sp*. strains were routinely maintained in Lennox LB broth or on agar plates and incubated at 30°C. Prior to all experiments, single colonies were used to inoculate 4 mL liquid cultures of LB broth buffered to a pH = 7 with 50 mM 3-(N-morpholino) propanesulfonic acid (MOPS) and incubated with shaking for 18 hours. These cultures were subsequently washed twice in a salt base containing 0.118% (w/v) $K_2HPO_4 \cdot 3\ H_2O$, 0.025% (w/v) $MgSO_4 \cdot 7\ H_2O$ and 50 mM MOPS. For the measurement of receptor expression levels, cultures were grown in casamino acids (CAA) medium, consisting of the salt base with 0.5% (w/v) CAA, 1 μM $FeCl_3 \cdot\ 6\ H_2O$. For competition experiments, the medium was supplemented with 0.5 mg/mL (140 mM) of the synthetic iron chelator EDDHA (CAA-EDDHA), a concentration chosen for consistency with previous studies. Cross-feeding experiments were instead supplemented with 100 μM. As we found through experimentation,140 mM far exceeds what is necessary, so concentrations were lowered

to conserve resources (Complete Green Co. El Segundo, California). As only 1 μM iron is present, both concentrations ensure that all iron is chelated and are functionally equivalent. In-frame deletion of the *pvdS* gene in Pf-5 (PFL_4190) was constructed by splicing-by-overlap-extension PCR and allelic exchange as described (Horton, 1995; Hoang *et al.*, 1998). The primers used for this are provided in Supporting Information, Table S3.2.

PVD quantification and supernatant supplementations

In all experiments, PVD was measured as relative fluorescence units (excitation and emission wavelengths of 400 nm and 460 nm, respectively) using a Tecan Infinite M200 plate reader (Tecan Group Ltd, Männedorf, Switzerland, Supporting Information Fig. S3.1). Molar concentrations were determined using a standard curve constructed with purified PVD (EMC, Micro-collections, Tübingen, Germany) (Meyer and Abdallah, 1978; Hoegy *et al.*, 2014). PVD-containing supernatants were diluted into indicated growth media to achieve either 10 μM or 100 μM PVD. To maintain consistent concentrations of nutrients in the growth media, supernatant supplements displaced equal volumes of water. For experiments designed to study the regulation of PVD biosynthesis, continued production of $PVD_{Pf\text{-}5}$ was observed as an increase of relative fluorescence units over the background levels present due to the heterologous PVDs added.

Real-time PCR

For comparison of receptor expression levels, Pf-5 Δ*pvdI* Δ*pchA* cultures were harvested after 18 hours of growth in the described CAA-based medium supplemented with the designated supernatant. RNA was extracted and converted to cDNA as described (Schuster, 2011). Primer pairs were designed specifically for each receptor using Primer Express 3.0.1 (Supporting Information, Table S3.1). The Pf-5 genome was considered in the primer design to avoid amplification of unintended products, and empirically corroborated by melt curve analysis. Real-Time PCR was performed with the ABI PRISM® 7500 FAST Sequence Detection System using SybrGreen. Data was analyzed

using 7500 Software v2.0.6. Transcript levels are expressed as the fold change relative to a "no supernatant" control.

Competitions and fitness measurement.

Overnight cultures of designated strains were mixed to 1:1 ratios and co-cultured in CAA-EDDHA. To distinguish sub-populations in interspecies competitions, CFUs were counted on both LB plates incubated at 37°C (selective for PAO1) and LB plates supplemented with 200 µg/mL carbenicillin (selective for Pf-5). For within-species competitions, antibiotic resistance markers for gentamicin and tetracycline were incorporated into the chromosome using the miniTn7 system (Choi and Schweizer, 2006). Pf-5 GmR and Pf-5 Δ*pvdS* TetR were distinguished by selective plating onto LB agar supplemented with gentamicin (50 µg/mL) or tetracycline (100 µg/mL)

Supporting information

SI Figures

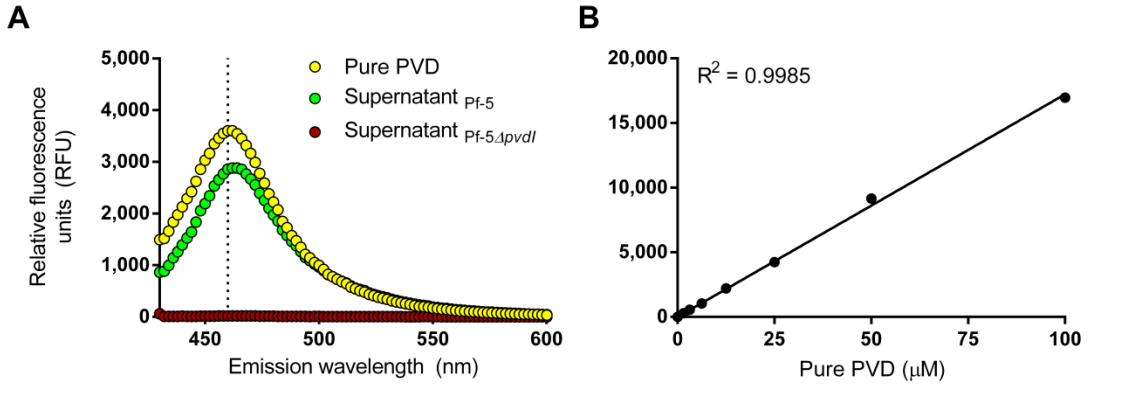

Figure S3.1 PVD detection based on inherent fluorescence properties using Tecan Infinite M200 plate reader. (A) A fluorescence emission scan with excitation set at 400 nm comparing RFU of purified PVD (yellow), supernatant from Pf-5 WT (green) and supernatant from Pf-5 Δ*pvdI* (red). Dotted line indicates emission wavelength of 460 nm, which was used for all quantitative measurements of PVD reported in this study. (B) PVD concentrations in bacterial supernatants were interpolated after constructing a standard curve with purified PVD (EMC, Microcollections).

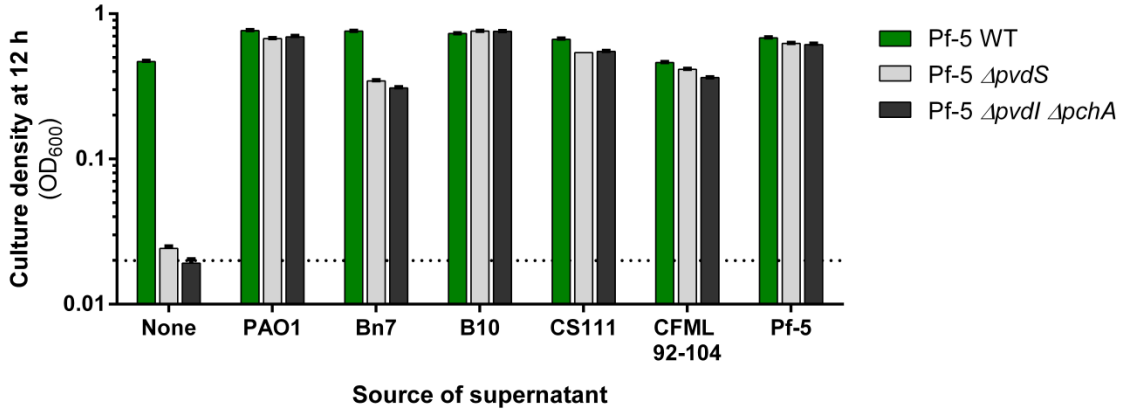

Figure S3.2 Confirmation of cross-feeding phenotypes. Pf-5 WT (green), Pf-5 Δ*pvdS* (light gray) and Pf-5 Δ*pvdI* Δ*pchA* (dark gray) were cultured in CAA-EDDHA alone or supplemented with supernatant from the strain indicated on the x-axis. Supernatants were adjusted to provide 10 µM of PVD. The dotted line on the Y-axis shows the starting inoculum density. Error bars show standard deviation of the mean (n=3) and are too small to be seen in most cases.

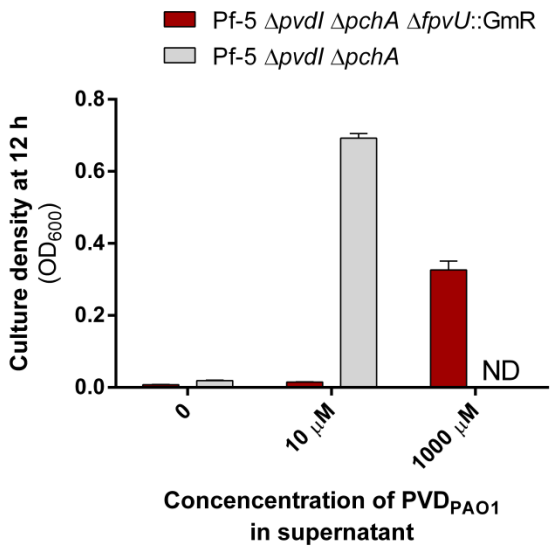

Figure S3.3 Selecting target concentration of PVD in cross-feeding experiments. FpvU specifically recognizes PVD_{PAO1}. However, if concentrations are high, we find that a Pf-5 Δ*pvdI* Δ*pchA* Δ*fpvU*::GmR mutant is able to grow on PVD_{PAO1}, likely due to non-specific binding with other receptors. By using supernatant concentrations equivalent to 10 µM PVD_{PAO1}, we can eliminate this effect while retaining robust cross-feeding. ND indicates not determined.

Table S3.1 Primers used for real-time PCR

Receptor gene and primers	Sequence in 5' to 3' direction
***fpvU* (PFL_2391[a])**	
Pf-5 FpvU F2	CGGCAGCACATGGAAGATTT
Pf-5 FpvU R2	TACCGTCGTACTGGAAGTTGTTGA
***fpvV* (PFL_2527)**	
Pf-5 FpvV F	CCAAGGTCAAGCGTGAAGAAA
Pf-5 FpvV R	GTAGACCACCCCGGCGTAA
***fpvW* (PFL_2293)**	
Pf-5 FpvW F	GGCCAGCACTCGCTCAA
Pf-5 FpvW R	AGGTTCTGGTCATCGAGCATCT
***fpvX* (PFL_3315)**	
Pf-5 FpvX F	GCGCGGACGCTTTGTC
Pf-5 FpvX R	TAGGCGATGTCCTTGGTGTTC
***fpvY* (PFL_3485)**	
Pf-5 FpvY F	TTCCAGTACGACGGGATTCC
Pf-5 FpvY R	GGTGTGGCCCGAGGAGTA
***fpvZ* (PFL_4092)**	
Pf-5 FpvZ F	CAGGACTTCGTCAGCAGTGAAC
Pf-5 FpvZ R	GCCAAAAGTGAAGGTGGTGTCT

[a]Indicates gene locus tag

Table S3.2 SOE Primers used for construction of Pf-5 Δ*pvdS*

Gene and primers	Sequence 5'-3'[a]
Pf-5 *ΔpvdS* (PFL_4190)	
Pf-5 pvdS F1b	$(N)_6$**GAGCTC**TTGAGGTCGATACCGAAGCCGCG
Pf-5 pvdS R1	TTCCGT*CAT*GGAAATCACCTTGTTGCAAAGAGGTTAGTG
Pf-5 pvdS F2	C*ATG*ACGGAAGCCCGTCGC*TGA*CTGGCGCCCTGCATGA
Pf-5 pvdS R2b	$(N)_6$**TCTAGA**TCGTCGCCCAGCGTCAGGGCG

[a] N indicates random base, bold font identifies restriction enzyme sites, italics indicate start and stop codons.

Chapter 4

Conclusions

Siderophore production is a cooperative behavior that has gained significant attention in the past 15 years (Griffin *et al.*, 2004; Buckling *et al.*, 2007). In addition to the use of siderophores as model systems, there is substantial evidence that social dynamics are relevant to the evolution of siderophore producing populations in natural and applied environments. However, it is often challenging to resolve whether a siderophore-negative isolate evolved as a social cheater or due to other non-social adaptations. Therefore, a current goal in the field is to better understand the fitness cost of siderophore production such that these two explanations can be more readily distinguished. In chapter 2 of this dissertation, we demonstrate the growth-limiting nutrient is a key determinant in distinguishing these two scenarios (Fig. 2.3). Perhaps counterintuitively, our findings indicate siderophore production should not be vulnerable to cheaters when iron is growth rate-limiting. Instead, a component of the siderophore itself must be limiting (i.e. C or N, in the case of PVD). However, the iron availability must still be low enough to stimulate siderophore production, a nuanced scenario that demands tedious consideration of how terms such as "limiting" are applied.

The relationship between nutrient limitation and fitness cost is certainly relevant to current conversations about siderophore-negative isolates observed in nature. In short, if the growth-limiting nutrient in the environment of question is also a building block of the siderophore, there should be potential for cheating. In the context of the cystic fibrosis lung, the sputum is known to contain high concentrations of debris from dead cells, amino acids and other macromolecules that are rich in carbon and nitrogen (Palmer *et al.*, 2007). The finding that PVD-negatives tend to retain their receptor when co-existing with a PVD-producer is certainly enticing (Andersen *et al.*, 2015); however, our data provide multiple examples where the ability to utilize another strain's siderophore does not necessarily manifest as a fitness advantage or burden on the producing sub-population (Fig. 2.3, S2.4, 3.5 and Table S2.2). Combined with other mechanisms known to limit cheaters, such as spatial structure and siderophore recycling (Kümmerli and Brown, 2010; Luján *et al.*, 2015), along with evidence that alternative iron acquisition

mechanisms are replacing siderophore production (Marvig *et al.*, 2014), non-social adaptation rather than social cheating may be a more parsimonious explanation for PVD-negative isolates in the cystic fibrosis lung.

In contrast, the potential for social cheating to explain siderophore-negative marine isolates seems more viable (D'Onofrio *et al.*, 2010; Cordero *et al.*, 2012). Indeed, one study was based on a collection of isolates from Plum Island Estuary (Cordero *et al.*, 2012), a site known to experience episodic blooms due to anthropogenic nitrogen run off, indicating that at least in some cases when such a bloom is not occurring, nitrogen is limiting. Our findings, combined with the relatively low spatial structure and higher diffusion rates associated with aquatic environments, corroborates the hypothesis that social cheating selects for siderophore-negative isolates in this case (Cordero *et al.*, 2012).

More broadly, our findings demonstrate how the stability of cooperation can rest on relative resource abundance. This principle has relevance to not only siderophores, but cooperation in general. There is growing evidence that supports this in other microbial secretions as well (Xavier *et al.*, 2011; Mellbye and Schuster, 2014). It is conceivable that even humans might improve efforts to cooperate by considering resource availability; if cooperation depletes a limiting resource, it is less likely to be stable than if it taxes something in excess.

In Chapter 3, we focused on the strategies at play during interspecies siderophore-mediated competition for iron. Such interactions are often more complex than the binary cooperator vs. obligate free-loader scenario that is more commonly studied. Specifically, many strains are capable of using siderophores originating from other species, yet retain the ability to produce their own. Although siderophore uptake capabilities have been characterized in some strains (Hartney *et al.*, 2013; Miethke *et al.*, 2013), less is known about how biosynthesis of the native siderophore responds to cross-feeding opportunities. Considering the extent to which bacteria can fine-tune gene expression, one might expect biosynthesis of the native siderophore to be repressed when another siderophore is available. However, in the agriculturally relevant biocontrol strain *P. protegens* Pf-5, we found this is not the case. Instead, Pf-5 continues to produce its native $PVD_{Pf\text{-}5}$ whether or

not other siderophores are available. Although an explanation for this was not initially clear, we soon found this behavior could be understood when in co-cultured with a competitor. We found $PVD_{Pf\text{-}5}$ has an antagonistic effect against *P. aeruginosa* that is needed for Pf-5 to maintain a competitive edge. This indicates the benefits of antagonizing a competitor outweigh the costs associated with PVD production for Pf-5.

The primary findings presented in this dissertation complement each other. Our chemostat work largely suggests PVD production should not come at a significant fitness cost, particularly when carbon and nitrogen are in excess. If there is little cost to PVD biosynthesis, it is then not so surprising that Pf-5 continues to produce $PVD_{Pf\text{-}5}$ irrespective of siderophore availability. For Pf-5, carrying a wide array of siderophore receptors may play a bigger role when invading an established niche, rather than representing a strategy to save biosynthetic costs (Loper and Buyer, 1991; McNally and Brown, 2015). Cross-feeding likely helps when getting established, but production of the native siderophore may be the key to taking over the niche. This suggests an optimistic prediction might be made regarding the stability of siderophore production for agricultural applications, although clearly this view is limited to considerations of just one of many interactions.

In summary, the work presented in this dissertation provides new insights to fundamental aspects of siderophore cooperation. These findings contribute to current conversations about the role of social dynamics in a number of contexts including natural microbial communities, human infections and agricultural applications. This work, and others like it, will help further refine the predictive power of the social evolution framework, which is needed to help understand the many cooperative behaviors of microorganisms, and even cooperation in general.

Bibliography

Adams, H., Zeder-Lutz, G., Schalk, I., Pattus, F., and Celia, H. (2006) Interaction of TonB with the outer membrane receptor FpvA of *Pseudomonas aeruginosa*. *J Bacteriol* **188**: 5752–5761.

Albrecht-Gary, A.-M., Blanc, S., Rochel, N., Ocaktan, A.Z., and Abdallah, M.A. (1994) Bacterial iron transport: Coordination properties of pyoverdin PaA, a peptidic siderophore of *Pseudomonas aeruginosa*. *Inorg Chem* **33**: 6391–6402.

Andersen, S.B., Marvig, R.L., Molin, S., Johansen, H.K., and Griffin, A.S. (2015) Long-term social dynamics drive loss of function in pathogenic bacteria. *Proc Natl Acad Sci* **112**: 10756–10761.

Barbhaiya, H. B., and Rao, K. K. (1985) Production of pyoverdine, the fluorescent pigment of *Pseudomonas aeruginosa* PAO1. *FEMS Microbiol Lett* **27**: 233–235.

Baron, C. (2010) Antivirulence drugs to target bacterial secretion systems. *Curr Opin Microbiol* **13**: 100–105.

Baysse, C., Budzikiewicz, H., Uria Fernandez, D., and Cornelis, P. (2002) Impaired maturation of the siderophore pyoverdine chromophore in *Pseudomonas fluorescens* ATCC 17400 deficient for the cytochrome c biogenesis protein CcmC. *FEBS Lett* **523**: 23–8.

Becker, S.A., Feist, A.M., Mo, M.L., Hannum, G., Palsson, B.Ø., and Herrgard, M.J. (2007) Quantitative prediction of cellular metabolism with constraint-based models: the COBRA Toolbox. *Nat Protoc* **2**: 727–738.

Boer, V.M., Crutchfield, C.A., Bradley, P.H., Botstein, D., and Rabinowitz, J.D. (2010) Growth-limiting intracellular metabolites in yeast growing under diverse nutrient limitations. *Mol Biol Cell* **21**: 198–211.

Brocchieri, L., and Karlin, S. (2005) Protein length in eukaryotic and prokaryotic proteomes. *Nucleic Acids Res* **33**: 3390–3400.

Brockhurst, M.A., Buckling, A., Racey, D., and Gardner, A. (2008) Resource supply and the evolution of public-goods cooperation in bacteria. *BMC Biol* **6**: 20.

Brown, S.P., and Taddei, F. (2007) The durability of public goods changes the dynamics and nature of social dilemmas. *Plos One* **2**: e593.

Buckling, A., Harrison, F., Vos, M., Brockhurst, M.A., Gardner, A., West, S.A., and Griffin, A. (2007) Siderophore-mediated cooperation and virulence in *Pseudomonas aeruginosa*. *FEMS Microbiol Ecol* **62**: 135–141.

Calcott, M.J., Owen, J.G., Lamont, I.L., and Ackerley, D.F. (2014) Biosynthesis of novel pyoverdines by domain substitution in a nonribosomal peptide synthetase of *Pseudomonas aeruginosa*. *Appl Environ Microbiol* **80**: 5723–5731.

Calderwood, S.B., and Mekalanos, J.J. (1988) Confirmation of the Fur operator site by insertion of a synthetic oligonucleotide into an operon fusion plasmid. *J Bacteriol* **170**: 1015–1017.

Caza, M., and Kronstad, J.W. (2013) Shared and distinct mechanisms of iron acquisition by bacterial and fungal pathogens of humans. *Front Cell Infect Microbiol* **3**: 80.

Challis, G.L., and Naismith, J.H. (2004) Structural aspects of non-ribosomal peptide biosynthesis. *Curr Opin Struct Biol* **14**: 748–756.

Choi, K.-H., and Schweizer, H.P. (2006) mini-Tn7 insertion in bacteria with single attTn7 sites: example *Pseudomonas aeruginosa*. *Nat Protoc* **1**: 153–161.

Cobessi, D., Celia, H., Folschweiller, N., Schalk, I.J., Abdallah, M.A., and Pattus, F. (2005) The crystal structure of the pyoverdine outer membrane receptor FpvA from *Pseudomonas aeruginosa* at 3.6 angstroms resolution. *J Mol Biol* **347**: 121–134.

Cordero, O.X., Ventouras, L.-A., DeLong, E.F., and Polz, M.F. (2012) Public good dynamics drive evolution of iron acquisition strategies in natural bacterioplankton populations. *Proc Natl Acad Sci* **109**: 20059–20064.

Cornelis, P., Matthijs, S., and Van Oeffelen, L. (2009) Iron uptake regulation in *Pseudomonas aeruginosa*. *Biometals Int J Role Met Ions Biol Biochem Med* **22**: 15–22.

Cornforth, D.M., and Foster, K.R. (2013) Competition sensing: the social side of bacterial stress responses. *Nat Rev Microbiol* **11**: 285–293.

Crosa, J.H., and Walsh, C.T. (2002) Genetics and assembly line enzymology of siderophore biosynthesis in bacteria. *Microbiol Mol Biol Rev* **66**: 223-249

Dandekar, A.A., Chugani, S., and Greenberg, E.P. (2012) Bacterial quorum sensing and metabolic incentives to cooperate. *Science* **338**: 264–266.

Darch, S.E., West, S.A., Winzer, K., and Diggle, S.P. (2012) Density-dependent fitness benefits in quorum-sensing bacterial populations. *Proc Natl Acad Sci U S A* **109**: 8259–8263.

Dauner, M., Storni, T., and Sauer, U. (2001) *Bacillus subtilis* metabolism and energetics in carbon-limited and excess-carbon chemostat culture. *J Bacteriol* **183**: 7308–7317.

De Vos, D., De Chial, M., Cochez, C., Jansen, S., Tummler, B., Meyer, J.M., and Cornelis, P. (2001) Study of pyoverdine type and production by *Pseudomonas aeruginosa* isolated from cystic fibrosis patients: prevalence of type II pyoverdine

isolates and accumulation of pyoverdine-negative mutations. *Arch Microbiol* **175**: 384–388.

Denayer, S., Matthijs, S., and Cornelis, P. (2007) Pyocin S2 (Sa) kills *Pseudomonas aeruginosa* strains via the FpvA type I ferripyoverdine receptor. *J Bacteriol* **189**: 7663–8.

D'Onofrio, A., Crawford, J.M., Stewart, E.J., Witt, K., Gavrish, E., Epstein, S., *et al.* (2010) Siderophores from neighboring organisms promote the growth of uncultured bacteria. *Chem Biol* **17**: 254–264.

Dumas, Z., Ross-Gillespie, A., and Kümmerli, R. (2013) Switching between apparently redundant iron-uptake mechanisms benefits bacteria in changeable environments. *Proc Biol Sci* **280**: 20131055.

Edgar, R.J., Xu, X., Shirley, M., Konings, A.F., Martin, L.W., Ackerley, D.F., and Lamont, I.L. (2014) Interactions between an anti-sigma protein and two sigma factors that regulate the pyoverdine signaling pathway in *Pseudomonas aeruginosa*. *BMC Microbiol* **14**: 287 e10.1186

Evans, C., Herbert, D., and Tempest, D. (1970) Continuous cultivation of micro-organisms: Construction of a chemostat. In *Methods Microbiol*. pp. 277–327.

Farmer, I.S., and Jones, C.W. (1976) The energetics of *Escherichia coli* during aerobic growth in continuous culture. *Eur J Biochem* **67**: 115–122.

Ghysels, B., Dieu, B.T.M., Beatson, S.A., Pirnay, J.-P., Ochsner, U.A., Vasil, M.L., and Cornelis, P. (2004) FpvB, an alternative type I ferripyoverdine receptor of *Pseudomonas aeruginosa*. *Microbiol Read Engl* **150**: 1671–1680.

Gledhill, M., and Buck, K.N. (2012) The organic complexation of iron in the marine environment: a review. *Front Microbiol* **3**: 69. e10.3389

Gore, J., Youk, H., and Oudenaarden, A. van (2009) Snowdrift game dynamics and facultative cheating in yeast. *Nature* **459**: 253–256.

Green, E.R., and Mecsas, J. (2016) Bacterial Secretion Systems: An Overview. *Microbiol Spectr* **4**: e10.1128

Greenwald, J., Hoegy, F., Nader, M., Journet, L., Mislin, G.L.A., Graumann, P.L., and Schalk, I.J. (2007) Real time fluorescent resonance energy transfer visualization of ferric pyoverdine uptake in *Pseudomonas aeruginosa*. A role for ferrous iron. *J Biol Chem* **282**: 2987–2995.

Greenwald, J., Zeder-Lutz, G., Hagege, A., Celia, H., and Pattus, F. (2008) The Metal Dependence of pyoverdine interactions with Its outer membrane receptor FpvA. *J Bacteriol* **190**: 6548–6558.

Gresham, D., and Dunham, M.J. (2014) The enduring utility of continuous culturing in experimental evolution. *Genomics* **104**: 399–405.

Griffin, A.S., West, S.A., and Buckling, A. (2004) Cooperation and competition in pathogenic bacteria. *Nature* **430**: 1024–1027.

Gupta, R., and Schuster, M. (2013) Negative regulation of bacterial quorum sensing tunes public goods cooperation. *ISME J* **7**: 2159–2168.

Haas, B., Kraut, J., Marks, J., Zanker, S.C., and Castignetti, D. (1991) Siderophore presence in sputa of cystic fibrosis patients. *Infect Immun* **59**: 3997–4000.

Haas, D., and Défago, G. (2005) Biological control of soil-borne pathogens by fluorescent pseudomonads. *Nat Rev Microbiol* **3**: 307–319.

Hall, A.R., and Colegrave, N. (2007) How does resource supply affect evolutionary diversification? *Proc Biol Sci* **274**: 73–78.

Hannauer, M., Yeterian, E., Martin, L.W., Lamont, I.L., and Schalk, I.J. (2010) An efflux pump is involved in secretion of newly synthesized siderophore by *Pseudomonas aeruginosa*. *FEBS Lett* **584**: 4751–4755.

Harder, W., and Dijkhuizen, L. (1983) Physiological responses to nutrient limitation. *Annu Rev Microbiol* **37**: 1–23.

Hardin, G. (1968) The tragedy of the commons. *Science* **162**: 1243–1248.

Harrison, F. (2013) Dynamic social behaviour in a bacterium: *Pseudomonas aeruginosa* partially compensates for siderophore loss to cheats. *J Evol Biol* **26**: 1370–1378.

Harrison, F., Browning, L.E., Vos, M., and Buckling, A. (2006) Cooperation and virulence in acute *Pseudomonas aeruginosa* infections. *BMC Biol* **4**: 21. e10.1186

Harrison, F., and Buckling, A. (2009) Siderophore production and biofilm formation as linked social traits. *ISME J* **3**: 632–634.

Harrison, F., Paul, J., Massey, R.C., and Buckling, A. (2007) Interspecific competition and siderophore-mediated cooperation in *Pseudomonas aeruginosa*. *ISME J* **2**: 49–55.

Hartney, S.L., Mazurier, S., Girard, M.K., Mehnaz, S., Davis, 2nd, E.W., Gross, H., *et al.* (2013) Ferric-pyoverdine recognition by Fpv outer membrane proteins of *Pseudomonas protegens* Pf-5. *J Bacteriol* **195**: 765–776.

Hartney, S.L., Mazurier, S., Kidarsa, T.A., Quecine, M.C., Lemanceau, P., and Loper, J.E. (2011) TonB-dependent outer-membrane proteins and siderophore utilization in *Pseudomonas fluorescens* Pf-5. *Biometals* **24**: 193–213.

Hassan, H.M., and Troxell, B. (2013) Transcriptional regulation by Ferric Uptake Regulator (Fur) in pathogenic bacteria. *Front Cell Infect Microbiol* **3**: e10.3389

Hider, R.C., and Kong, X. (2010) Chemistry and biology of siderophores. *Nat Prod Rep* **27**: 637-657

Hoang, T.T., Karkhoff-Schweizer, R.R., Kutchma, A.J., and Schweizer, H.P. (1998) A broad-host-range Flp-FRT recombination system for site-specific excision of chromosomally-located DNA sequences: application for isolation of unmarked *Pseudomonas aeruginosa* mutants. *Gene* **212**: 77–86.

Hoegy, F., Mislin, G.L.A., and Schalk, I.J. (2014) Pyoverdine and pyochelin measurements. *Methods Mol Biol* **1149**: 293–301.

Horton, R.M. (1995) PCR-mediated recombination and mutagenesis. SOEing together tailor-made genes. *Mol Biotechnol* **3**: 93–99.

Imperi, F., Tiburzi, F., and Visca, P. (2009) Molecular basis of pyoverdine siderophore recycling in *Pseudomonas aeruginosa*. *Proc Natl Acad Sci U S A* **106**: 20440–20445.

Jain, R., and Srivastava, R. (2009) Metabolic investigation of host/pathogen interaction using MS2-infected *Escherichia coli*. *BMC Syst Biol* **3**: 121.

Jiricny, N., Diggle, S.P., West, S.A., Evans, B.A., Ballantyne, G., Ross-Gillespie, A., and Griffin, A.S. (2010) Fitness correlates with the extent of cheating in a bacterium. *J Evol Biol* **23**: 738–747.

Joshi, F., Archana, G., and Desai, A. (2006) Siderophore cross-utilization amongst rhizospheric bacteria and the role of their differential affinities for Fe3+ on growth stimulation under iron-limited conditions. *Curr Microbiol* **53**: 141–147.

King, E.O., Ward, M.K., and Raney, D.E. (1954) Two simple media for the demonstration of pyocyanin and fluorescein. *J Lab Clin Med* **44**: 301–307.

Kloepper, J.W., Leong, J., Teintze, M., and Schroth, M.N. (1980) Enhanced plant growth by siderophores produced by plant growth-promoting rhizobacteria. *Nature* **286**: 885–886.

Koster, M., Klompenburg, W. van, Bitter, W., Leong, J., and Weisbeek, P. (1994) Role for the outer membrane ferric siderophore receptor PupB in signal transduction across the bacterial cell envelope. *EMBO J* **13**: 2805–2813.

Kümmerli, R., Berg, P. van den, Griffin, A.S., West, S.A., and Gardner, A. (2010) Repression of competition favours cooperation: experimental evidence from bacteria. *J Evol Biol* **23**: 699–706.

Kümmerli, R., and Brown, S.P. (2010) Molecular and regulatory properties of a public good shape the evolution of cooperation. *Proc Natl Acad Sci* **107**: 18921–18926.

Kümmerli, Rolf, Gardner, A., West, S.A., and Griffin, A.S. (2009) Limited dispersal, budding dispersal, and cooperation: an experimental study. *Evol Int J Org Evol* **63**: 939–949.

Kümmerli, Rolf, Griffin, A.S., West, S.A., Buckling, A., and Harrison, F. (2009) Viscous medium promotes cooperation in the pathogenic bacterium *Pseudomonas aeruginosa*. *Proc Biol Sci* **276**: 3531–3538.

Kümmerli, R., Jiricny, N., Clarke, L.S., West, S.A., and Griffin, A.S. (2009) Phenotypic plasticity of a cooperative behaviour in bacteria. *J Evol Biol* **22**: 589–598.

Kümmerli, R., and Ross-Gillespie, A. (2014) Explaining the sociobiology of pyoverdin producing *Pseudomonas*: a comment on Zhang and Rainey (2013). *Evol Int J Org Evol* **68**: 3337–3343.

Kümmerli, R., Schiessl, K.T., Waldvogel, T., McNeill, K., and Ackermann, M. (2014) Habitat structure and the evolution of diffusible siderophores in bacteria. *Ecol Lett* **17**: 1536–1544.

Lamont, I.L., Beare, P.A., Ochsner, U., Vasil, A.I., and Vasil, M.L. (2002) Siderophore-mediated signaling regulates virulence factor production in *Pseudomonas aeruginosa*. *Proc Natl Acad Sci U S A* **99**: 7072–7077.

Lee, W., Baalen, M. van, and Jansen, V.A.A. (2012) An evolutionary mechanism for diversity in siderophore-producing bacteria. *Ecol Lett* **15**: 119–125.

Lehmann, L., and Keller, L. (2006) The evolution of cooperation and altruism--a general framework and a classification of models. *J Evol Biol* **19**: 1365–1376.

Lenski, R.E. (1991) Quantifying fitness and gene stability in microorganisms. *Biotechnol Read Mass* **15**: 173–192.

Lim, C.K., Hassan, K.A., Tetu, S.G., Loper, J.E., and Paulsen, I.T. (2012) The effect of iron limitation on the transcriptome and proteome of *Pseudomonas fluorescens* Pf-5. *Plos One* **7**.e10.1371

Loper, J.E., and Buyer, J.S. (1991) Siderophores in microbial interactions on plant-surfaces. *Mol Plant Microbe Interact* **4**: 5–13.

Loper, J.E., Kobayashi, D.Y., and Paulsen, I.T. (2007) The genomic sequence of *Pseudomonas fluorescens* Pf-5: Insights into biological control. *Phytopathology* **97**: 233–238.

Luján, A.M., Gómez, P., and Buckling, A. (2015) Siderophore cooperation of the bacterium *Pseudomonas fluorescens* in soil. *Biol Lett* **11**:

Lyczak, J.B., Cannon, C.L., and Pier, G.B. (2002) Lung infections associated with cystic fibrosis. *Clin Microbiol Rev* **15**: 194–222.

Marvig, R.L., Damkiær, S., Khademi, S.M.H., Markussen, T.M., Molin, S., and Jelsbak, L. (2014) Within-host evolution of *Pseudomonas aeruginosa* reveals adaptation toward iron acquisition from hemoglobin. *mBio* **5**: e00966-00914.

McMorran, B.J., Merriman, M.E., Rombel, I.T., and Lamont, I.L. (1996) Characterisation of the pvdE gene which is required for pyoverdine synthesis in *Pseudomonas aeruginosa*. *Gene* **176**: 55–59.

McNally, L., and Brown, S.P. (2015) Building the microbiome in health and disease: niche construction and social conflict in bacteria. *Phil Trans R Soc B* **370**: 20140298.

Mellbye, B., and Schuster, M. (2011) The sociomicrobiology of antivirulence drug resistance: a proof of concept. *MBio* **2**. e00131-11

Mellbye, B., and Schuster, M. (2014) Physiological framework for the regulation of quorum sensing-dependent public goods in *Pseudomonas aeruginosa*. *J Bacteriol* **196**: 1155–1164.

Meyer, J.M., and Abdallah, M.A. (1978) The fluorescent pigment of *Pseudomonas fluorescens*: Biosynthesis, purification and physicochemical properties. *Microbiology* **107**: 319–328.

Meyer, J.M., Geoffroy, V.A., Baida, N., Gardan, L., Izard, D., Lemanceau, P., *et al.* (2002) Siderophore typing, a powerful tool for the identification of fluorescent and nonfluorescent pseudomonads. *Appl Environ Microbiol* **68**: 2745–2753.

Meyer, J.-M., Gruffaz, C., Raharinosy, V., Bezverbnaya, I., Schäfer, M., and Budzikiewicz, H. (2008) Siderotyping of fluorescent *Pseudomonas*: molecular mass determination by mass spectrometry as a powerful pyoverdine siderotyping method. *Biometals Int J Role Met Ions Biol Biochem Med* **21**: 259–271.

Meyer, J.M., Neely, A., Stintzi, A., Georges, C., and Holder, I.A. (1996) Pyoverdin is essential for virulence of *Pseudomonas aeruginosa*. *Infect Immun* **64**: 518–523.

Miethke, M., Kraushaar, T., and Marahiel, M.A. (2013) Uptake of xenosiderophores in *Bacillus subtilis* occurs with high affinity and enhances the folding stabilities of substrate binding proteins. *Febs Lett* **587**: 206–213.

Minandri, F., Imperi, F., Frangipani, E., Bonchi, C., Visaggio, D., Facchini, M., *et al.* (2016) Role of iron uptake systems in *Pseudomonas aeruginosa* virulence and airway infection. *Infect Immun* **84**: 2324–2335.

Moore, C.M., Mills, M.M., Arrigo, K.R., Berman-Frank, I., Bopp, L., Boyd, P.W., *et al.* (2013) Processes and patterns of oceanic nutrient limitation. *Nat Geosci* **6**: 701–710.

Moreau-Marquis, S., Bomberger, J.M., Anderson, G.G., Swiatecka-Urban, A., Ye, S., O'Toole, G.A., and Stanton, B.A. (2008) The ΔF508-CFTR mutation results in increased biofilm formation by *Pseudomonas aeruginosa* by increasing iron availability. *Am J Physiol Lung Cell Mol Physiol* **295**: L25–L37.

Morris, J.J., Lenski, R.E., and Zinser, E.R. (2012) The Black Queen Hypothesis: evolution of dependencies through adaptive gene loss. *mBio* **3**. e00036-12

Nadell, C.D., Bassler, B.L., and Levin, S.A. (2008) Observing bacteria through the lens of social evolution. *J Biol* **7**: 27.

Nadell, C.D., Drescher, K., and Foster, K.R. (2016) Spatial structure, cooperation and competition in biofilms. *Nat Rev Microbiol* **14**: 589–600.

Nagata, T., Oobo, T., and Aozasa, O. (2013) Efficacy of a bacterial siderophore, pyoverdine, to supply iron to *Solanum lycopersicum* plants. *J Biosci Bioeng* **115**: 686–690.

Neidhardt, F.C., Ingraham, J.L., and Schaechter, M. (1990) Physiology of the bacterial cell: A molecular approach. *Sinauer Associates*

Niehus, R., Picot, A., Oliveira, N.M., Mitri, S., and Foster, K.R. (2017) The evolution of siderophore production as a competitive trait. *Evolution*. *In press*

Noinaj, N., Guillier, M., Travis J. Barnard, and Buchanan, S.K. (2010) TonB-dependent transporters: Regulation, structure, and function. *Annu Rev Microbiol* **64**: 43–60.

Nowak, M.A., and Sigmund, K. (1998) What two legs can learn from four legs. *Nature* **395**: 760–761.

Oberhardt, M.A., Puchałka, J., Fryer, K.E., Martins dos Santos, V.A.P., and Papin, J.A. (2008) Genome-scale metabolic network analysis of the opportunistic pathogen *Pseudomonas aeruginosa* PAO1. *J Bacteriol* **190**: 2790–2803.

Oberhardt, M.A., Puchałka, J., Martins dos Santos, V.A.P., and Papin, J.A. (2011) Reconciliation of genome-scale metabolic reconstructions for comparative systems analysis. *PLoS Comput Biol* **7**: e1001116.

Ochsner, U.A., Johnson, Z., Lamont, I.L., Cunliffe, H.E., and Vasil, M.L. (1996) Exotoxin A production in *Pseudomonas aeruginosa* requires the iron-regulated *pvdS* gene encoding an alternative sigma factor. *Mol Microbiol* **21**: 1019–1028.

Ochsner, U.A., Wilderman, P.J., Vasil, A.I., and Vasil, M.L. (2002) GeneChip expression analysis of the iron starvation response in *Pseudomonas aeruginosa*: identification of novel pyoverdine biosynthesis genes. *Mol Microbiol* **45**: 1277–1287.

Pai, A., Tanouchi, Y., and You, L. (2012) Optimality and robustness in quorum sensing (QS)-mediated regulation of a costly public good enzyme. *Proc Natl Acad Sci U S A* **109**: 19810–19815.

Palmer, K.L., Aye, L.M., and Whiteley, M. (2007) Nutritional cues control *Pseudomonas aeruginosa* multicellular behavior in cystic fibrosis sputum. *J Bacteriol* **189**: 8079–8087.

Parray, J.A., Jan, S., Kamili, A.N., Qadri, R.A., Egamberdieva, D., and Ahmad, P. (2016) Current perspectives on plant growth-promoting rhizobacteria. *J Plant Growth Regul* **35**: 877–902.

Parret, A.H., and De Mot, R. (2002) Bacteria killing their own kind: novel bacteriocins of *Pseudomonas* and other gamma-proteobacteria. *Trends Microbiol* **10**: 107–112.

Poole, K., Neshat, S., Krebes, K., and Heinrichs, D.E. (1993) Cloning and nucleotide sequence analysis of the ferripyoverdine receptor gene fpvA of *Pseudomonas aeruginosa*. *J Bacteriol* **175**: 4597–4604.

Rankin, D.J., Bargum, K., and Kokko, H. (2007) The tragedy of the commons in evolutionary biology. *Trends Ecol Evol* **22**: 643–651.

Ratledge, C., and Dover, L.G. (2000) Iron metabolism in pathogenic bacteria. *Annu Rev Microbiol* **54**: 881–941.

Rédly, G.A., and Poole, K. (2003) Pyoverdine-Mediated Regulation of FpvA Synthesis in *Pseudomonas aeruginosa*: Involvement of a Probable Extracytoplasmic-Function Sigma Factor, FpvI. *J Bacteriol* **185**: 1261–1265.

Rédly, G.A., and Poole, K. (2005) FpvIR control of fpvA ferric pyoverdine receptor gene expression in *Pseudomonas aeruginosa*: demonstration of an interaction between FpvI and FpvR and identification of mutations in each compromising this interaction. *J Bacteriol* **187**: 5648–5657.

Reid, D.W., Carroll, V., O'May, C., Champion, A., and Kirov, S.M. (2007) Increased airway iron as a potential factor in the persistence of *Pseudomonas aeruginosa* infection in cystic fibrosis. *Eur Respir J* **30**: 286–292.

Rella, M., Mercenier, A., and Haas, D. (1985) Transposon insertion mutagenesis of *Pseudomonas aeruginosa* with a Tn5 derivative: application to physical mapping of the arc gene cluster. *Gene* **33**: 293–303.

Ross-Gillespie, A., Gardner, A., Buckling, A., West, S.A., and Griffin, A.S. (2009) Density dependence and cooperation: Theory and a test with bacteria. *Evolution* **63**: 2315–2325.

Ross-Gillespie, A., Gardner, A., West, S.A., and Griffin, A.S. (2007) Frequency dependence and cooperation: theory and a test with bacteria. *Am Nat* **170**: 331–342.

Russell, J.B., and Cook, G.M. (1995) Energetics of bacterial growth: balance of anabolic and catabolic reactions. *Microbiol Rev* **59**: 48–62.

Saha, M., Sarkar, S., Sarkar, B., Sharma, B.K., Bhattacharjee, S., and Tribedi, P. (2016) Microbial siderophores and their potential applications: a review. *Environ Sci Pollut Res Int* **23**: 3984–3999.

Sandoz, K.M., Mitzimberg, S.M., and Schuster, M. (2007) Social cheating in *Pseudomonas aeruginosa* quorum sensing. *Proc Natl Acad Sci* **104**: 15876–81.

Schalk, I.J., and Guillon, L. (2013) Pyoverdine biosynthesis and secretion in *Pseudomonas aeruginosa*: implications for metal homeostasis. *Environ Microbiol* **15**: 1661–1673.

Scholz, R.L., and Greenberg, E.P. (2015) Sociality in *Escherichia coli*: Enterochelin is a private good at low cell density and can be shared at high cell density. *J Bacteriol* **197**: 2122–2128.

Schuster, M. (2011) Global expression analysis of quorum-sensing controlled genes. *Methods Mol Biol Clifton NJ* **692**: 173–187.

Schuster, M., Sexton, D.J., Diggle, S.P., and Greenberg, E.P. (2013) Acyl-homoserine lactone quorum sensing: from evolution to application. *Annu Rev Microbiol* **67**: 43–63.

Sexton, D.J., and Schuster, M. (2017) Nutrient limitation determines the fitness of cheaters in bacterial siderophore cooperation. *Nature comm in review* .

Smith, D.R., and Chapman, M.R. (2010) Economical evolution: microbes reduce the synthetic cost of extracellular proteins. *mBio* **1**. 3 e00131-10

Smith, E.E., Buckley, D.G., Wu, Z., Saenphimmachak, C., Hoffman, L.R., D'Argenio, D.A., *et al.* (2006) Genetic adaptation by *Pseudomonas aeruginosa* to the airways of cystic fibrosis patients. *Proc Natl Acad Sci U S A* **103**: 8487–8492.

Smith, E.E., Sims, E.H., Spencer, D.H., Kaul, R., and Olson, and M.V. (2005) Evidence for diversifying selection at the pyoverdine locus of *Pseudomonas aeruginosa*. *J Bacteriol* **187**: 2138-2147

Stites, S.W., Walters, B., O'Brien-Ladner, A.R., Bailey, K., and Wesselius, L.J. (1998) Increased iron and ferritin content of sputum from patients with cystic fibrosis or chronic bronchitis. *Chest* **114**: 814–819.

Stover, C.K., Pham, X.Q., Erwin, A.L., Mizoguchi, S.D., Warrener, P., Hickey, M.J., *et al.* (2000) Complete genome sequence of *Pseudomonas aeruginosa* PAO1, an opportunistic pathogen. *Nature* **406**: 959–964.

Toll-Riera, M., San Millan, A., Wagner, A., and MacLean, R.C. (2016) The genomic basis of evolutionary innovation in *Pseudomonas aeruginosa*. *PLoS Genet* **12**: e1006005.

Traxler, M.F., Watrous, J.D., Alexandrov, T., Dorrestein, P.C., and Kolter, R. (2013) Interspecies interactions stimulate diversification of the *Streptomyces coelicolor* secreted metabolome. *mBio* **4** e00459-13

Vansuyt, G., Robin, A., Briat, J.-F., Curie, C., and Lemanceau, P. (2007) Iron Acquisition from Fe-Pyoverdine by *Arabidopsis thaliana*. *Mol Plant Microbe Interact* **20**: 441–447.

Velicer, G.J., and Vos, M. (2009) Sociobiology of the myxobacteria. *Annu Rev Microbiol* **63**: 599–623.

Visca, P., Imperi, F., and Lamont, I.L. (2007) Pyoverdine siderophores: from biogenesis to biosignificance. *Trends Microbiol* **15**: 22–30.

Wandersman, C., and Delepelaire, P. (2004) Bacterial iron sources: from siderophores to hemophores. *Annu Rev Microbiol* **58**: 611–647.

West, S.A., Diggle, S.P., Buckling, A., Gardner, A., and Griffin, A. (2007) The social lifes of microbes. *Annu Rev Ecol Evol Syst* **38**: 53–77.

West, S.A., Griffin, A.S., and Gardner, A. (2007) Evolutionary explanations for cooperation. *Curr Biol* **17**: 661-672.

West, S.A., Griffin, A.S., Gardner, A., and Diggle, S.P. (2006) Social evolution theory for microorganisms. *Nat Rev Microbiol* **4**: 597–607.

Winsor, G.L., Griffiths, E.J., Lo, R., Dhillon, B.K., Shay, J.A., and Brinkman, F.S.L. (2016) Enhanced annotations and features for comparing thousands of *Pseudomonas* genomes in the *Pseudomonas* genome database. *Nucleic Acids Res* **44**: D646-653.

Xavier, J.B. (2011) Social interaction in synthetic and natural microbial communities. *Mol Syst Biol* **7**: 483.

Xavier, J.B., Kim, W., and Foster, K.R. (2011) A molecular mechanism that stabilizes cooperative secretions in *Pseudomonas aeruginosa*. *Mol Microbiol* **79**: 166–179.

Yeterian, E., Martin, L.W., Guillon, L., Journet, L., Lamont, I.L., and Schalk, I.J. (2010) Synthesis of the siderophore pyoverdine in *Pseudomonas aeruginosa* involves a periplasmic maturation. *Amino Acids* **38**: 1447–1459.

Youard, Z.A., Mislin, G.L.A., Majcherczyk, P.A., Schalk, I.J., and Reimmann, C. (2007) *Pseudomonas fluorescens* CHA0 produces enantio-pyochelin, the optical antipode of the *Pseudomonas aeruginosa* siderophore pyochelin. *J Biol Chem* **282**: 35546–35553.

Zhang, X.X., and Rainey, P.B. (2013) Exploring the sociobiology of pyoverdin-producing *Pseudomonas*. *Evolution* **67**: 3161–3174.

Appendix 3: Abstracts of other published work

"Acyl-Homoserine Lactone Quorum Sensing: From Evolution to Application"

Martin Schuster,[1] D. Joseph Sexton,[1] Stephen P. Diggle,[2] and E. Peter Greenberg[3]

Abstract

Quorum sensing (QS) is a widespread process in bacteria that employs autoinducing chemical signals to coordinate diverse, often cooperative activities such as bioluminescence, biofilm formation, and exoenzyme secretion. Signaling via acyl-homoserine lactones is the paradigm for QS in Proteobacteria and is particularly well understood in the opportunistic pathogen *Pseudomonas aeruginosa*. Despite thirty years of mechanistic research, empirical studies have only recently addressed the benefits of QS and provided support for the traditional assumptions regarding its social nature and its role in optimizing cell-density-dependent group behaviors. QS-controlled public-goods production has served to investigate principles that explain the evolution and stability of cooperation, including kin selection, pleiotropic constraints, and metabolic prudence. With respect to medical application, appreciating social dynamics is pertinent to understanding the efficacy of QS-inhibiting drugs and the evolution of resistance. Future work will provide additional insight into the foundational assumptions of QS and relate laboratory discoveries to natural ecosystems.

Published
Annual Review of Microbiology
May. 2013, Vol. 67: 43-63

"Uncovering effects of antibiotics on the host and microbiota using transkingdom gene networks". Morgun A, Dzutsev A, Dong X, Greer RL, Sexton DJ, Ravel J, Schuster M, Hsiao W, Matzinger P, Shulzhenko N

Abstract

Despite widespread use of antibiotics for the treatment of life-threatening infections and for research on the role of commensal microbiota, our understanding of their effects on the host is still very limited. Using a popular mouse model of microbiota depletion by a cocktail of antibiotics, we analysed the effects of antibiotics by combining intestinal transcriptome together with metagenomic analysis of the gut microbiota. In order to identify specific microbes and microbial genes that influence the host phenotype in antibiotic-treated mice, we developed and applied analysis of the transkingdom network. We found that most antibiotic-induced alterations in the gut can be explained by three factors: depletion of the microbiota; direct effects of antibiotics on host tissues and the effects of remaining antibiotic-resistant microbes. Normal microbiota depletion mostly led to downregulation of different aspects of immunity. The two other factors (antibiotic direct effects on host tissues and antibiotic-resistant microbes) primarily inhibited mitochondrial gene expression and amounts of active mitochondria, increasing epithelial cell death. By reconstructing and analysing the transkingdom network, we discovered that these toxic effects were mediated by virulence/quorum sensing in antibiotic-resistant bacteria, a finding further validated using in vitro experiments. In addition to revealing mechanisms of antibiotic-induced alterations, this study also describes a new bioinformatics approach that predicts microbial components that regulate host functions and establishes a comprehensive resource on what, why and how antibiotics affect the gut in a widely used mouse model of microbiota depletion by antibiotics.

Published
Gut
Nov. 2015, Vol. 64: 1732-43

Hypothesis and Theory

"Why quorum sensing controls private goods"

Martin Schuster, D. Joseph Sexton, and Burkhard A. Hense

Abstract

Cell-cell communication, also termed quorum sensing (QS), is a widespread process that coordinates gene expression in bacterial populations. The generally accepted view is that QS optimizes the cell density-dependent benefit attained from cooperative behaviors, often in the form of secreted "public goods". This view is challenged by an increasing number of cell-associated "private goods" reported to be under QS-control for which a collective benefit is not apparent. A prominent example is nucleoside hydrolase from *Pseudomonas aeruginosa*, a periplasmic enzyme that catabolizes adenosine. Several recent studies have shown that private goods can function to stabilize cooperation by co-regulated public goods, seemingly explaining their control by QS. Here we argue that this property it is a by-product for other benefits rather than an adaptation. Emphasizing ecophysiological context, we propose alternative explanations for the QS control of private goods. We suggest that the benefit attained from private goods is associated with high cell density, either because a relevant ecological condition correlates with density, or because the private good is, directly or indirectly, involved in cooperative behavior. Our analysis helps guide a systems approach to QS, with implications for antivirulence drug design and synthetic biology.

Frontiers Microbiology

Provisionally accepted

April 2017

Appendix B

“Studies on the QS regulation of nucleoside hydrolase”

D. Joseph Sexton and Martin Schuster

Rationale

In a mechanism known as quorum sensing (QS), bacteria use small chemical signals to coordinate a wide variety of species-specific behaviors as a function of cell density. Current theory indicates QS circuits evolved to optimize cooperative behaviors, as individual cells can avoid investing resources until enough contributing neighbors are present to make cooperation efficient (Schuster *et al.*, 2013). However, this explanation is seemingly contradicted by the existence of QS-regulated behaviors which appear private rather than cooperative in nature. The degradation of adenosine into ribose and adenine by the periplasmic enzyme nucleoside hydrolase (Nuh) in *Pseudomonas aeruginosa* has been considered one such example (Heurlier *et al.*, 2005; Mellbye and Schuster, 2011; Dandekar *et al.*, 2012). In an effort to resolve this apparent discrepancy, we explored several plausible explanations for the QS regulation of Nuh. First, we re-assessed a previously proposed role for Nuh in creating a metabolic penalty for cheaters. Second, we tested a novel hypothesis that suggests metabolite leakage may confer attributes characteristic of a cooperative secretion to Nuh activity. We also considered the potential for Nuh to influence the concentration of the QS signal itself, through a putative role in recycling the pool of a signal precursor. The evidence collected to date has not provided conclusive support for these explanations. Current work is evaluating these data and considering yet alternative explanations.

Results

Re-assessment of proposed role of Nuh in metabolic constraining cheaters

In a previous report, it was proposed that Nuh is regulated by QS because co-regulating a private good along with other public goods would create a fitness penalty for defectors of cooperation (Dandekar *et al.*, 2012). This conclusion was based on an *in vitro* evolution experiment performed in caseinate, adenosine or both mixed at various ratios. As was shown previously, QS cheaters consistently evolved in caseinate media through mutations in *lasR*, a gene encoding the global regulator of the LasI/R QS circuit in *P. aeruginosa* strain PAO1. However, when the adenosine concentration was increased to 75% of the total carbon source or above, *lasR* mutants did not arise. The authors

concluded *lasR* mutants forfeit access to adenosine, creating a metabolic penalty that discouraged social cheaters (Dandekar *et al.*, 2012). This explanation fit within a broader concept of pleotropic cheater constraint, where cooperative and non-cooperative behaviors are coordinated under the same regulatory mechanism (Foster *et al.*, 2004). A cheater strategy is discouraged because of a penalty associated with losing an unrelated but important or essential function.

However, the author's experimental design increased adenosine by displacing caseinate, offering overall less QS dependent growth substrate (Dandekar *et al.*, 2012). This should create less opportunity for QS cheaters independent of the presence of adenosine. We re-assessed this explanation by recreating the conditions described in the original report, but held caseinate concentrations constant when provided adenosine. In a series of co-culture experiments between PAO1 wild-type (WT) and a QS mutant, (PAO1 Δ*lasR* Tp^R), we find sequential consumption of carbon sources temporally separates adenosine metabolism from the cooperative degradation of caseinate (Fig. B1). Because the metabolism of the two carbon sources does not occur simultaneously, it does not seem likely pleiotropic constraints are at play. More importantly, we see the presence of adenosine does not prevent enrichment of the QS mutant when caseinate is present (Fig. B.1B).

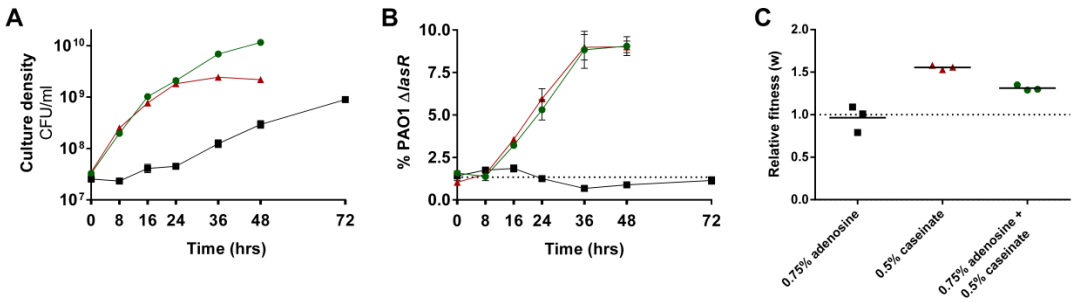

Figure B.1. Co-cultures between PAO1 and PAO1 Δ*lasR* Tp^R. Co-cultures were grown in caseinate (red triangles), adenosine (black squares) or caseinate + adenosine (green circles). The data show the change in total population density (CFU/mL) over time (a), change in frequency of PAO1 Δ*lasR* Tp^R over time (b) and fitness of PAO1 Δ*lasR* Tp^R relative to PAO1 WT after 48 hours growth in caseinate and caseinate + adenosine or after 72 hours in when grown on adenosine (c).

Potential for metabolite leakage to confer public characteristics to Nuh activity

An alternative explanation for QS regulation of Nuh considers the unique sub-cellular localization of Nuh. Contrasting from the cytoplasmic location of Nuh in *E. coli*, Nuh is located in the periplasm of *P. aeruginosa* (Imperi *et al.*, 2009). Periplasmic contents are known to be inherently leaky, particularly at high cell densities (Rinas and Hoffmann, 2004). If leakage of Nuh or the degradation products into the extracellular environment is substantial, this private good may have public good attributes under some conditions, offering a potential explanation for QS regulation of Nuh.

To test this hypothesis, we first set out to determine whether Nuh activity is leaky in *P. aeruginosa*. For this purpose, we adapted a previously published assay for Nuh activity in *P. aeruginosa* that is based on the detection of ribose, a product of Nuh mediated adenosine degradation (Heurlier *et al.*, 2005). Using this method, we measured ribose in the supernatant from *P. aeruginosa* cells after incubation with varying concentrations of adenosine for 1 hour (Fig B.2). To ensure Nuh was expressed at constant levels, we used a *lasI* signal synthase mutant and activated the QS circuit by exogenously adding 5 μM of QS signal 3-oxo-C12. Cell-free and adenosine-free controls were performed to resolve whether any ribose originated from cell-independent degradation of adenosine or cell lysis, respectively (Fig B.2A). At the highest concentration tested (28.1 mM adenosine), ribose was not detected in the cells-only control. An average of 8 nM ribose was detected in the adenosine-only control, suggesting some degree of cell-independent breakdown does occur (Fig B.2A). With both cells and adenosine however, an average of 55 nM ribose was detected in the supernatant, providing evidence of leakage attributable to cell activity. An extension of this permutation was designed to help resolve whether enzymes or metabolites were leaking. Cells were removed yet the assay was permitted to continue for another hour. We reasoned that if enzyme had leaked, the ribose concentration would continue to increase. We did indeed observe a slight increase, suggesting some enzyme had leaked, but only contributing only a minor fraction of the total ribose we had detected. This suggests leakage of the metabolites is more relevant than leakage of the protein. Specific activity was calculated and plotted as a function of adenosine concentration. We found our data

fit Michaelis-Menten kinetics, corroborating the idea that the ribose was enzymatically derived (Fig B.2B).

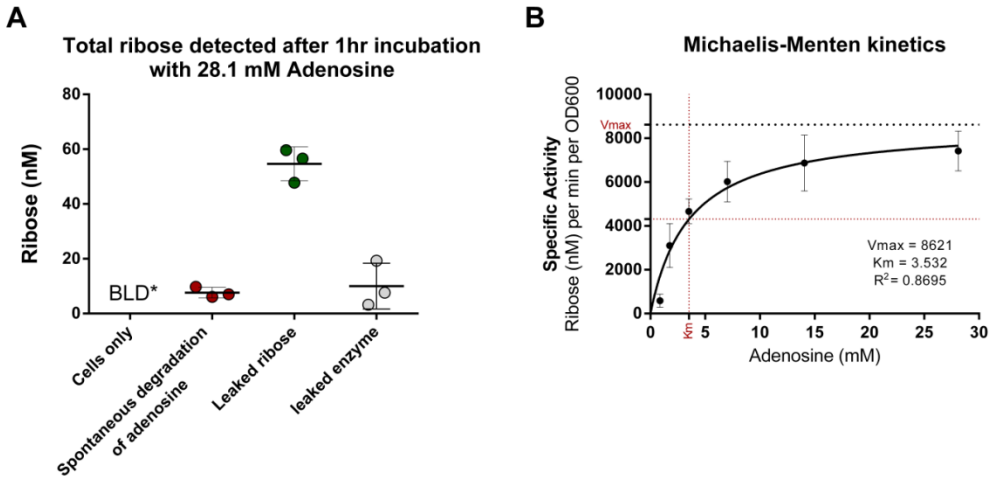

Figure B.2. Ribose leaks from *P. aeruginosa* cells after incubation with adenosine. (A) Total ribose detected after 1hr incubation (B) Plotting the specific activity as a function of adenosine concentration reveals that ribose leakage from the cell follows a Michaelis-Menten kinetics model.

After demonstrating that metabolites from adenosine degradation leak into the extracellular medium, we then wanted to determine if the amount of leakage was biologically significant. To address this question, we designed a bioassay that utilized the anticipated phenotype of a *nuh* mutant. Because Nuh is required to break down adenosine, we expect a mutation in *nuh* would render the strain unable to grow on adenosine as the sole carbon source. If co-cultured with a WT, any increase in biomass would be quantitatively related to the amount of leaked metabolites. To accomplish this, a mutant *nuh* allele with an in-frame deletion was constructed and exchanged with the WT allele in the *P. aeruginosa* PAO1 background (Horton, 1995). A tetracycline marker was then inserted into a neutral site so the mutant and WT sub-populations could be distinguished by selective plating (Choi and Schweizer, 2006). Before initiating the co-culture bioassay, we tested the mutant phenotype by evaluating mono-culture in a defined M9 salts media with adenosine as the sole carbon source. As expected, PAO1 WT was able to grow in adenosine, while PAO1 Δ*nuh* Tc^R was not (Fig. C.3A, n = 4). To verify this growth deficiency was attributable to the *nuh* mutation, we cultured both strains with

adenine and ribose as the sole carbon sources, which are the products of Nuh mediated adenosine degradation (Fig. B.3B, n = 2). We observed comparable growth of both strains, showing that PAO1 Δ*nuh* Tc^R was a suitable strain for our intended bioassay experiment. The PAO1 WT and PAO1 Δ*nuh* Tc^R were then co-cultured in adenosine, with sub-populations distinguished at 0, 72 and 144 hrs. Interestingly, we found the biomass did not increase at all, and for reasons that remain unclear, actually decreased in density (Fig C.3C, n = 4). This result suggests that although there is clearly some degree of metabolite leakage (Fig C.2), it does not appear to be enough to be significant in a social context, at least under these conditions. This finding was not consistent with the hypothesis that metabolite leakage confers public characteristics to Nuh activity and encouraged us to consider alternative explanations.

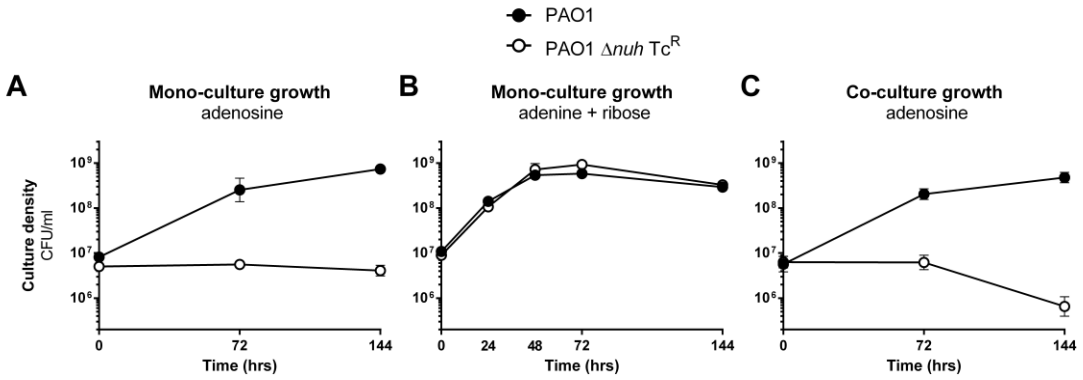

Figure B.3. Co-culture bioassay to measure metabolite leakage. PAO1 WT (black circles) and PAO1 Δ*nuh* TetR (white circles) were grown independently in adenosine (A) or in ribose + adenine (B) or in co-culture in adenosine (C). PAO1 and PAO1 Δ*nuh* Tc^R densities were determined by CFU counts on LB or LB + Tc_{100}, respectively.

Evaluating the influence of Nuh on QS signal concentrations

Interestingly, it has been suggested that Nuh activity may be involved with recycling S-adenosylmethionine (SAM), a precursor of the acyl-homoserine lactone (AHL) signals responsible for activating the QS circuit (Heurlier *et al.*, 2005). This perspective would shift the perceived role of Nuh away from nutrient acquisition and instead towards supporting the QS circuit more directly. If true, the QS regulation of Nuh could be understood. However, this potential role has not been explored empirically. We compared the concentrations of AHLs produced by PAO1 and the PAO1 Δ*nuh* when

cultured in defined media with caseinate and glucose as the sole carbon sources, representative of QS-dependent and QS-independent conditions, respectively (Fig. C4). We investigated the AHLs made by both LasI and RhlI, which produce 3-oxo-C12-HSL and C4-HSL, respectively, using previously published β-galactosidase reporter strains (Pearson *et al.*, 1995). However, both signals were detected at similar concentrations in all permutations explored, indicating Nuh does not likely influence QS signal concentration (Fig B.4).

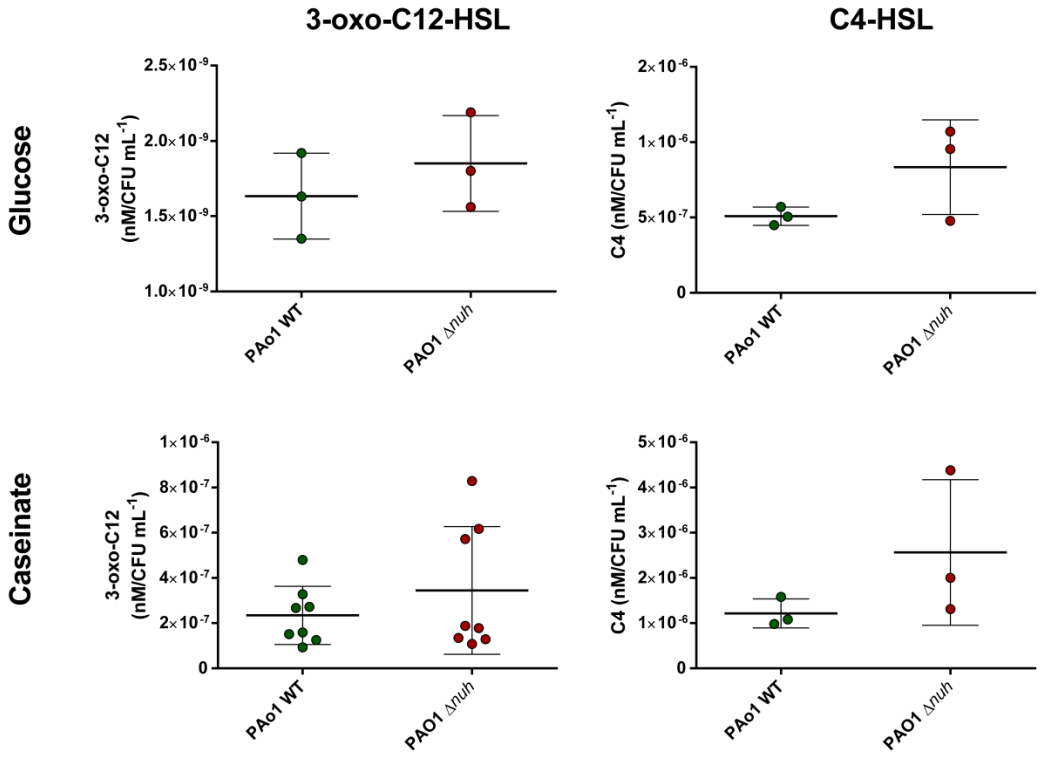

Figure B.4. Role of Nuh in QS signal production. Concentrations of 3-oxo-C12-HSL (left panels) and C4-HSL (right panels) AHLs were determined from WT (green) and *nuh* mutant (red) after 18 hours of growth in glucose (top panels) or caseinate (bottom panels) minimal medias. Signal concentrations were normalized to cultured density. Signal concentrations were not significantly different between PAO1 and PAO1 Δ*nuh* (two-sample t-test, $\alpha = 0.05$).

Conclusions

The density-dependent coordination of gene expression using QS systems is ubiquitous in the microbial world (Pearson *et al.*, 1995a). Although significant progress

has been made resolving the molecular characteristics and diversity of QS systems, less is known about the fitness advantages QS offers relative to other regulatory mechanisms (Schuster *et al.*, 2013). In other words, why might a gene be regulated by QS rather than an alternative mechanism? This evolutionary question has important implications as many pathogenicity factors are controlled by QS systems (Schuster *et al.*, 2003). This has stimulated significant interest in anti-QS therapies, warranting a better understanding of the selective pressures shaping the QS regulon (Hentzer and Givskov, 2003; Kohler *et al.*, 2010; Mellbye and Schuster, 2011).

Current theory suggests QS evolved as to stabilize cooperative secretions, which are inherently more efficient at higher densities (Schuster *et al.*, 2013). This interpretation is corroborated by the observation that secreted products are over-represented in the QS regulon of *P. aeruginosa* (Schuster *et al.*, 2003). Recent work has also shown more explicitly that the fitness benefits of some QS behaviors increase with density (Darch *et al.*, 2012; Pai *et al.*, 2012). However, not all QS behaviors involve secreted proteins, an observation that seemingly contrasts this theory. The field is therefore challenged to resolve this discrepancy to improve the ability to predict whether a behavior is likely to be regulated by QS.

We explored this question by evaluating the QS regulated degradation of intracellular adenosine by Nuh in *P. aeruginosa*. Although we pursued several plausible explanations, the current evidence has not provided a clear answer as to why Nuh is regulated by QS. The previously proposed role in metabolically constraining cheaters through the co-regulation of private (adenosine metabolism) and public (caseinate metabolism) benefits seemed convincing initially (Dandekar *et al.*, 2012). However, our data clearly demonstrate that the presence of adenosine does not constrain cheaters so long as relevant caseinate concentrations are maintained (Fig. B.1). Our novel idea that the benefits of Nuh activity may be leaky and share attributes with a traditional "cooperative secretion" was also intriguing considering the sub-cellular localization of Nuh in the periplasm (Imperi *et al.*, 2009). This hypothesis was initially supported by the detection of ribose in the extracellular medium (Fig. B.2). However, we found the amount of intracellular metabolites that leak is not likely to be biologically significant,

which motivated us to explore another alternative (Fig. B.3). The proposed role of Nuh in influencing QS signals was also attractive (Heurlier *et al.*, 2005), but we found that PAO1 and PAO1 Δ*nuh* generate comparable concentrations of QS signals, casting doubt on this role of Nuh in *P. aeruginosa* (Fig. B4).

This work demonstrates the inherent challenges when attempting to resolve the evolutionary benefits of a given behavior. We approached this question using Nuh activity to build on precedent literature that has considered the social dynamics of Nuh production (Mellbye and Schuster, 2011; Dandekar *et al.*, 2012). However, using Nuh came with certain disadvantages. Most notably, the function of Nuh for the cell in the natural environment is not fully understood. The concept of metabolic constraint was founded on the premise that adenosine serves as a carbon source (Dandekar *et al.*, 2012). Yet there is reason to believe adenosine may be more relevant as a nitrogen source (Appendix A). Other work has demonstrated Nuh activity is not specific to adenosine, but can degrade other nucleosides as well (Fields, 2002). The idea that Nuh could influence signal concentrations further emphasizes how resolving biochemical function does not always translate into a clear understanding of what happens in a natural context (Heurlier *et al.*, 2005). Our efforts have provided new insights into the function of Nuh that ultimately will help resolve its biological role. Once this is better understood, addressing why it is regulated by QS will be a more tangible task.

Methods

Bacterial strains and growth conditions

Bacterial cultures were routinely maintained at 37°C in Lennox LB liquid medium or on Lennox LB agar plates. Growth experiments with defined carbon sources were performed in M9 minimal medium (0.68% (w/v) Na_2HPO_4, 0.3% (w/v) KH_2PO_4, 0.05% (w/v) NaCl, 0.1% (w/v) NH_4Cl, 0.01% (w/v) $MgSO_4$, 0.001% (w/v) $CaCl_2$) and contained 0.5% (w/v) caseinate, 0.75% (w/v) adenosine, or both as indicated. PAO1 Δ*nuh* was constructed using splicing-by-overlap-extension PCR and allelic exchange as described as described (Horton, 1995). The Δ*nuh* allele was built using 5'-N^6TCTAGACCCGCGGCTCGATGAGCCT and 5'-

N^6AAGCTTTTGAACCTGATGCTGGCGGTGCCTT as external primers and 5'-AGAGACTCAGGGCAGGCGGCGTGACATGGGGCGGCT and 5'-AGCCGCCCCATGTCACGCCGCCTGCCCTGAGTCTCTCGTCGTA as overlapping internal primers. Restriction enzyme sites (XbaI and HindIII, respectively) for cloning into an allelic exchange vector are underlined. The resulting PAO1 Δ*nuh* mutant was subsequently tagged with a tetracycline resistance marker as described (Choi and Schweizer, 2006). PAO1 Δ*lasI* and PAO1 Δ*lasR* Tp^R mutants were previously constructed in the Schuster lab by Cara Wilder (Wilder *et al.*, 2011).

Co-culture experiments

PAO1 and PAO1 Δ*lasR* Tp^R were co-cultured with shaking at 37°C in M9 minimal media with either 0.5% (w/v) caseinate, 0.75% (w/v) adenosine or 0.5% (w/v) caseinate + 0.75% (w/v) adenosine. Cultures were inoculated with 1% initial PAO1 Δ*lasR* Tp^R. PAO1 and PAO1 Δ*lasR* Tp^R sub-populations were distinguished at the indicated intervals by selective plating onto LB and LB + 100 µg/mL trimethoprim, respectively. Relative fitness (*w*) of non-producers was calculated as the ratio of average growth rates or Malthusian parameters as described (Lenski, 1991). For the Nuh leakage bioassay, PAO1 and PAO1 Δ*nuh* Tc^R were co-cultured with shaking at 37°C in M9 minimal media with 3.74 mM adenosine (which corresponds to 0.1% w/v). Strains were initiated at 1:1 ratios and sub-populations were distinguished at 0,72 and 144 hours by selective plating onto LB and LB + 100 µg/mL tetracycline, respectively.

Ribose assay

PAO1 Δ*lasI* cultures were grown to saturation in M9 minimal media with 3.74 mM adenosine + 5 µM 3-oxo-C12-HSL. Cells were washed and resuspended to an OD_{600} of 0.1 in the same media and incubated for 1 hour for ribose to accumulate. The reaction was stopped with 1N HCl and subsequently neutralized with 1N NaOH. Neocuprioine and reducing sugar reagent (4% (w/v) Na_2CO_3, 1.6% (w/v) glycine and 0.045% (w/v) $CuSO_4$) were added for color development and incubated for 2 hours at 80°C. Total

absorbance at 450 nm was measured and used to interpolate ribose concentrations from a standard curve.

QS Signal assay

QS signals were extracted from culture supernatants in acidified ethyl acetate. The concentration of signal in these extracts was determined using *E. coli* reporter strains DH5α pECP61.5 and MG4 pKDT17, which express β-galactosidase in response to 3-oxo-C12-HSL and C4-HSL, respectively (Pearson *et al.*, 1995). Luminescence was developed with the GALACTO-light kit (applied Biosystems) and measured in a TECAN Infinite 200 plate reader (Tecan Group Ltd, Männedorf, Switzerland). Signal concentrations were interpolated from a standard curve.

Bibliography

Choi, K.-H., and Schweizer, H.P. (2006) mini-Tn7 insertion in bacteria with single attTn7 sites: example *Pseudomonas aeruginosa*. *Nat Protoc* **1**: 153–161.

Dandekar, A.A., Chugani, S., and Greenberg, E.P. (2012) Bacterial quorum sensing and metabolic incentives to cooperate. *Science* **338**: 264–266.

Darch, S.E., West, S.A., Winzer, K., and Diggle, S.P. (2012) Density-dependent fitness benefits in quorum-sensing bacterial populations. *Proc Natl Acad Sci U S A* **109**: 8259–8263.

Fields, C. (2002) Comparative biochemistry and genetic analysis of nucleoside hydrolase in *Escherichia coli*, *Pseudomonas aeruginosa*, and *Pseudomonas fluorescens*. *University of North Texas* A Dissertation.

Foster, K.R., Shaulsky, G., Strassmann, J.E., Queller, D.C., and Thompson, C.R. (2004) Pleiotropy as a mechanism to stabilize cooperation. *Nature* **431**: 693–6.

Hentzer, M., and Givskov, M. (2003) Pharmacological inhibition of quorum sensing for the treatment of chronic bacterial infections. *J Clin Invest* **112**: 1300–7.

Heurlier, K., Dénervaud, V., Haenni, M., Guy, L., Krishnapillai, V., and Haas, D. (2005) Quorum-Sensing-Negative (lasR) Mutants of *Pseudomonas aeruginosa* Avoid Cell Lysis and Death. *J Bacteriol* **187**: 4875–4883.

Horton, R.M. (1995) PCR-mediated recombination and mutagenesis. SOEing together tailor-made genes. *Mol Biotechnol* **3**: 93–99.

Imperi, F., Ciccosanti, F., Perdomo, A.B., Tiburzi, F., Mancone, C., Alonzi, T., *et al.* (2009) Analysis of the periplasmic proteome of *Pseudomonas aeruginosa*, a metabolically versatile opportunistic pathogen. *Proteomics* **9**: 1901–1915.

Kohler, T., Perron, G.G., Buckling, A., and Delden, C. van (2010) Quorum sensing inhibition selects for virulence and cooperation in *Pseudomonas aeruginosa*. *PLoS Pathog* **6**: e1000883.

Lenski, R.E. (1991) Quantifying fitness and gene stability in microorganisms. *Biotechnol Read Mass* **15**: 173–192.

Mellbye, B., and Schuster, M. (2011) The sociomicrobiology of antivirulence drug resistance: a proof of concept. *MBio* **2**:e00131-11.

Pai, A., Tanouchi, Y., and You, L. (2012) Optimality and robustness in quorum sensing (QS)-mediated regulation of a costly public good enzyme. *Proc Natl Acad Sci U S A* **109**: 19810–19815.

Pearson, J.P., Passador, L., Iglewski, B.H., and Greenberg, E.P. (1995) A second N-acylhomoserine lactone signal produced by *Pseudomonas aeruginosa*. *Proc Natl Acad Sci* **92**: 1490–1494.

Rinas, U., and Hoffmann, F. (2004) Selective leakage of host-cell proteins during high-cell-density cultivation of recombinant and non-recombinant *Escherichia coli*. *Biotechnol Prog* **20**: 679–687.

Schuster, M., Lostroh, C.P., Ogi, T., and Greenberg, E.P. (2003) Identification, timing, and signal specificity of *Pseudomonas aeruginosa* quorum-controlled genes: a transcriptome analysis. *J Bacteriol* **185**: 2066–2079.

Schuster, M., Sexton, D.J., Diggle, S.P., and Greenberg, E.P. (2013) Acyl-homoserine lactone quorum sensing: from evolution to application. *Annu Rev Microbiol* **67**: 43–63.

Wilder, C.N., Diggle, S., and Schuster, M. (2011) Cooperation and cheating in *Pseudomonas aeruginosa*: The roles of the *las*, *rhl*, and *pqs* quorum sensing systems. *ISME J* **8**:1332-43.

Appendix C

"Chemostat construction and operation"

D. Joseph Sexton, Brett Mellbye, Martin Schuster

Summary

Chemostats are a way of achieving microbial continuous-cultures, where growth rate is determined by the dilution rate of the media and population density by the concentration of the limiting nutrient (Evans *et al.*, 1970; Ziv *et al.*, 2013; Gresham and Dunham, 2014). For evolutionary questions, they represent a gold standard as defined selective conditions can be held constant, which cannot be achieved in any other biological system. Although bioreactors can be purchased, they are expensive and come with their own inherent limitations. This protocol describes a home-made chemostat design that is cheap, adaptable and has been refined in-house over years. Sufficient details are provided to recreate this design exactly along with pertinent rationale helpful for adapting it as needed.

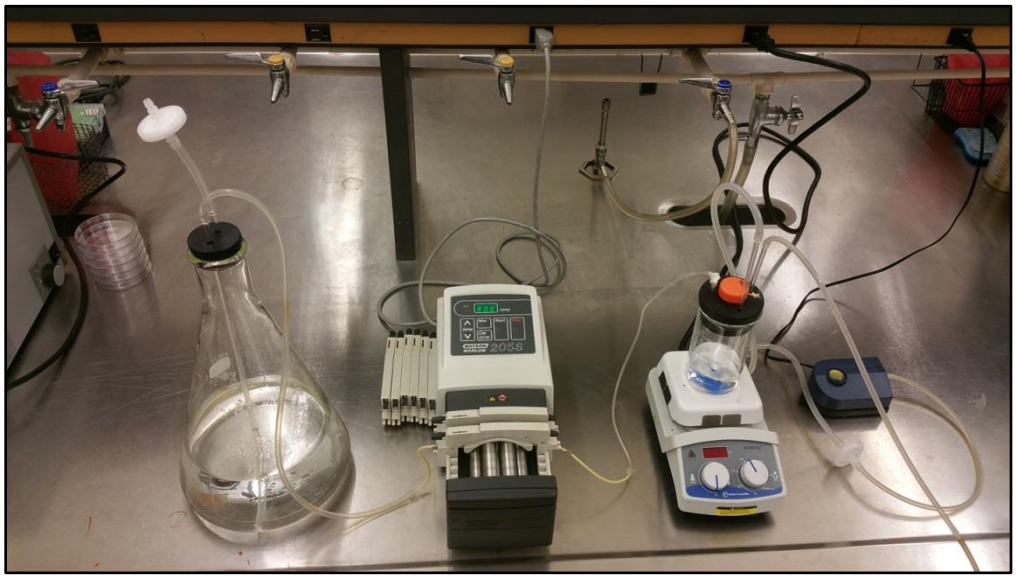

Figure C.1. The Schuster lab chemostat. Sterile media is pulled from a 4 L reservoir (left) using a peristalatic pump (center). Media enters the chemostat bioreactor (right). Effluent is collected in a waste reservoir (not in of frame).

Chemostat construction

The Schuster lab chemostat design can largely be constructed from ordinary lab supplies, with a peristaltic pump being the most unique requirement. The only tools needed are an electric drill with a standard bit set plus a 1 ¼ in spade bit, along with a blade for cutting plastic tubing and device for cutting glass tubing. For plastic tubing other than the peristaltic pump lines, use 0.125 in I.N. 0.25 in O.D Silastic laboratory tubing (Dow Corning #515-012).

How to size the glass tubing

Glass tubing is needed at various lengths for the media reservoir and chemostat bioreactor. Glass tubing comes in rods of stock length and must be cut down to the desired size using a glass tubing cutter (Fig C.2A). This tool is used to lightly score the outside circumference of the tube. The tubing can then be cleanly broken by hand at the site of the score. The new glass edges will be sharp and need to be blunted (Fig. C.2B). This is done by heating the new edge of the glass tubing over a bunsen burner (Fig. C.2C). Once hot, the sharp edge can be gently pressed onto the lab bench to round off the edge (Fig. C.2D). This should be modest and not done such that the shape of the tube is significantly distorted. The hole should be enlarged if the glass tube cannot be manipulated easily to avoid the risk of breaking the glass. Small amounts of mineral oil can be used to lubricate the rubber stopper to help with installation.

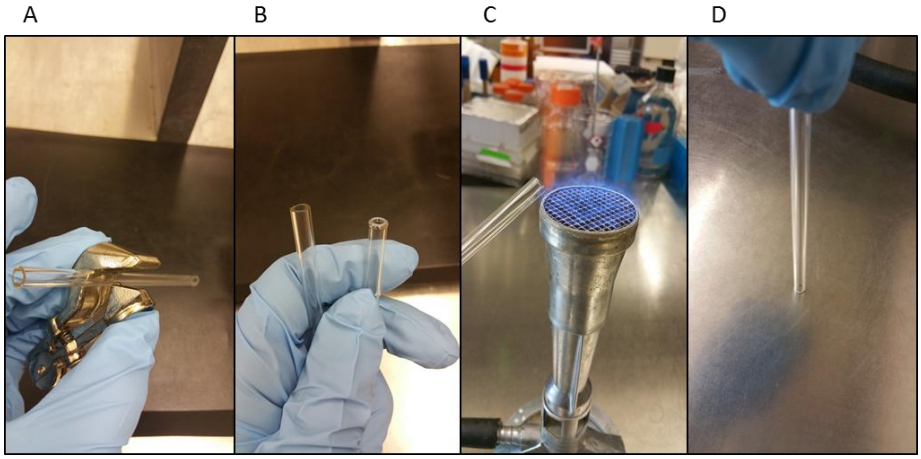

Figure C.2 Sizing glass. Glass cutter tool (A), contrast of freshly cut sharp edge and one that has been rounded (B), heating of sharp edge (C) and rounding of heated cut edge on lab bench (D).

The media reservoir

The media reservoir consists of a 4L flask capped with a size 10 rubber stopper with 2 holes that can hold glass tubing (Fig C.3). One hole serves as the sterile air intake to prevent a vacuum from forming in the reservoir. The glass tube is relatively short (no more than 2-4 inches) connected by minimal plastic tubing (Dow Corning #515-012) to a directional air filter (PALL Bacterial Air Vent autoclavable – part #4210).The air intake line can be longer, but reducing unnecessary hose when possible will make the chemostat more manageable (Fig C.3A).

The second hole in the rubber stopper holds the media feed line. The glass tubing reaches to about 2-3 inches from the bottom of the reservoir. A piece of rubber hose with a beveled cut is added to extend the reach fully to the bottom. The beveled cut prevents the rubber tubing from butting directly against the reservoir wall, which could potentially block media access (Fig C.3B). On the topside of the glass tube, a plastic tubing is attached which will run to the peristaltic pump. This length is be variable based on the work space, but should also be minimized to avoid excessive tubing.

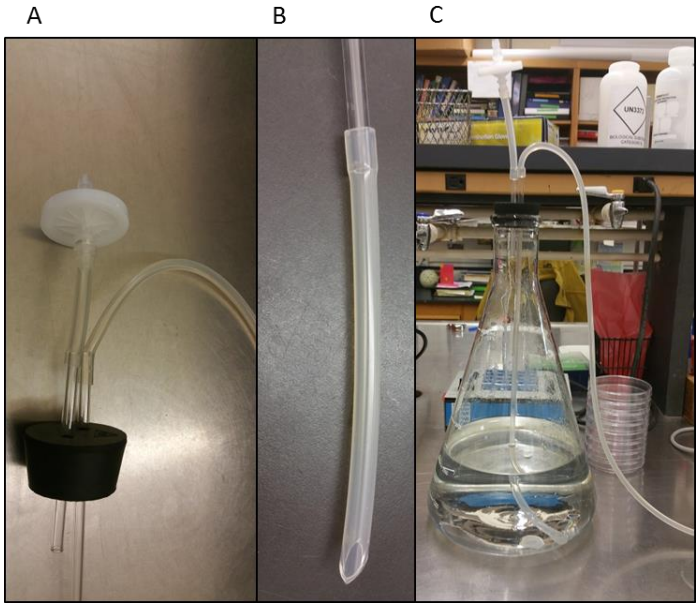

Figure C.3. Media reservoir. Cap of media reservoir showing air intake and media feed line (A), beveled cut of flexible hose at the bottom of media feedline and reservoir assembled in 4 L flask (C).

The pump

We use a Watson Marlow 205S peristaltic pump, which has 8 lanes and variable speed from 3 RPM to 90 RPM (Fig. C.4A). As the pump speed is set in RPM, the flow rate is determined by collecting effluent over a set amount of time at several speeds. A standard curve can be used to determine the RPM setting that will achieve the desired dilution rate. This provides the potential to run up to 8 chemostats simultaneously, although space and other resources may limit what is reasonable at one time. The selection of tubing that goes through the pump is important. We use 1.3 mm ID Pharmed BPT tubing (Cat# 95713-32) and replace after every 3-4 runs, as the lines will wear quickly. For example, there are gray plastic components which lock the line into the pump cassettes. These gray plastic components often fall off after repeated use (Fig. C.4C). Barbed plastic adapters are used to connect the peristaltic pump line to the larger media feed line (Fig. C.4B).

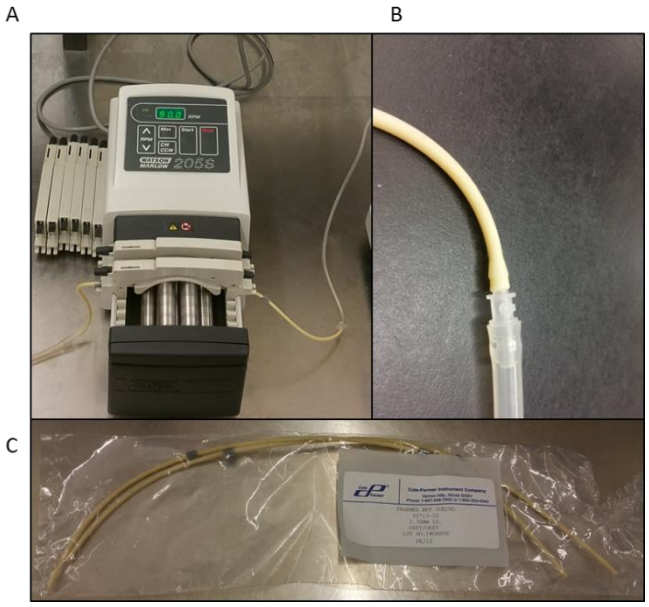

Figure C.4. Media pump. The peristaltic pump assembly with unused cassettes removed for visibility (A). Media feed line must adapt to a peristaltic pump line using a plastic barbed adaptor (B). Picture of peristaltic pump lines, which have plastic fittings that provide points for the pump cassettes to hold onto (C).

Chemostat bioreactor

The chemsotat bioreactor is built with a 400 mL KIMAX beaker (#14040) capped with a size 13.5 rubber stopper. The stopper is modified to have 4 symmetrically arranged ports (Fig. C.5B). The holes should be drilled before any components are installed. The sampling port is installed first before glass components have been added. A spade bit is used to cut a 1 ¼ hole out of the center of the 13.5 stopper. It is important the sampling port is centered; previous attempts to move it to the side to increase accessibility for sampling resulted in warping of the stopper after autoclaving, preventing it from sitting evenly on the beaker. A 50 mL conical tube is inserted through the 1 ¼ hole with light mineral oil if needed. The bottom half of the conical is removed after inserting into the rubber stopper and is cut as high up to the stopper as possible (Fig. C.4B).

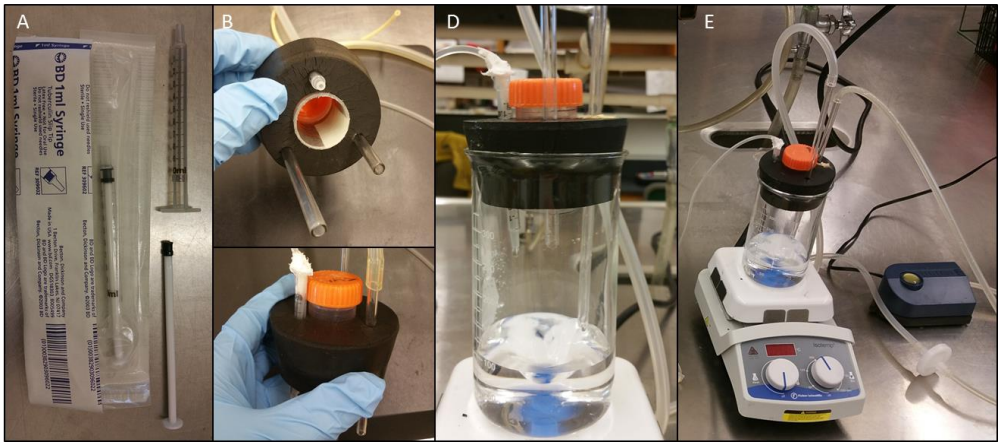

Figure C.5. Chemostat bioreactor. The housing of a 1 mL syringe is used for the media inlet (A). View of underside of chemostat bioreactor cap, showing center sampling port with media inlet on top, air intake bottom right and the waste-out line bottom left (B). Top view of assembled bioreactor cap (C). Side view of chemostat bioreactor to show position of waste-out line position (D). Full chemostat assembly on stir plate with aquarium pump shown in background.

The media inlet is build out of a disassembled 1 mL syringe casing adapted to the media inlet line with silicone sealant (Fig. C.5A&C). This design is suitable because the syringe produces small uniform droplets and is sturdy enough to be pressed through the hole in the rubber stopper. The sterile air intake forces air into the chemostat bioreactor using a standard fish aquarium pump (Fig. C.5E). This is accomplished by inserting a short piece of glass tubing through the stopper and connecting it with plastic tubing to the

aquarium pump, with a PALL bacterial air vent in line. As with the media reservoir, this glass piece should be short (2-4 inches) and is set to not protrude minimally into airspace of the chemostat bioreactor.

The waste-out line operates based on air pressure created by the aquarium pump. As air is forced in, pressure is relieved through the waste-out line. Therefore media which contacts the opening of waste-out tube will be pushed out of the chemostat and into the waste reservoir. The position of the waste-outline determines the volume in the chemostat (Fig. C.5D). Because the stir bar forms a vortex, the waste-outline is positioned when stirring at the experimental speed. The stir speed is set as fast as the system can go without causing splattering. The glass piece is set as straight as possible to avoid contacting the side wall or ending up in the center of the chemostat, which can interfere with sampling. On the top side, rubber tubing is attached and runs to a waste reservoir. In addition to holding all the waste, the waste reservoir must also fit in the autoclave. The chemostat must be air tight; air leaks will disrupt the waste removal mechanism and lead to a volume increasing. This will continue spill out of the chemostat bioreactor through the location of the air leak if not caught sooner.

Chemostat preparation

Cleaning and sterilizing

Although glass components can be cleaned, inner parts of tubing cannot. However, running the system with ddH_2O can flush out debris from construction, media from previous runs or residual chemicals from manufacturing of tubing. It also provides an opportunity to review the condition of the chemostat and inspect the system for any leaks. For these reasons, it is good habit to assemble the chemostat and run 2-3 L of ddH_20 through before preparing for the next run. The chemostat beaker glass walls are treated before each run with the siliconizing reagent SigmaCote (sigma #SL2-100ML) to prevent biofilm formation. This procedure is done in the chemical fume hood and involves pipetting or otherwise manipulating 1000 µL of SigmaCote along the inner walls of the beaker. After all surface area has been covered with redundancy, the excess

volume is reused in the next beaker or discarded. The reagent is baked onto the glass in a drying oven set to 80°C.

Sterilizing the chemostat is inherently cumbersome due to the size and connectivity of the components. With the system described here, it is most convenience to sterilize the chemostat when disassembled (Fig. C.6). Ends of open hoses should be covered with tin foil (Fig. C.6B&C). The cap of the sampling port is turned back a turn or two and the cap is held in place with autoclave indicator. The stir bar is also placed in the bioreactor before sterilizing. Chemostat bioreactor and media reservoir cap are autoclaved together in a dry cycle with 25 minutes sterilization and 10 minutes of drying (Fig. C.6A-C). As the dry cycle does not dry completely, bioreactor and media reservoir cap are transfered to a drying oven until completely dry. This is especially important for the bacterial air vents, as water will compromise the function of the filter and create potential for contamination. After autoclaving and drying, the chemostat is assembled in a sterile cabinet before moving the system to a temperature controlled room. The media reservoir is autoclaved separately in a liquid cycle for 60 minutes. The water needs to cool overnight before heat sensitive ingredients can be added.

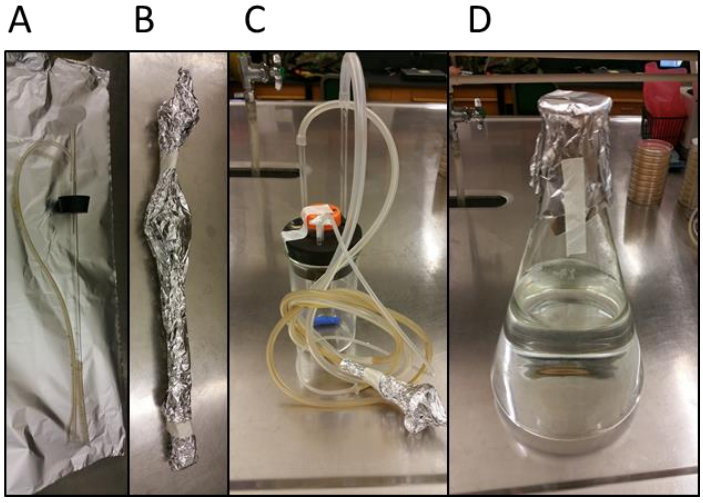

Figure C.6. Disassembled chemostat before sterilization. Media-feed line is disconnected on the "media-reservoir" side of peristaltic pump. Media reservoir cap and tubing before wrapping in aluminum foil (A). Media reservoir cap and tubing after wrapped into aluminum foil (B). Chemostat bioreactor before being autoclaved has the ends of all three lines collectively wrapped in aluminum foil. Braiding the tubing helps keep things organized (C). Chemostat bioreactor and media reservoir cap are autoclaved on a dry

cycle for 25 minutes with 10 minutes of drying. Media reservoir with ddH_2O is autoclaved separately on a liquid cycle for 1 hour (D).

Operating the chemostat

Equilibrate chemostat

The assembled chemostat is moved to the 37°C warm room the night before starting the run, so the media and other components can equilibrate. When preparing the cells for inoculation, the peristaltic pump is turned on to run ~ 0.5 L of the experimental medium through the system as a final measure to push out anything left over from previous steps and as a final check for leaks. The chemostat is left operating at a slow speed up until the point of inoculation. This ensures the volume is correct when cells are added to the system.

Starting the chemostat

The peristaltic pump is turned off. The sampling port is used to inoculate the bioreactor to a cell density (OD_{600}) that will enable at least several doublings before saturating the media. For experiments where the saturating density is at an OD_{600} of 1, starting at 0.05 has been good. This batch phase of growth gives the cells an opportunity to adapt to the conditions of the chemostat. The pump is turned on just before the cells transition to stationary phase. If timed well, density oscillations are minimized. Sampling volumes should be small to avoid disrupting the steady-state. Sampling 2 mL from a 100 mL culture every 24 hours has been successful in this respect. Once operating, the chemostat should be stable until the media is depleted. When sampling, or at other regular intervals, the system is evaluated for biofilm formation. Although the Sigmacote treatment generally works well, biofilms may still form starting on scratches in the glassware or at the water air interface. The latter is most likely to occur if the stir speed is too high, and leads to splattering. Even slow rate of splatter will lead to biofilm formation. If biofilms appear, the run should be discarded. After an experiment is completed, the chemostat system is autoclaved (90 minutes for waste, 45 minutes for everything else) shortly to prevent cells or media from drying onto any components. Glassware is cleaned gently with soap to avoid scratching.

Evans, C., Herbert, D., and Tempest, D. (1970) Continuous cultivation of micro-organisms: Construction of a chemostat. In *Met Microbiol*. pp. 277–327.

Gresham, D., and Dunham, M.J. (2014) The Enduring Utility of Continuous Culturing in Experimental Evolution. *Genomics* **104**: 399–405.

Ziv, N., Brandt, N.J., and Gresham, D. (2013) The use of chemostats in microbial systems biology. *J Vis Exp JoVE* . doi: 10.3791/50168.